AD-A283 379

STRUCTURAL INTERMETALLICS

PERSPECTIVES ON SCIENCE AND TECHNOLOGY

February 5 & 6, 1994

DEFENCE METALLURGICAL RESEARCH LABORATORY
HYDERABAD
INDIA

Vol. II

Metals Group,
MATERIALS RESEARCH SOCIETY OF INDIA

ASIAN OFFICE OF AEROSPACE RESEARCH & DEVELOPMENT
US Air Force

This document has been approved for public release and sale; its distribution is unlimited.

Best
Available
Copy

DISCLAIMER NOTICE

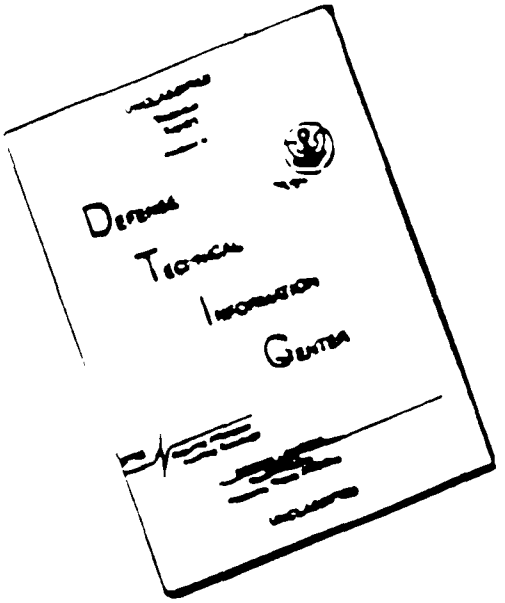

THIS DOCUMENT IS BEST QUALITY AVAILABLE. THE COPY FURNISHED TO DTIC CONTAINED A SIGNIFICANT NUMBER OF PAGES WHICH DO NOT REPRODUCE LEGIBLY.

STRUCTURAL INTERMETALLICS

PERSPECTIVES ON SCIENCE AND TECHNOLOGY

February 5 & 6, 1994

DEFENCE METALLURGICAL RESEARCH LABORATORY
HYDERABAD
INDIA

Vol. II

Metals Group,
MATERIALS RESEARCH SOCIETY OF INDIA

ASIAN OFFICE OF AEROSPACE RESEARCH & DEVELOPMENT
US Air Force

Accesion For
NTIS CRA&I ☑
DTIC TAB ☐
Unannounced ☐
Justification
By
Distribution /
Dist
A-1

19408
94-25385

94 8 11 053

CONTENTS

Vol. II

1. FOREWORD

2. PROGRAMME

3. European Intermetallics Activities and Contribution from France
   T.Khan and S.Naka
   ONERA, France

4. Microstructure, Processing and Properties of $MoSi_2$
   D.A. Hardwick
   Rockwell Science Centre, USA

5. Effect of Microstructure on the Creep of Molybdenum Disilicides and their Composites
   K. Sadananda and R. Feng
   Naval Research Laboratory, USA

6. Ordered Ground State Structures in HCP Alloys
   A.K. Singh
   Defence Metallurgical Research Laboratory, India
   and
   Prof. S.Lele
   Banaras Hindu University, India

7. Stability
   S. Raju, E.Mohandas and V.S.Raghunathan
   Indira Gandhi Centre for Atomic Research, India

FOREWORD

A two day symposium on "Structural Intermetallics - Perspectives on Science and Technology" was held at the Defence Metallurgical Research Laboratory, Hyderabad, India on February 5 and 6, 1994, preceding the Annual General Meeting of the Materials Research Society of India. The Symposium was organised by the Metals Group of the Materials Research Society of India and co-sponsored by the Asian Office of Aerospace Research and Development, US Air Force. C.V.Sundaram, Chairman, Metals Group of the Materials Research Society of India noted in his introductory remarks that the progress towards the development of intermetallics to application has been 'exasperatingly' slow. Robert Cahn of the University of Cambridge, UK, in a keynote lecture provided a historical perspective on early research on 'weakly ordered' alloys and examples of more recent work on 'strongly ordered' compounds.

The symposium featured ten overview talks. Dan Miracle of Air Force Wright Laboratory addressed both science-based issues and engineering concerns related to the metallurgy of NiAl. He noted that NiAl could be significantly strengthened to the levels of several superalloys and, in any case, possessed a variety of attractive properties such as low density, high thermal conductivity and excellent environmental resistance. Nevertheless, a reasonable combination of toughness and high temperature strength continues to be an elusive goal, and the current approach emphasises design methodologies which can use low toughness materials with adequate factors of safety. The alloy system presents large opportunities for research in fabrication (casting technology), strengthening and deformation behaviour. Vinod Sikka presented the status of Fe_3Al and Ni_3Al from an applications engineering perspective with emphasis on work at the Oak Ridge National Laboratory, USA. He stressed specially the excellent corrosion and sulphidation resistance of the Fe_3Al base alloys and their cost benefits in relation to stainless steel. High temperature strength levels continue to be of concern and strong environmental effects on ductility at room temperature have been identified. It appears unlikely that Ni_3Al base alloys will find aeroengine applications, but their excellent carburisation resistance and high temperature strength lend them to applications in heat treatment furnaces, automotive vehicles and in manufacturing. Cost is a key concern in these applications. A summary of the work on Ti_3Al and Ti_2AlNb base alloys at the Defence Metallurgical Research Laboratory, with emphasis on the key issues that limit application, was provided by Ashok Gogia. He described microstructural and compositional effects on primary creep in some detail emphasising that this area has not received adequate attention

in the literature, although the major contribution to creep strain arises from transient behaviour. Other drawbacks relate to oxygen induced dynamic embrittlement over the range of application temperatures and poor burn resistance, a feature common to all titanium alloys with the exception of TiAl. Patrick Martin from Rockwell Science Centre, USA described the current status on TiAl. Successful engine ground tests at General Electric of cast Ti-47Al-2Cr-Nb offer a positive outlook for application of an intermetallic alloy in rotating applications. His talk emphasised issues related to thermomechanical processing of these alloys as they affect microstructure evolution and emphasised the need to refine the processing-microstructure-property envelope in full scale ingot conversion and the development of low cost processing approaches for potential automotive applications.

Work on molybdenum disilicide was covered in two presentations : Dallis Hardwick summarised the physical metallurgy of $MoSi_2$ and described in some detail Rockwell Science Centre work on this material, while Sadananda from the Naval Research Laboratory, USA concentrated on the effect of SiC particulates and whisker composites with $MoSi_2$ on creep resistance. While composite microstructure can be designed to provide creep resistance much superior to superalloys and approaching ceramic-ceramic systems at temperatures greater than 1000°C, it was clear that low temperature toughness must be enhanced, perhaps utilising ductile phase toughening or laminate design. Two approaches to the stability of intermetallics were described by Raju from Indira Gandhi Centre for Atomic Research, India, and Ashok Singh from the Defence Metallurgical Research Laboratory, India. Raju described the variety of semi-empirical approaches using alloy theory parameters and concluded with his own work in developing a new structure map parameter which offers advantages over the Pettifor scheme. Ashok Singh offered a description of a variety of thermodynamic approaches including CVM to developing ground state structures in ordered hexagonal systems. Tassaduq Khan of ONERA, France described the nature and substance of European Community Schemes such as BRITE-EURAM, COST and CEASI as related to intermetallic programmes and provided a summary of ONERA work on B2 alloys based on the Ti-Al-Nb system and approaches to TiAl alloy development.

A variety of contributed presentations from various research groups in India covered work on phase transformations in TiAl, Zr_3Al and B2-DO_3 systems, powder metallurgy and ingot approaches to processing Fe_3Al and Al_3Ti alloys, the mechanical behaviour of alloys of the Ti_3Al-Nb system and oxidation resistance of Ti_3Al alloys. A dominant metallurgical theme that emerged from the symposium was the dichotomy that exists between high temperature strength and low temperature ductility in the

intermetallics. Alloying and processing schemes that enhance the one, almost inevitably do so at the expense of the other.

A hard copy of the material presented in the overview talks is provided in two volumes. The first covers the aluminides : NiAl, TiAl, Ni_3Al, Fe_3Al and Ti_3Al. The second presents the material on European intermetallic activities, molybdenum disilicide and its composites, the ground state structures and stability of intermetallics.

March, 1994

D. Banerjee
Defence Metallurgical Research Laboratory
Hyderabad-500258, India

PROGRAMME

Saturday, Feb 5

9.00 - 9.45	Intermetallics - The Fashionable and Unfashionable *R.W.Cahn* University of Cambridge, U.K.
9.45 - 10.15	Coffee
10.15 - 11.00	Understanding and Applications of NiAl *D.B.Miracle* Air Force Wright Laboratory, USA
11.00 - 11.45	Technology and Applications of Ni_3Al-Based Materials *V. K. Sikka* Oakridge National Laboratory, USA
11.45 - 12.05	Development of Cold Rolling Texture in Ni_3Al (B) *R.K.Ray* Indian Institute of Technology, Kanpur, India
12.05 - 12.25	Recrystallisation of Ni_3Al *A.K.Jena* Indian Institute of Technology, Kanpur, India
12.25 - 1.15	Lunch
1.15 - 2.00	Promise versus Reality for High Temperature Applications of Gamma TiAl - A Perspective *P.L.Martin* Rockwell Science Centre, USA
2.00 - 2.20	Diffusional Composition Invariant and Coarsening Phase Transformations in TiAl Base Alloys *R.V.Ramanujam* Bhabha Atomic Research Centre, Bombay, India
2.20 - 2.40	Interface Modification in two phase ($\gamma+\alpha_2$) Titanium Aluminide by Ternary Additions and their Deformation Behaviour *S.R.Singh* National Metallurgical Laboratory, Jamshedpur, India
2.40 - 3.15	Tea
3.15 - 4.00	The Stability of Intermetallics *S.Raju* Indira Gandhi Centre for Atomic Research, Kalpakkam, India
4.00 - 4.45	Ground State Structures of Ordered Alloys *S. Lele & A.K.Singh* Banaras Hindu University, Varanasi, India

Sunday, Feb 6

9.00 - 9.45	European Intermetallic Activities - Contributions from France *T. Khan* ONERA, France
9.45 - 10.15	Coffee
10.15 - 11.00	Composites Based on Molybdenum Silicide : Progress and Prospects *D.A. Hardwick* Rockwell Science Centre, USA
11.00 - 11.45	Technology and Applications of Fe_3Al-based materials *V.K. Sikka* Oak Ridge National Laboratory, USA
11.[illegible] - 12.05	Preparation and Processing of Fe_3Al Strips through Ingot and P/M processing *S.Bagchi, S.Suwas, S.Bhargava, S.Sangal and R.K.Dube* Indian Institute of Technology, Kanpur, India
12.05 - 12.25	Anti-phase boundaries in B2 and DO_3 Fe-Al-X (X=Cr, Mo) and $DO_{22}/L1_2$ Al-Ti-Ni Intermetallics *Ujjwal Prakash* Defence Metallurgical Research Laboratory, Hyderabad, India
12.25 - 12.45	Improvement in Mechanical Properties of Iron Aluminides *Aruna Bahadur* National Metallurgical Laboratory, Jamshedpur, India
12.45 - 2.00	Lunch
2.00 - 2.45	The Metallurgy of Ti_3Al Base alloys *A.K.Gogia* Defence Metallurgical Research Laboratory, Hyderabad, India
2.45 - 3.05	Low Cycle Fatigue Behaviour of Ti-27Al-15Nb *P.N.Singh, B.K.Singh, C.Ramachandra and V.Singh* Banaras Hindu University, Varanasi, India
3.05 - 3.25	High Temperature Oxidation of Ti_3Al *T.K.Roy, R.Balasubramaniam and A.Ghosh* Indian Institute of Technology, Kanpur, India
3.25 - 4.00	Tea
4.00 - 4.20	Morphological Features of Ti_3Al Based Intermetallic Alloys Prepared by Reaction Synthesis *M.Sujata, S.Bhargava and S.Sangal* Indian Institute of Technology, Kanpur, India
4.20 - 4.40	Phase Transformations in Zr_3Al Base Alloys *R.Tewari, G.K.Dey and P.Mukhopadhyay* Bhabha Atomic Research Centre, Bombay, India

3. European Intermetallics Activities and Contribution from France

T.Khan and S.Naka
ONERA, France

European Intermetallics Activities and Contribution from France

T. KHAN and S. NAKA

ONERA, 29, Av. de la Division Leclerc, 92322 Châtillon, France

February, 5-6, 1994, Hyderabad

Principal European Programme on Advanced Materials

1) BRITE/EURAM

2) COST 513

3) CEASI

ONERA

BRITE - EURAM

TABLE 1: GENERAL CONDITIONS FOR PARTICIPATION

Type 1 Projects
(up to 90% of available budget)

Industrial Applied Research -indicative Priority Themes -precompetitive and collaborative -potential for exploitation -subsequent development expected	Size	-10 Man-years minimum -1 to 3 Mecu
	Duration	-2 to 4 years
	Partners	-at least 2 independent industrial enterprises -at least 2 different Member States

Type 2 Projects
(7% to 10% of available budget)

Focused Fundamental Research -upstream of Type 1 -indicative Priority Themes -precompetitive and collaborative -industrial endorsement from 2 Member States	Size	-10 Man-years minimum 0.4 to 1 Mecu
	Duration	-2 to 4 years
	Partners	-at least 2 organisations -at least 2 different Member States

Co-ordinated Activity

Co-ordination of related research -within Technical Areas -in different Member States -co-ordination activities only -proposers must justify activity	EC Funding	-up to 100% coordination costs -not research costs
	Partners	-as appropriate
	Calls	-continuous

COST

PRESENTING NEW PROPOSALS & JOINING PROJECTS
Flow Charts on Project Procedures

*** Proposing a new project**
Preparation phase

Individual Scientists or Research Institutes or industry have a proposal for a new project

↓

Technical Committee of New Project Group for approval

↓

Initiator of project with COST Secretariat formulate de final MoU

↓

Committee of Senior Officials approves the MoU

↓

National Authorities sign the MoU

↓

New COST project

CONTACTS

⇓

COST Secretariat

Council of the EC (GD D1)
170 rue de la Loi Charl. 9/47
B. 1048 Brussels
Tél. 32 2 234.73.62 or 66.44

*** Joining a project as a member**
Project already under execution

Individual Scientists or Research Institute or Industry

↓

Cost Secretariat

↓

Project Management Committee

↓

National Authority

↓

New member of a COST project

Joining the project

Concerted European Action on Structural Intermetallics (CEASI)

The objectives of CEASI are:

(i) To provide a framework by which a coherent pre-competitive research programme can be carried out in the field of structural intermetallic-based alloys.

(ii) To ensure that there is a balance of activity in the research programme across the whole discipline, so that European intermetallics research goes ahead in a well-balanced way.

(iii) To supply, process and circulate reference materials to participants.

(iv) To develop a fundamental understanding of alloying behaviour in intermetallics so that alloy development and alloy processing is on a firm basis for future application to the manufacture of components.

CEASI Project Management

EEC Brussels

Industrial Advisory Board

Thien (Siemens) and Smarsly (MTU) Germany

Lasalmonie (SNECMA) and Brun (Turbomeca) France

Regis (ENEL) Italy

Harkegard (ABB) and Harkegar (Sulzer) Switzerland

Kearns (IMI) and Postans (Rolls-Royce) UK

Project Management Board

Loretto (IRC Birmingham, UK)
Project coordinator

Khan (ONERA, Paris, France)
Coordinator of processing and applications

Sauthoff (Max Planck Düsseldorf, Germany)
Coordinator for property assessment

Plus seven elected members from CEASI

Participant groups

Alloy development

Material properties

Material Processing

Joining

French Programmes

- Various Intermetallics
  - Ti_3Al (or Ti_2AlNb) and Nb-base intermetallic alloys
  - TiAl
  - NiAl
  - Ni_3Al
  - Fe_3Al and FeAl
  - Two-phase A2+B2 alloys

- Interaction with the industry
  SNECMA, Turboméca, Aérospatiale Dassault and SEP

- Formation of a GDR (research group)
  Basic research oriented

ONERA

Ti_3Al or Ti_2AlNb base

High Niobium Titanium Aluminides (B2)

Increasing Nb beyond 25 at.%

Advantages

- Fine microstructure ⇒ yield stress
- Higher amount of ordered β phase
  - ⇒ high temperature strength
  - ⇒ room temperature ductility
- Orthorhombic phase ⇒ room temperature ductility

Disadvantage

- High density (> 5)

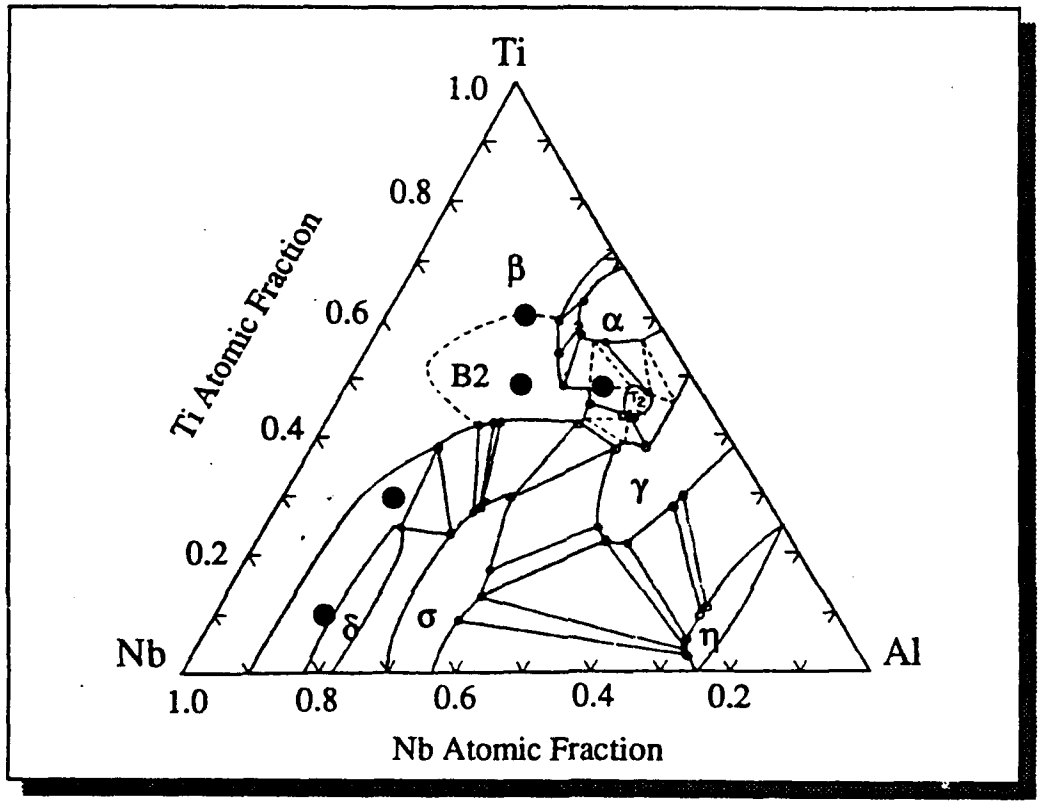

Compositions of alloys of the Ti-Al-Nb system in which the B2 phase was observed. They were plotted in the phase diagram of the Ti-Al-Nb system (Isothermal section at 1200°C), proposed by Perepezko et al. (1990).

TiAl base

Activities on $\gamma+\alpha_2$ TiAl-based Alloys

- Effect of various alloying elements
  - Fe, Cr, Mo, W : γ-stabilizing
  - Nb, Ta : α_2-stabilizing
  - $\Rightarrow$ Development of new compositions
- Thermomechanical processings (isothermal forging and extrusion)
  - e.g. on $Ti_{48}Al_{48}Nb_2Cr_2$
  - • microstructure control before and after processing
- Casting : e.g. on TiAl-Fe-V-B
  - • good castability : addition of B? and/or β-phase solidification?
- Powder metallurgy
  - • reactive sintering
- Basic study on phase transformation mechanisms

ONERA

Key Metallurgical Factors

ONERA

- Alloy composition
  - Some beneficial alloying elements identified
- Microstructure
  - Lamellar structure : most frequent and important
  - Various microstructures resulting from various phase-transformation sequences
- Texture
  - Solidification texture often extremely pronounced
- Porosity
  - Macro- and micro-porosities
- Impurity level
  - High purity materials required
- Machining
  - Good quality of the surface

Texture

During solidification

$L \Rightarrow \alpha$

α : HCP $\Rightarrow$ crystal growth direction // [0001]

During the formation of lamellar structure

$\alpha \Rightarrow \alpha+\gamma \Rightarrow \alpha_2+\gamma$ (or $\alpha \Rightarrow \alpha_2 \Rightarrow \alpha_2+\gamma$)

$(0001)\alpha$ or α_2 // $\{111\}\gamma$

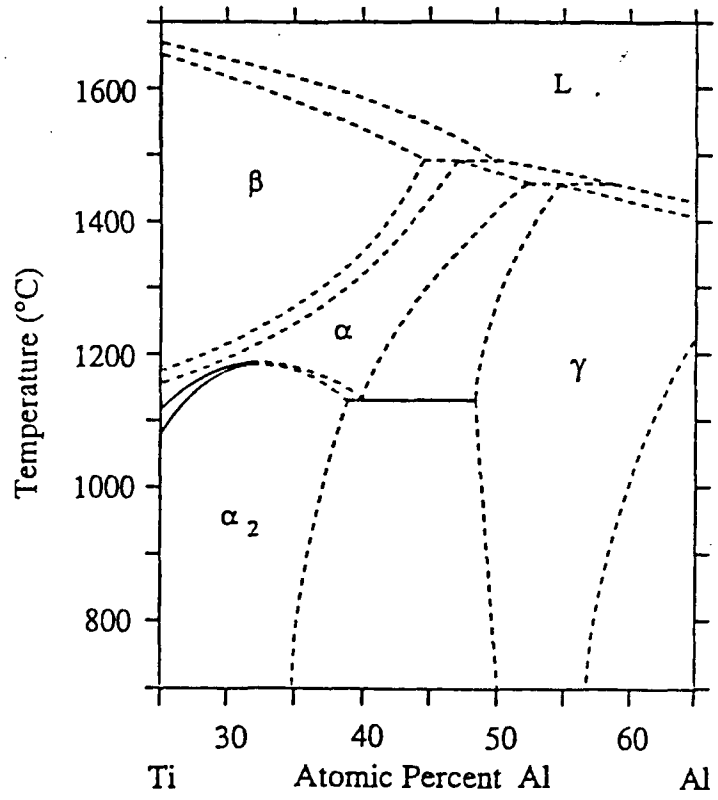

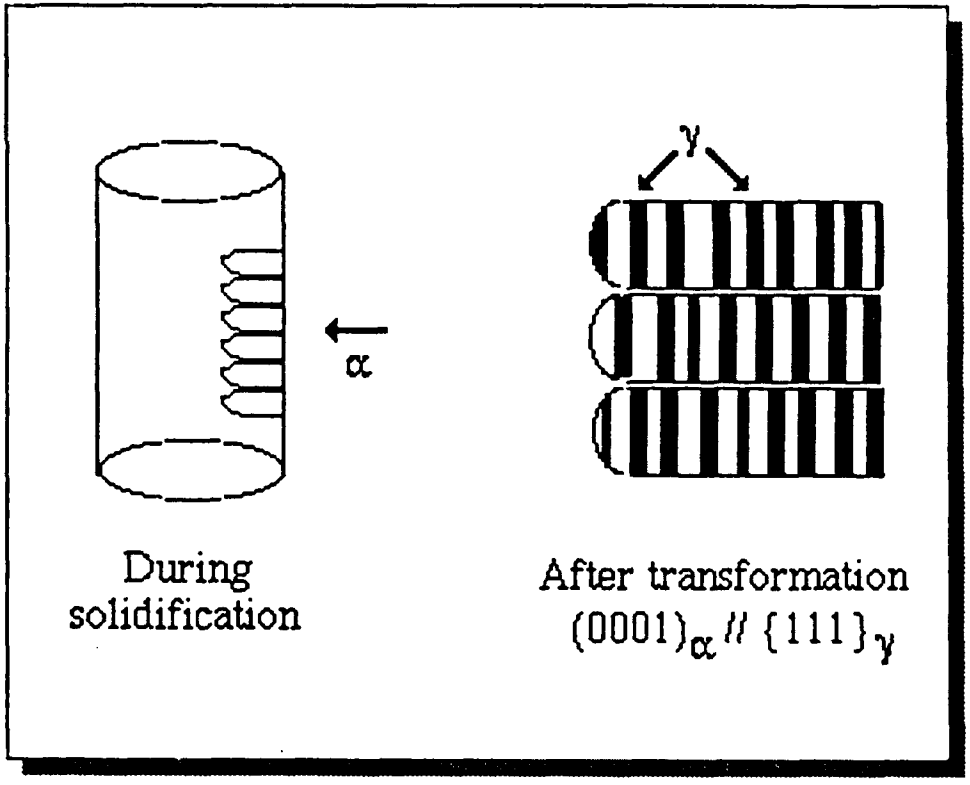

ONERA

– **Acute solidification texture**
⇒ scattering of mechanical properties data

✓ **Future directions in the research activities related to the texture**

- Investigate the evolution of texture during thermal and thermomechanical processings
  ⇒ reduce or suppress the solidification texture

⇒ • Identify suitable alloy compositions to promote solidification with the β phase ⇒ weaker texture

Phase transition sequence

$L \Rightarrow \beta + \gamma$ (interdendritic)

$\Downarrow$ 12 variants due to the Burgers

$\Downarrow$ relationship : $\{110\}_\beta // \{0001\}_\alpha$

$\Downarrow$ $\langle 111 \rangle_\beta // \langle 1120 \rangle_\alpha$

α

$\Downarrow$

$\gamma + \alpha_2 + \beta$ (B2)

Impurity level

- Atom-probe analysis of the two phases γ and α_2 in the lamellar structure
  Maximum solubility of oxygen is very low : ≈300at.ppm.
- Tentatitive explanation of the origin of a better ductility
  of $\gamma+\alpha_2$ two-phase alloys, compared to γ single-phase alloys
  - in two-phase alloys : oxygen is "dispersed" throughout the α_2 lamellae.
  - in single phase : oxygen is strongly segregated in the form of oxide.

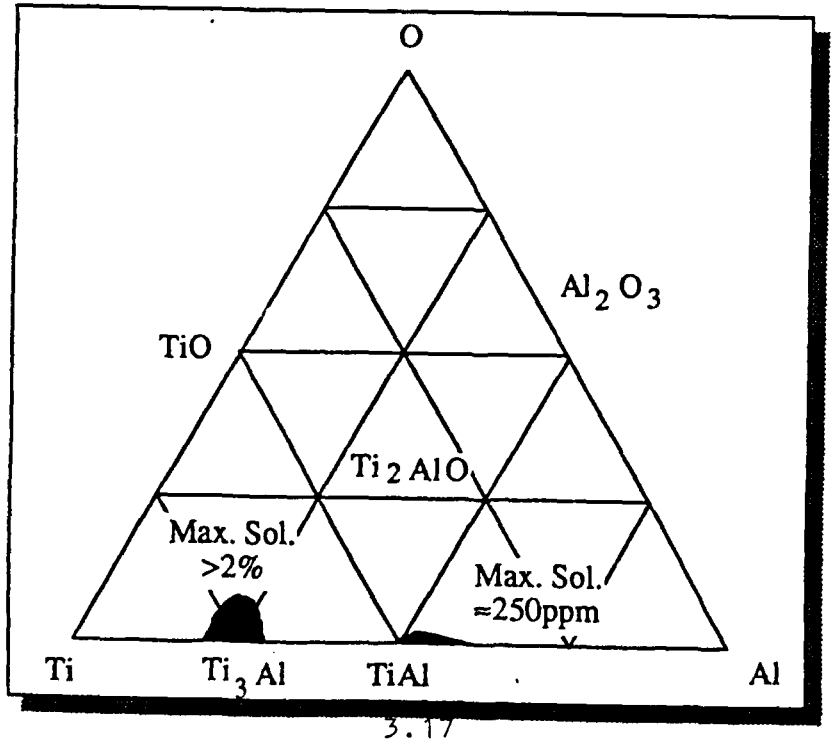

ONERA

ONERA

Composition determined by Chemical Analysis and Volume Fraction of the α_2 Phase estimated through TEM.

	$Ti_{52}Al_{48}$	$Ti_{54}Al_{46}$
Aluminium	47.9±0.4 at.%	46±0.4 at.%
Titanium	51.8±0.4 at.%	53.7±0.4 at.%
Oxygen	2290±230 at.ppm	2505±250 at.ppm
$F_{v\ \alpha 2}$	10±5%	30±5%

Oxygen Concentrations as well as Volume Fractions of the α_2 Phase deduced from Atom-Probe Analysis.

	$Ti_{52}Al_{48}$		$Ti_{54}Al_{46}$	
	α_2	γ	α_2	γ
Oxygen	19200±1200 at.ppm	230±70 at.ppm	8100±700 at.ppm	200±100 at.ppm
$F_{\alpha 2}$	10 ±2%		29 ±7%	

ONERA

Future directions in the research activities related to the impurity level

- Prepare two phase $\gamma+\alpha_2$ alloys
  containing less than 250 at.ppmO ($\approx$ 100 wt.ppmO)

- Investigate their deformation behaviour
  $\Rightarrow$ change in plastic deformation mechanisms ?
  mobility of 1/2<110] and 1/2<112] dislocations
  $\Rightarrow$ influence on macroscopic ductility ?

ONERA

Various transformation modes

1) Formation of lamellar structure

- $\alpha \Rightarrow \alpha+\gamma \Rightarrow \alpha_2+\gamma$ or $\alpha \Rightarrow \alpha_2 \Rightarrow \alpha_2+\gamma$
- nature of various interfaces :

  γ/α_2 and γ/γ (TB's, ODB's, PTB's, MB's)

2) Massive transformation

- $\alpha \Rightarrow \gamma$
- numerous defects and interfaces including γ APB's

3) Discontinuous coarsening of γ lamellae

- solute redistribution through moving grain boundaries ?
- mechanism less clarified

Two-Phase Systems

ONERA

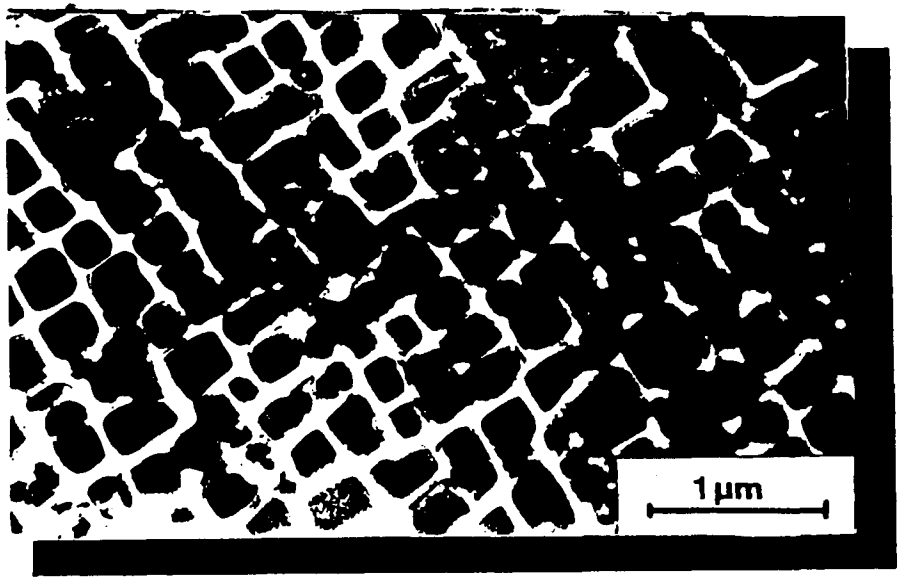

γ-γ' microstructure

(Ni-base superalloy)

Two-phase A2+B2 (or A2+$L2_1$) alloys

(γ-γ' type microstructure)

Nb base, Ta base, Fe base etc.

- A2 matrix containing a high volume fraction of sencond "compatible" phase

  "compatible" : crystal structure and lattice parameter

- Solid state decomposition of solid solution into two phases
- Empirical "Crystallo-chemical approach

  evaluate both size effect and chemical interaction

ONERA

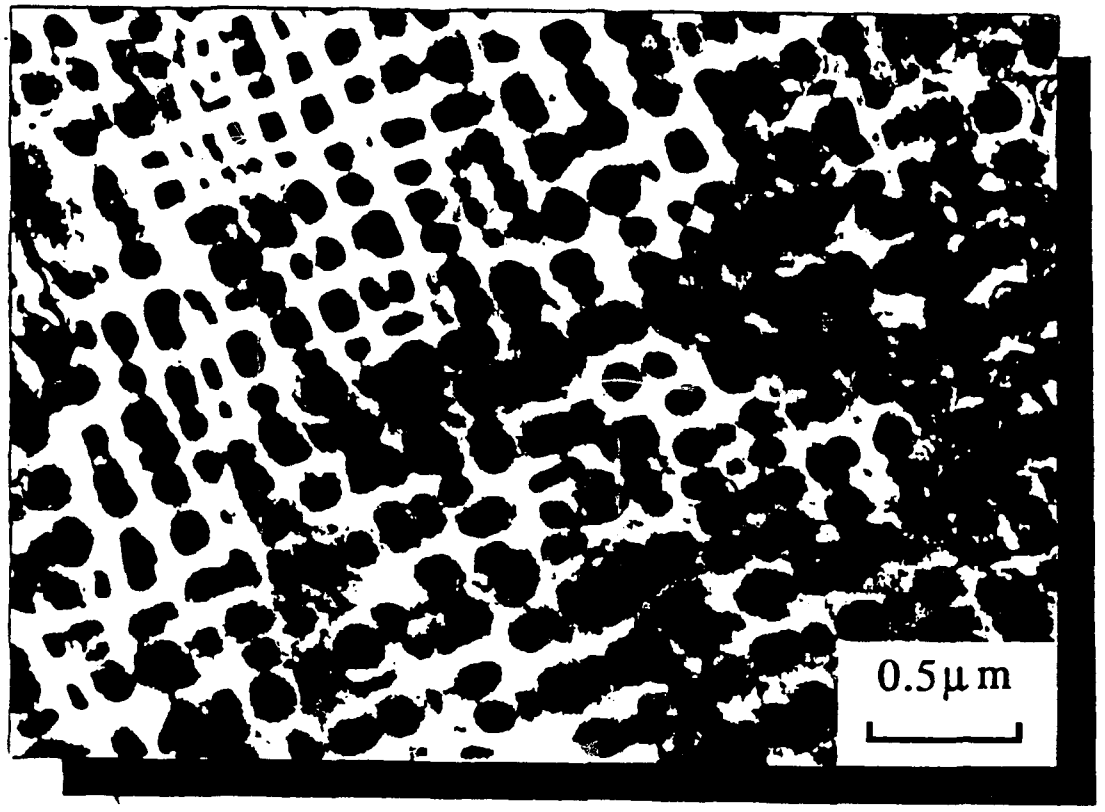

Two-phase ($A2+L2_1$) microstructure

observed in $Fe\text{-}Ni_2AlTi$ system

ONERA

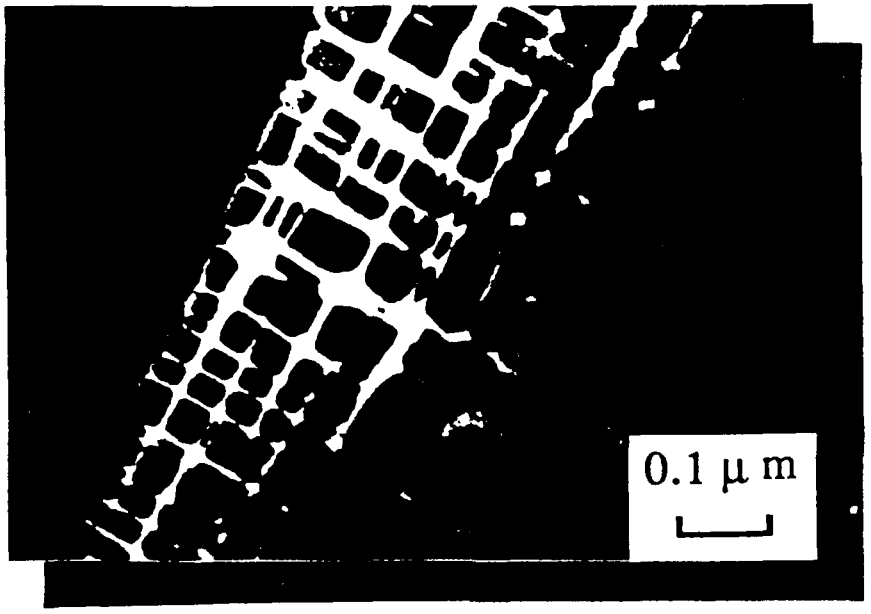

Two-phase (B2+A2) microstructure observed in a Ta-base alloy (Ta-Ti-Zr-Al-Nb-Mo system)

ONERA

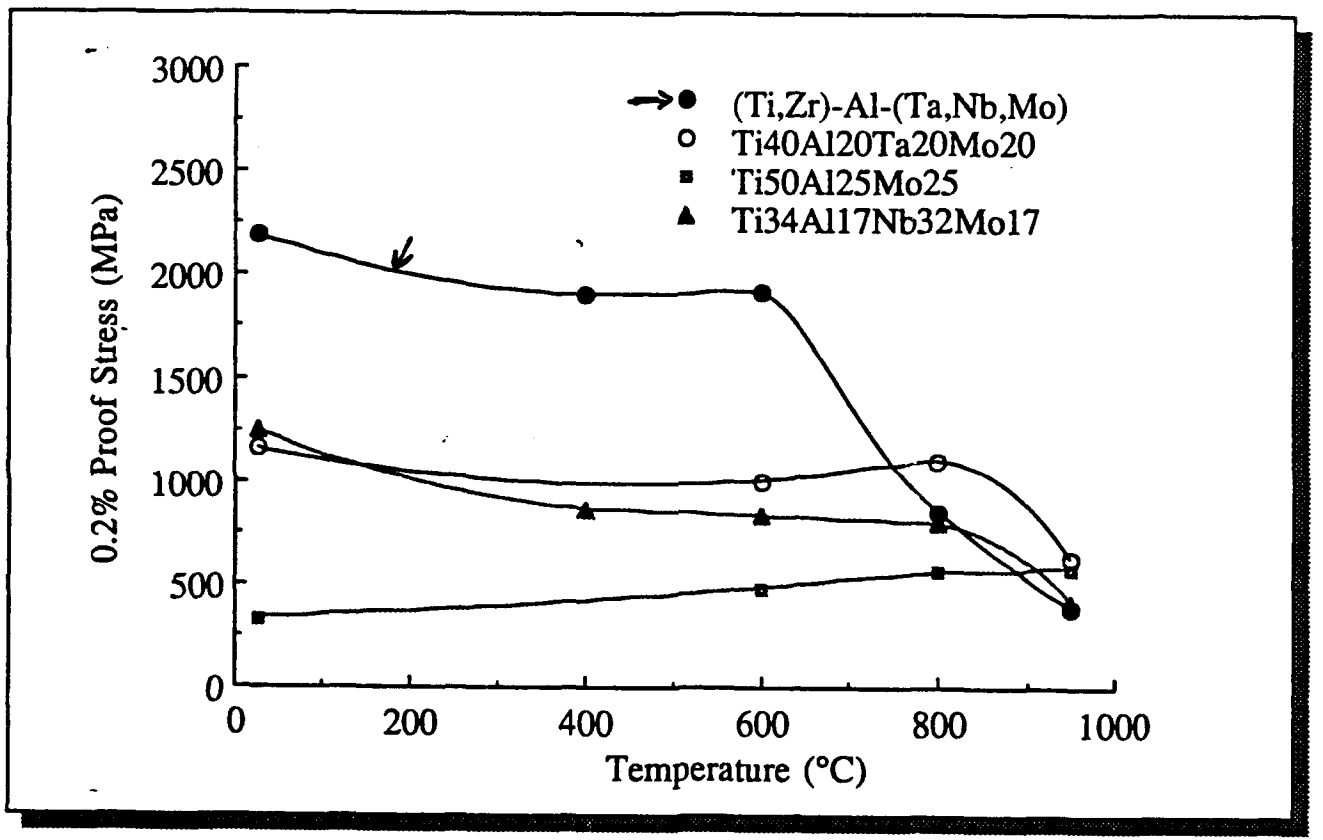

Temperature dependence of yield stress for various alloys : Comparison made between a two-phase B2+A2 alloy and three single-phase B2 alloys

NiAl base

ONERA

Travaux ONERA

ductilité

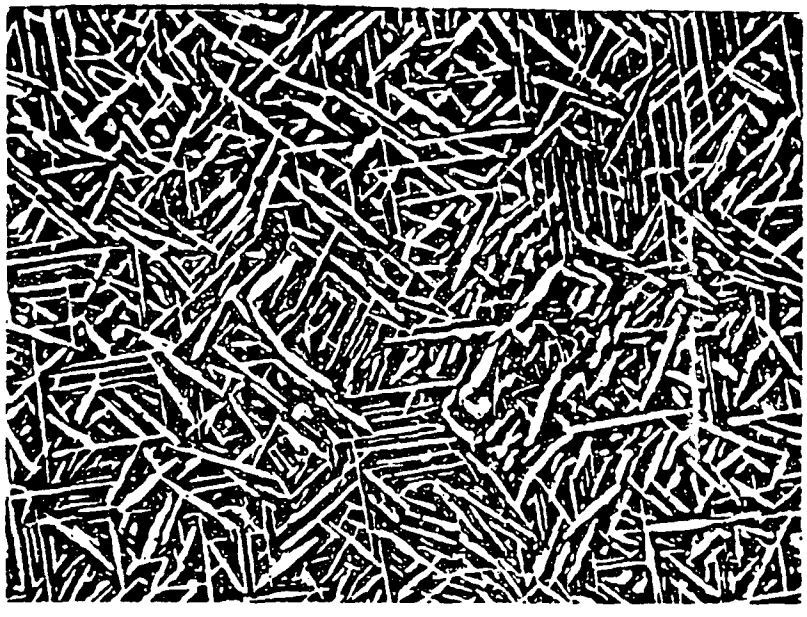

20µm

durcissement

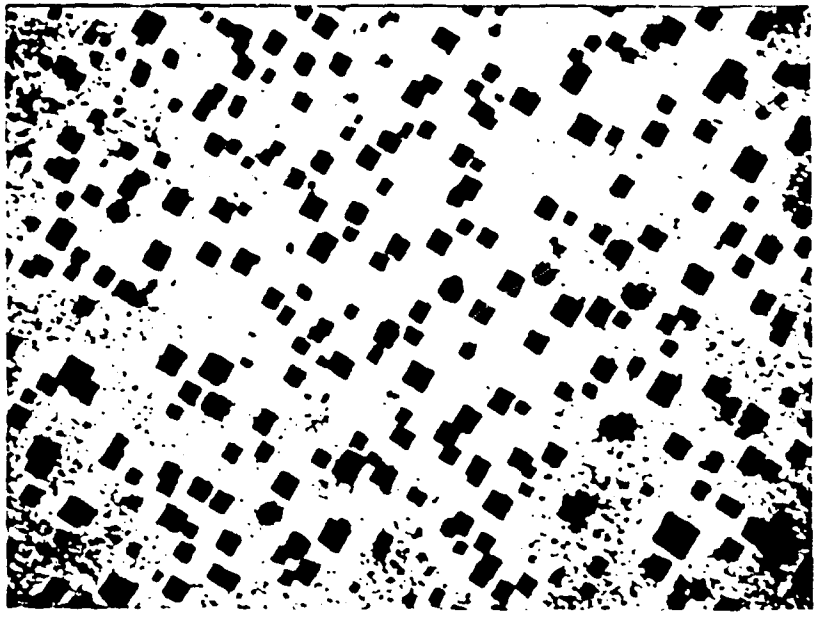

100nm

4. Microstructure, Processing and Properties of $MoSi_2$

D.A. Hardwick
Rockwell Science Centre, USA

Microstructure, Processing and Properties of $MoSi_2$

D. A. Hardwick
Rockwell International Science Center

work supported by AFOSR

Rockwell International
Science Center

SUMMARY

Introduction	:	Historical Background Crystal Structure, Dislocations DBTT, Oxidation Silica as Impurity
RISC Work	:	Our AFOSR program Processing, Microstructure, Properties Comments on Future Directions
Composites	:	Bright Phase Ductile Phase Laminates Composite Design

Background of $MoSi_2$ Development

- Early NACA reports, R. A. Long and W. A. Maxwell; 1950 - 1952
  - Hot pressed PM material; <100% dense
  - Oxygen, carbon and grain size effects quantified
  - Hot tensile, hot compression, tensile creep and oxidation measured to at least 1300°C
  - Thermal shock resistance (under stress) of turbine blade shapes
- German work began in early 50's as well; Fitzer and students which has continued to the present time
  - Ductile phase (wire) composites with Ta and Nb
- Soviet reports beginning in mid 50's; Samsonov and coworkers on transition element silicides
  - Thermophysical properties
- SiC whisker composites work began in mid 80's in US; Carter, Gibbs, Petrovic (LANL)
  - Strength and toughness benefits

Los Alamos

Assessed Mo-Si Phase Diagram

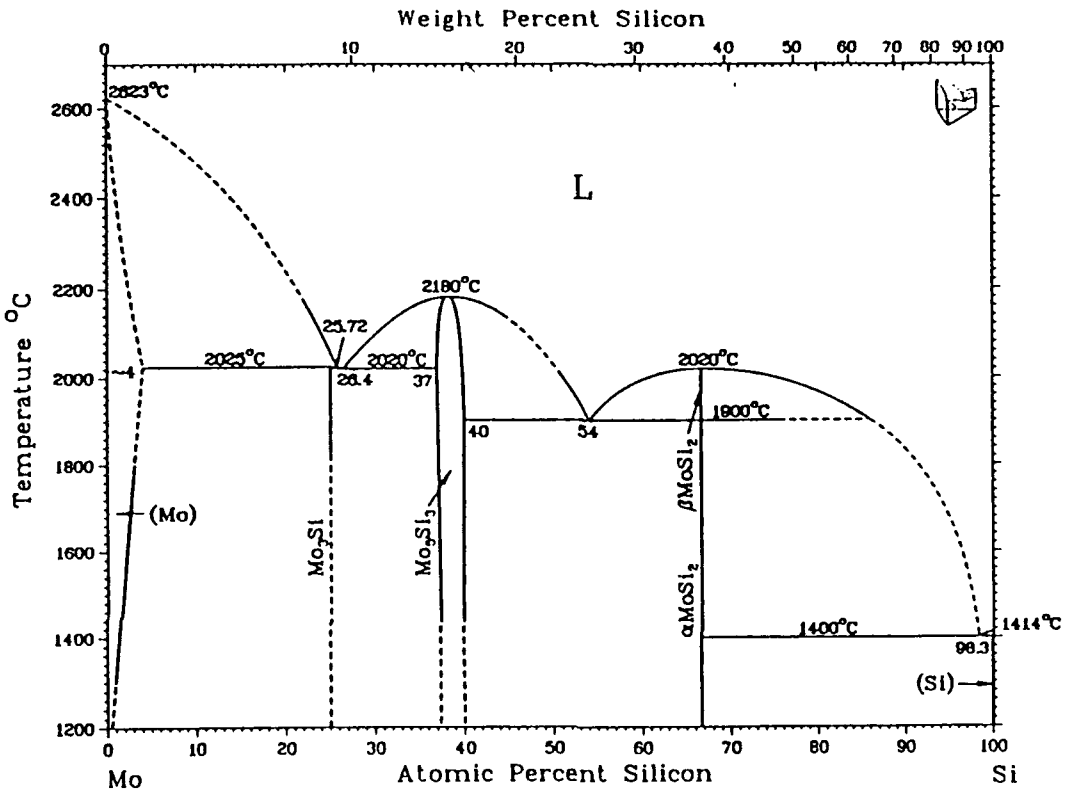

Mo-Si Crystal Structure Data

Phase	Composition, at.% Si	Pearson symbol	Space group	Struktur-bericht designation	Prototype
(Mo)	0	*cI*2	*Im*3*m*	*A*2	W
Mo_3Si	25	*cP*8	*Pm*3*n*	*A*15	Cr_3Si
Mo_5Si_3	37.5	*tI*38	*I*4/*mcm*	$D8_m$	W_5Si_3
$\alpha MoSi_2$	66.7	*tI*6	*I*4/*mmm*	$C11_b$	$MoSi_2$
$\beta MoSi_2$	66.7	...	$C6_22$	...	...
(Si)	100	*cF*8	*Fd*3*m*	*A*4	C (diamond)

Dislocations in $MoSi_2$

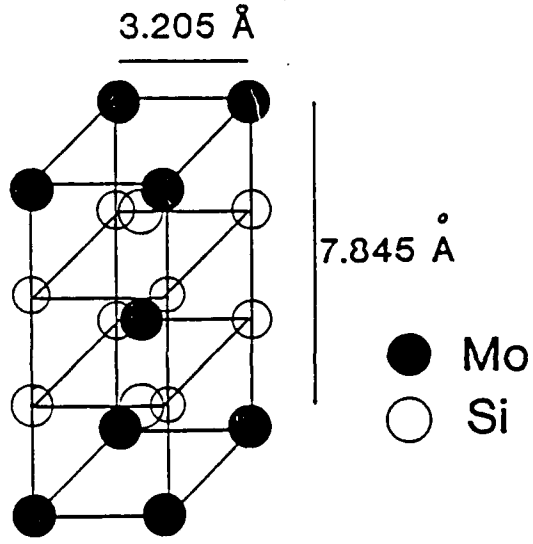

TABLE 1. Possible Burger's vectors and slip planes for $MoSi_2$

b	Slip planes	b (Å)	$\lvert b\rvert^2$ (Å^2)
✓⟨100⟩	{0kl} 011, 001	3.21 •	10.24
✓⟨110⟩	{110}, {111}	4.54	20.61
✓(1/2){111}	✓{101}, {110}✓	4.53 •	20.56
[001]	{100}, {110}	7.85	61.62
(1/2)[001]	{110}, {013}	2.62	6.84
✓(1/2)⟨331⟩	{110}, {013}✓	7.86	61.78
(1/6)⟨331⟩	{110}, {013}	2.61	6.82

Boldt et al. Mat. Sci. Eng A

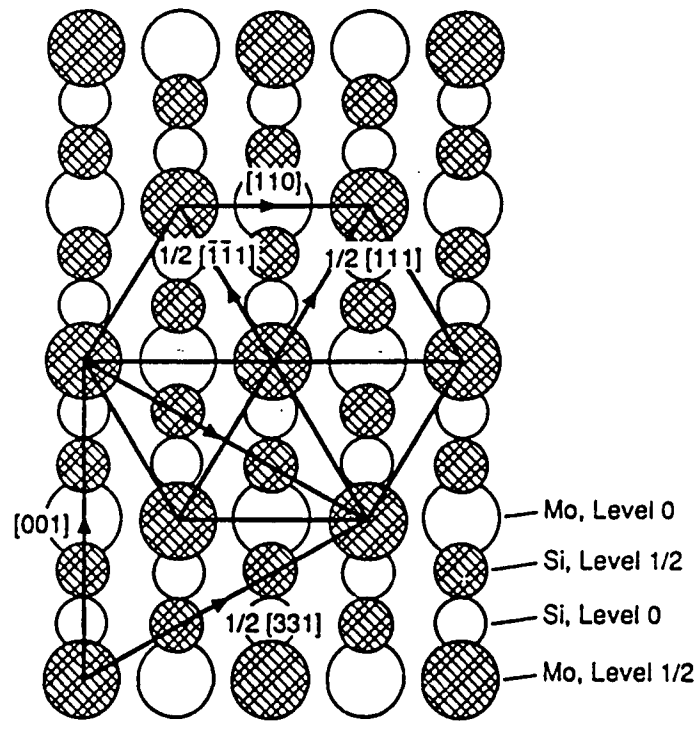

Mitchell et al. Mat. Sci. Eng A

Compression of Single Crystals

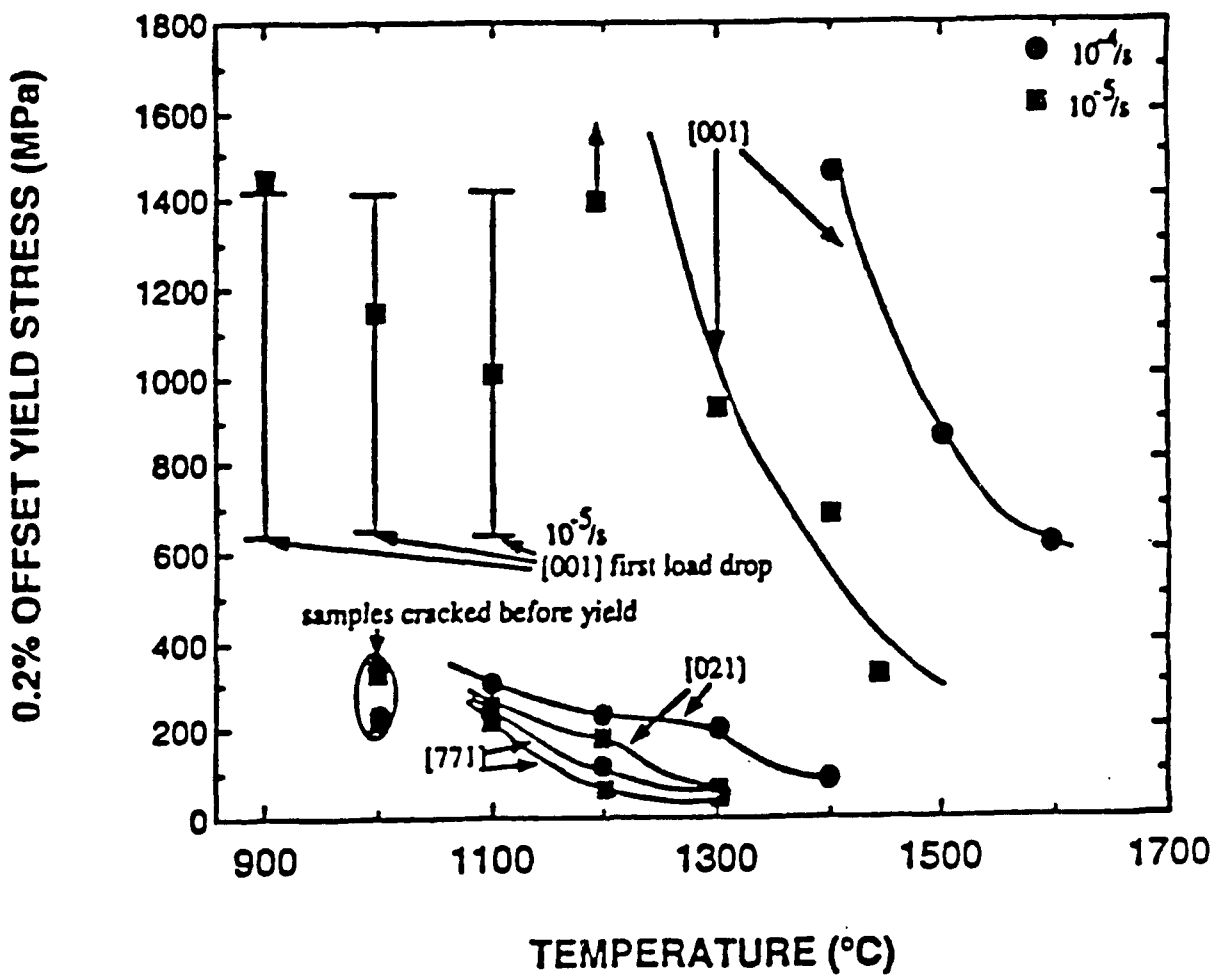

Ductile to Brittle Transition Temperature

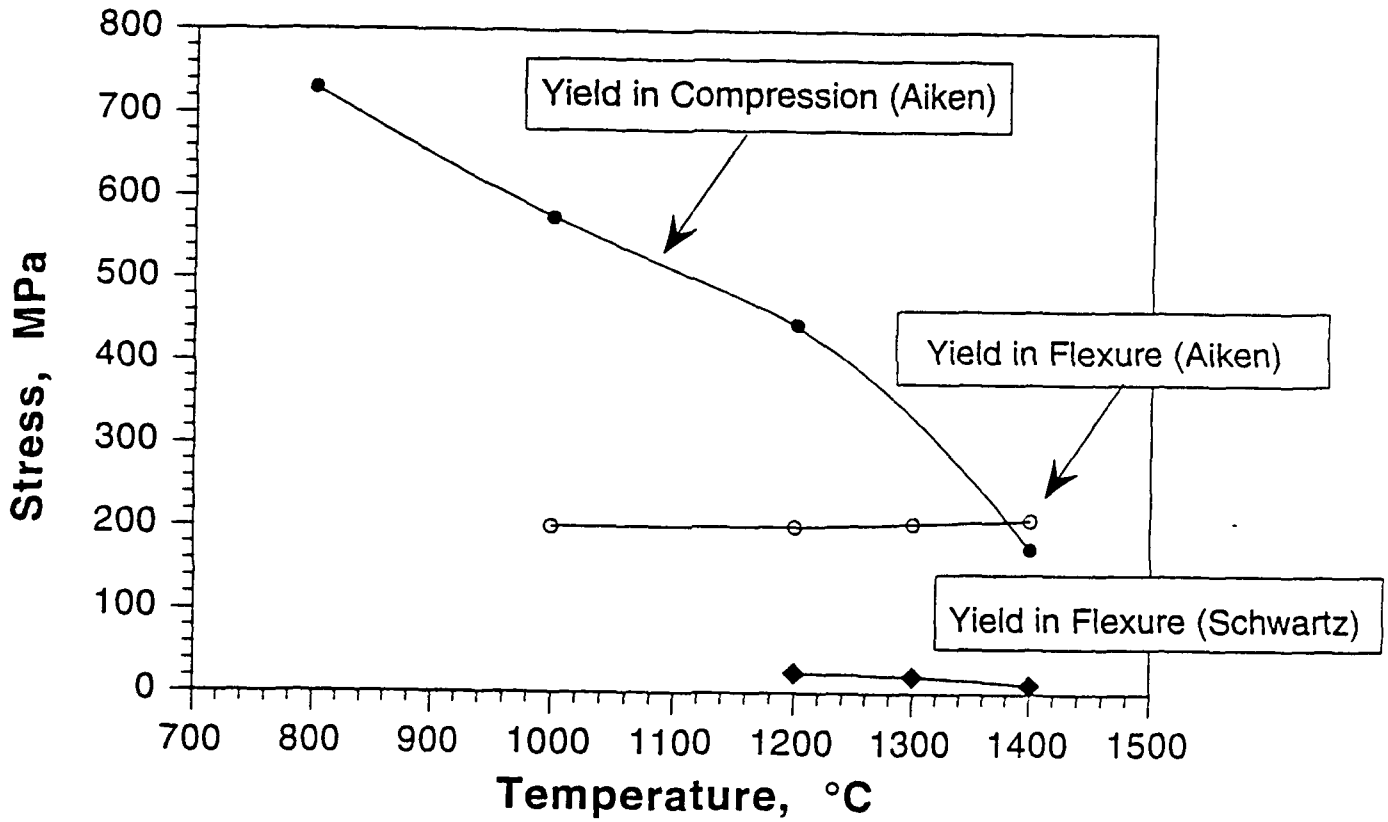

Accelerated Oxidation of $MoSi_2$

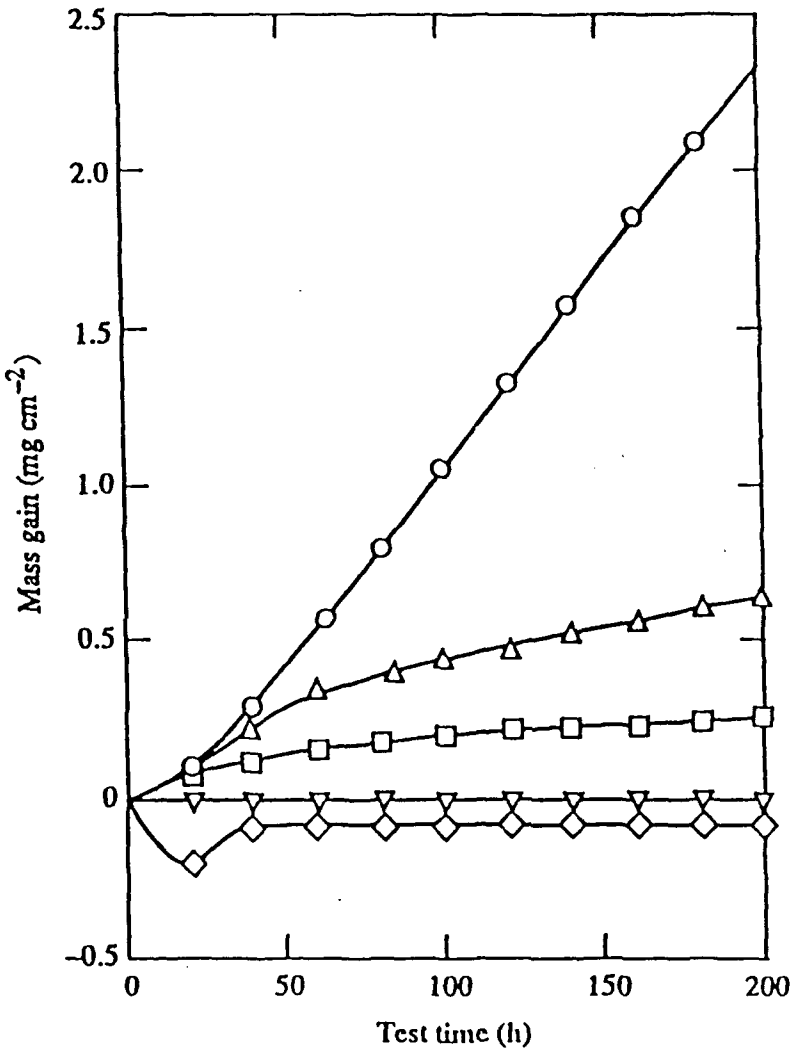

Fig. 2—Cyclic oxidation of CERAC $MoSi_2$ samples in dry air as a function of temperature: (□) 400 °C; (△) 450 °C; (○) 500 °C; (◇) 550 °C; and (▽) 600 °C.

Meschter, Met. Trans. 6 (1992)

Schematic of Reactive HIP Process

SC-0575-C

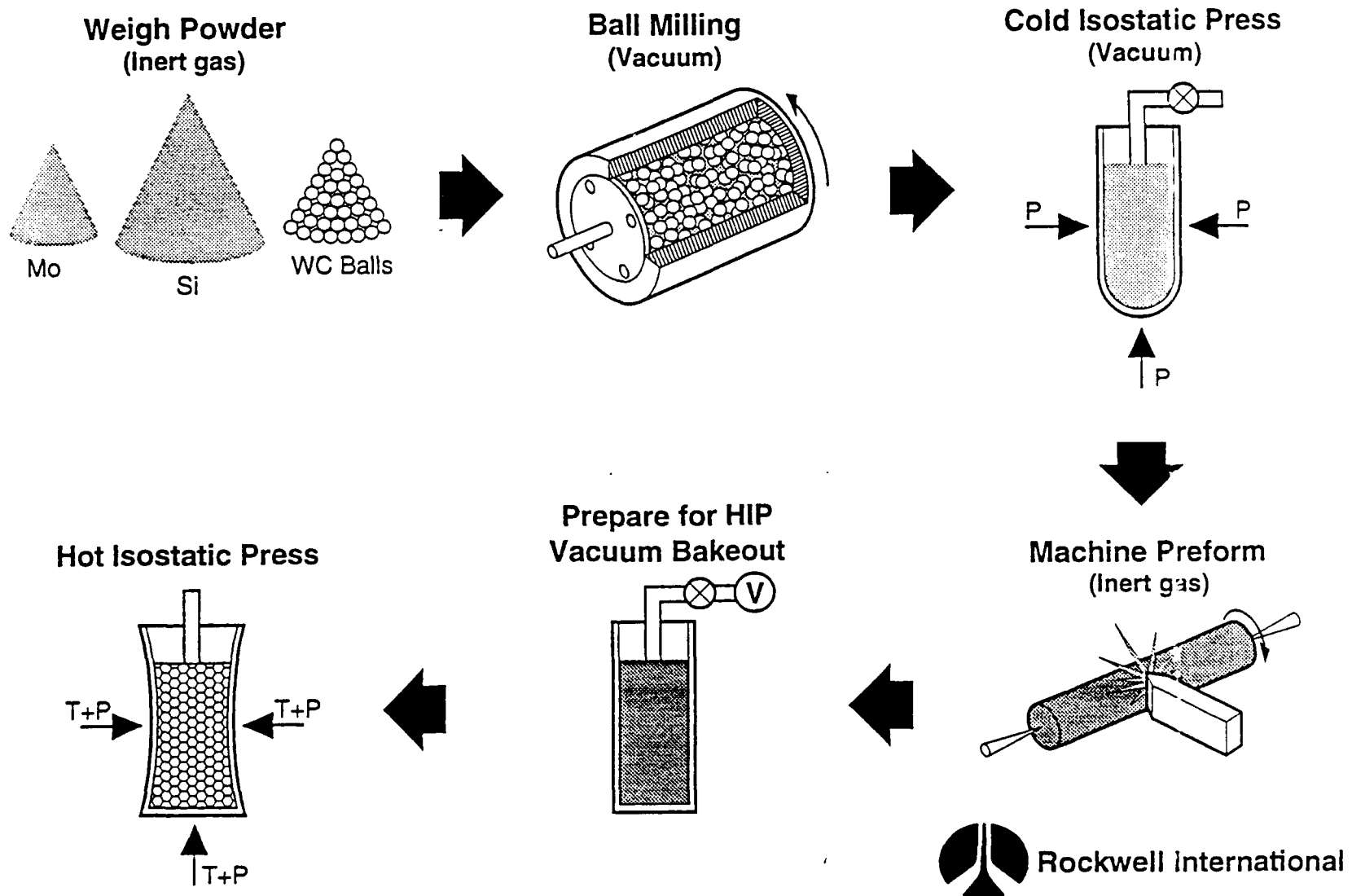

Rockwell International
Science Center

Characteristics of Our Processing Route

- Begins with high purity elemental powder, not commercial silicide powder
- All processing steps in inert environment ⇒ clean but tedious
- Produces a 98% dense material with large grain size and low silica content
- Densification assisted by adiabatic heating - low external heat input
- Probably not a feasible process for large scale production

Microstructure of $MoSi_2$; as processed

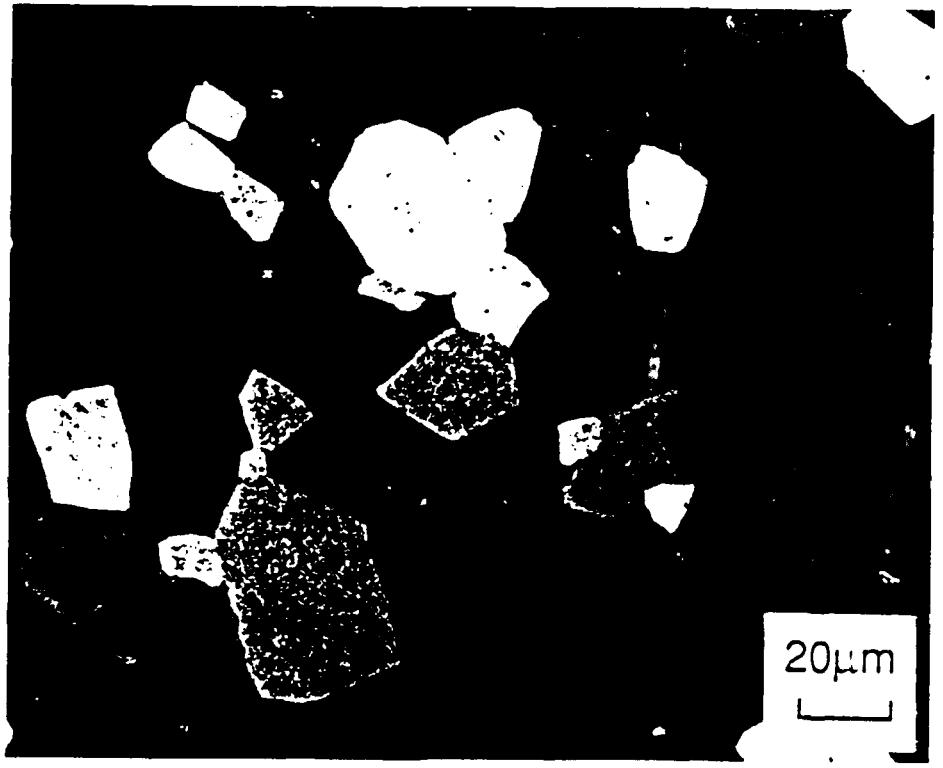

Optical - polarized light

Rockwell International
Science Center

Experimental Parameters

- Compression of right circular cylinders
  Simple specimen geometry, simple stress state (cf. bending)
- Temperature range: 1200°C - 1400°C (likely range for DBTT)
- Strain rate range: 10^{-3} sec^{-1} to 10^{-5} sec^{-1}
- Strain range: 1% to 50% (average strain ≈10%)
- Flow stress, influence of stress on microstructure, deformation mechanisms

Rockwell International
Science Center

Effect of Microstructure on Mechanical Properties

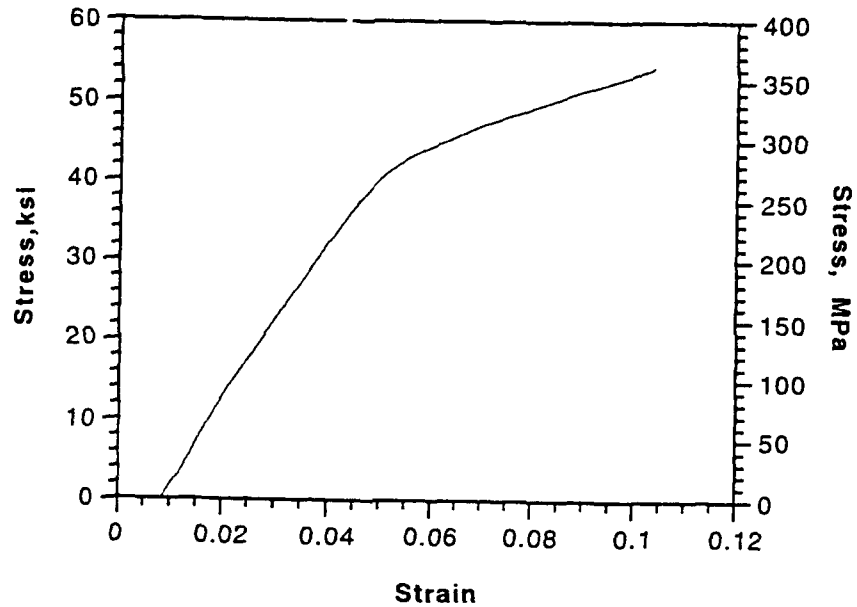

Stress-Strain Curve for Sample Tested at 1200°C and 10^{-5}/sec

Non-linearity in Stress-Strain Curve ≡ Plastic Deformation ?

Yield Stress vs Temperature and Strain Rate

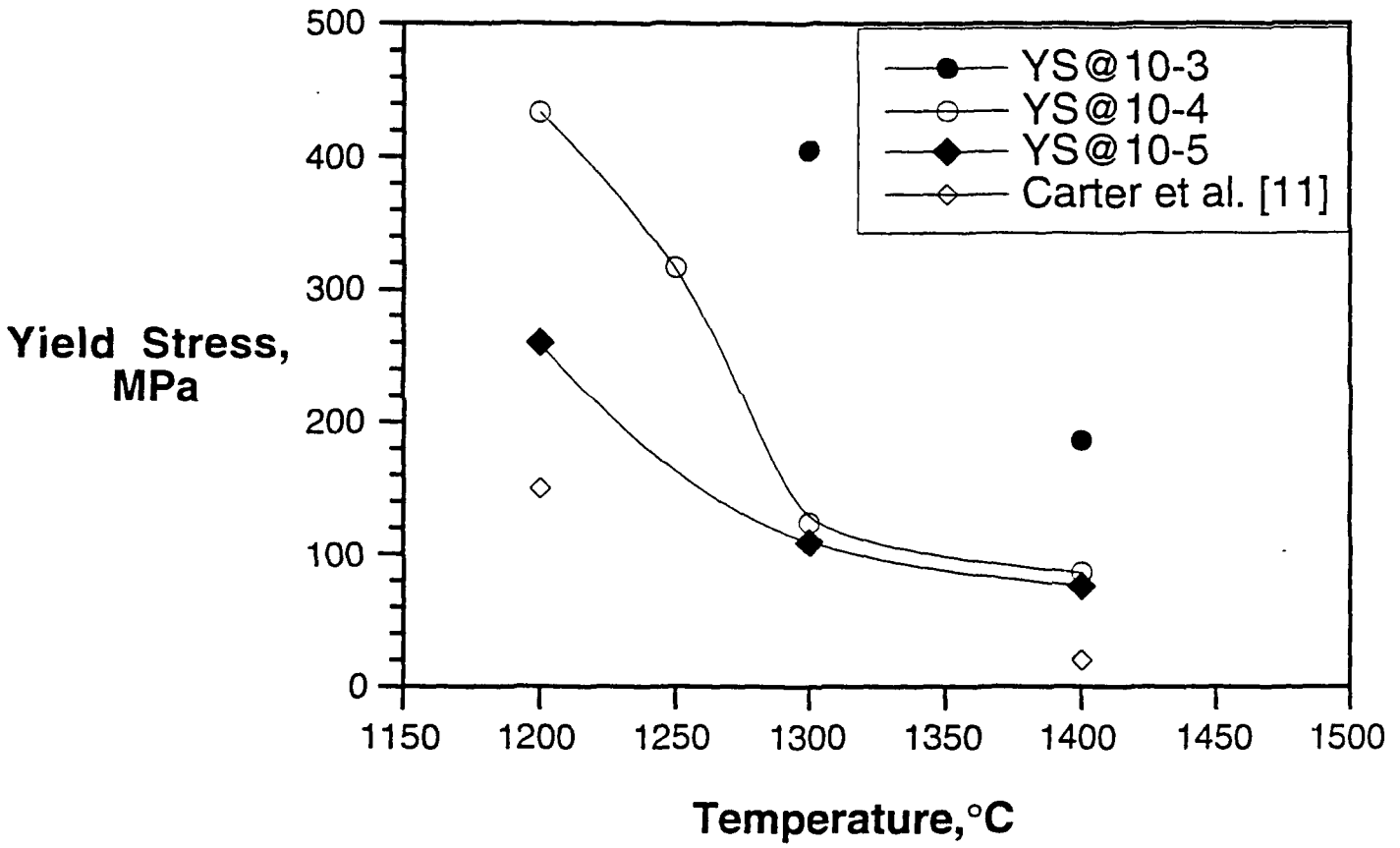

Rockwell International
Science Center

Microstructure of $MoSi_2$ deformed at $10^{-4}sec^{-1}$

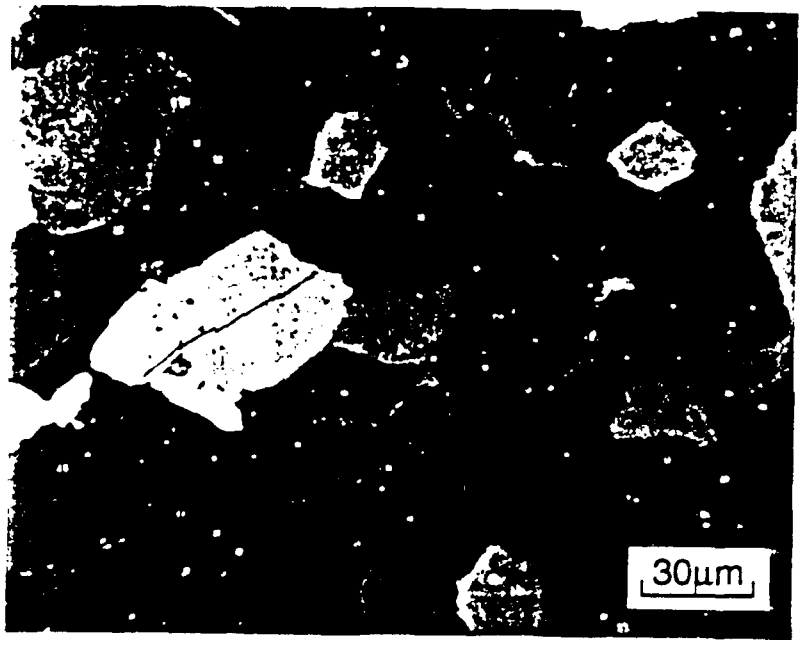

1250°C; $\varepsilon_\tau = 0.087$

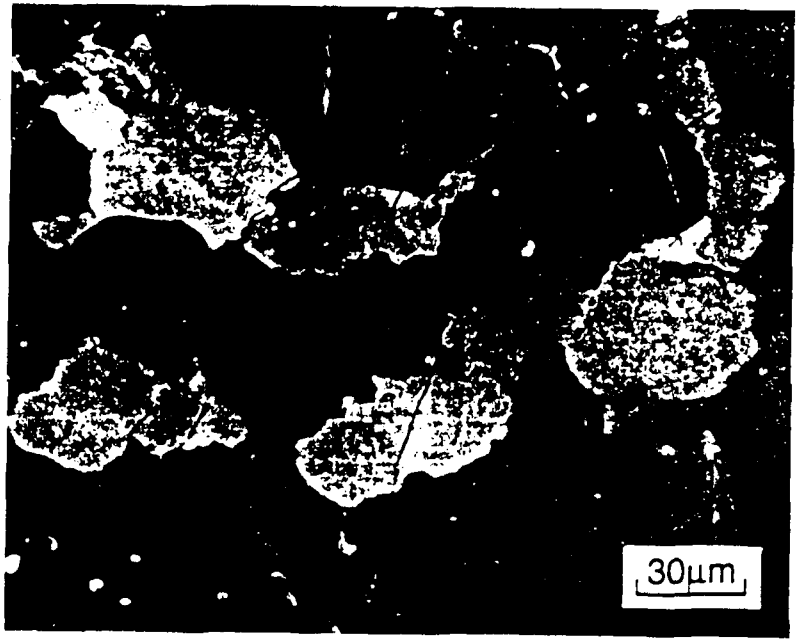

1300°C; $\varepsilon_t = 0.15$

Rockwell International
Science Center

Microstructure of $MoSi_2$ deformed at $10^{-4}sec^{-1}$

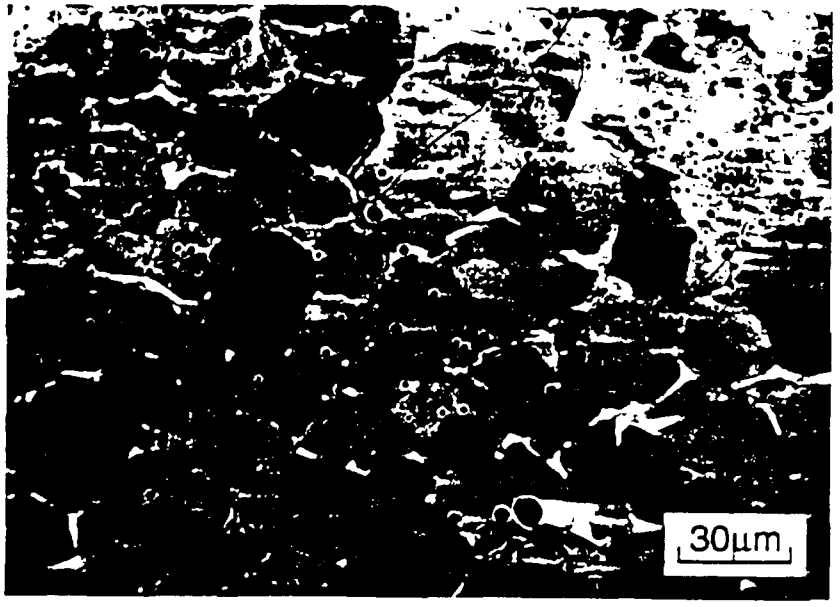

1250°C; $\varepsilon_\tau = 0.087$

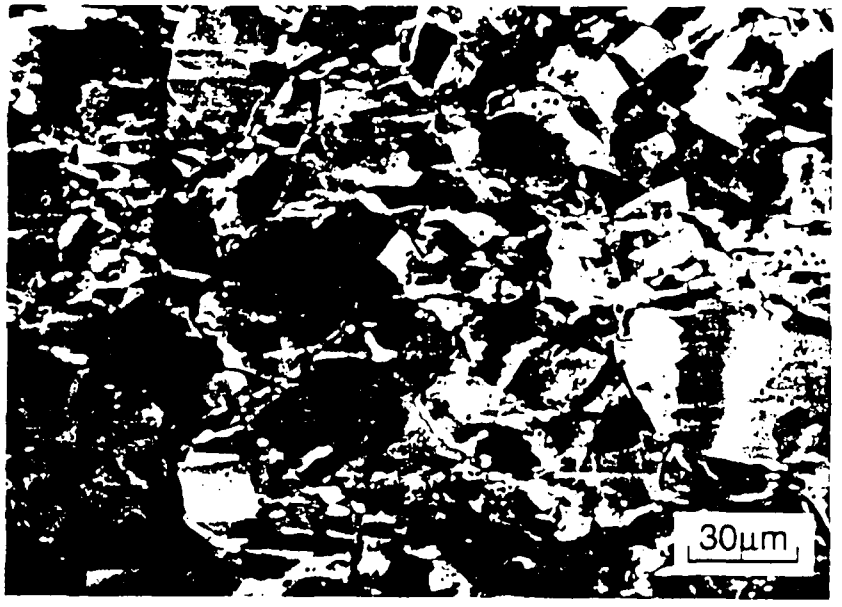

1300°C; $\varepsilon_t = 0.15$

Rockwell International
Science Center

Large Strain Deformation of $MoSi_2$

1 cm

$\varepsilon = 0.5$ / T= 1300° / $\dot{\varepsilon} = 1 \times 10^{-5} sec^{-1}$

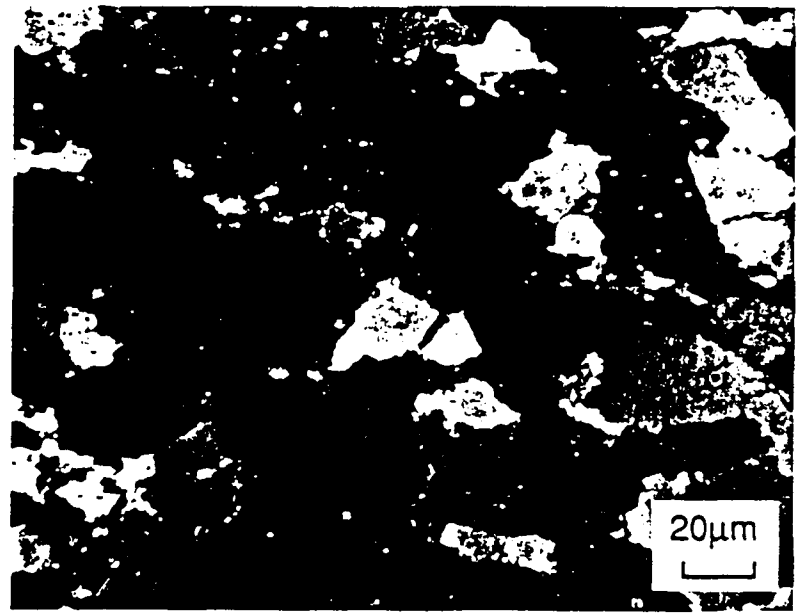

Optical - polarized light

Microstructure of $MoSi_2$; $e_t = 0.57$ at 1300°C and $10^{-4}sec^{-1}$

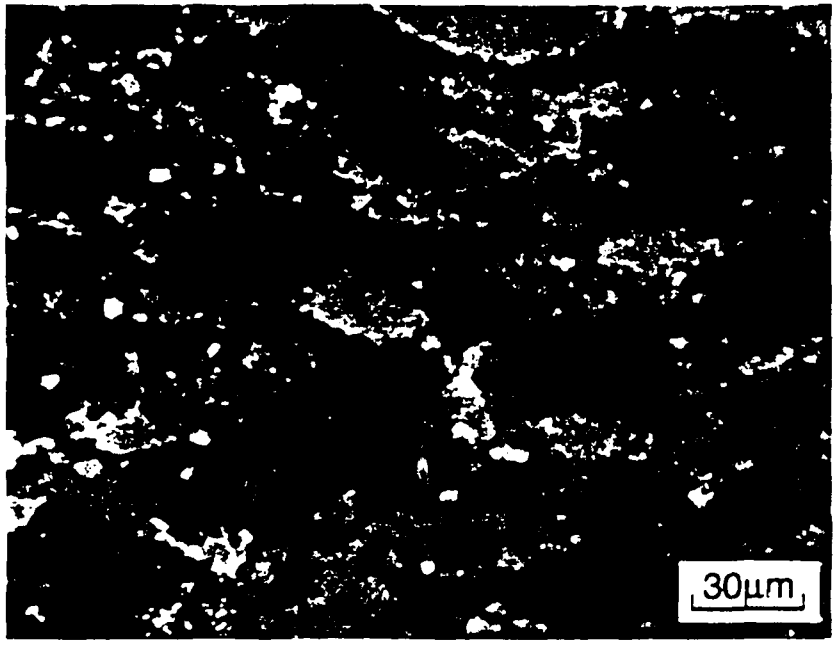

Optical - polarized light

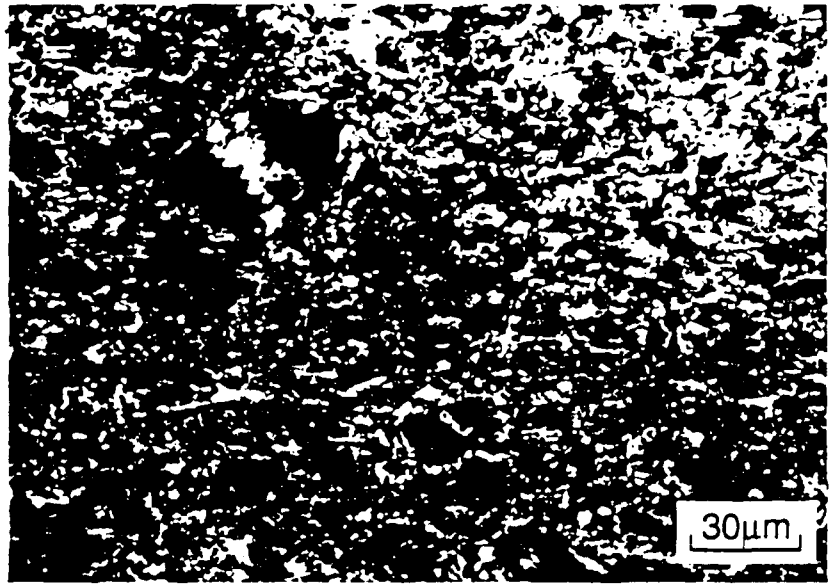

SEM - backscatter contrast

Rockwell International
Science Center

Dislocations in $MoSi_2$ strained at $10^{-4}sec^{-1}$

$\varepsilon_t = 0.16$; T = 1300°C

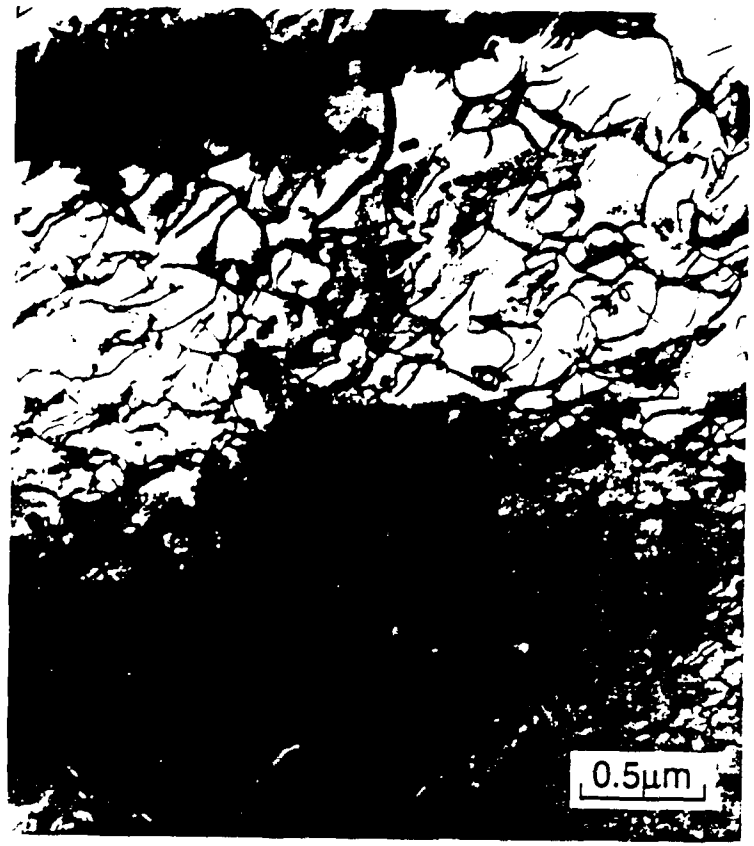

$\varepsilon_t = 0.14$; T = 1400°C

Rockwell International
Science Center

Implications for Future Work

- Reduce CRSS of hardest orientations by alloying - must be done in single crystals
- Alloying to promote additional slip systems - altering the crystal structure
- Directional solidification to enhance "soft" orientations
- Additions of benign second phase to reduce grain size - decrease slip length so that initial cracks are not catastrophic

  Additions of C or rare earths would have combined effect of producing second phase while scavanging oxygen
- Silica should be avoided - it does promote a fine grain size but, in high concentrations, enhances grain boundary sliding. This is one way to avoid microcracking but not the best way!

Rockwell International
Science Center

$MoSi_2$ Composite Approaches

- Brittle Whiskers or Rods: Increase in creep strength and toughness (via pull-out)
- Hard Dispersoids: Increase in flow stress and work hardening rate
- Ductile Phases (Particulates, Whiskers, Wires): Increase in low temperature toughness (via energy absorption) -- implied creep detriment (?)
- Laminates: Can dramatically affect both strength and toughness depending on the details of the interfacial properties

Strength and Toughness of $MoSi_2$ Composites

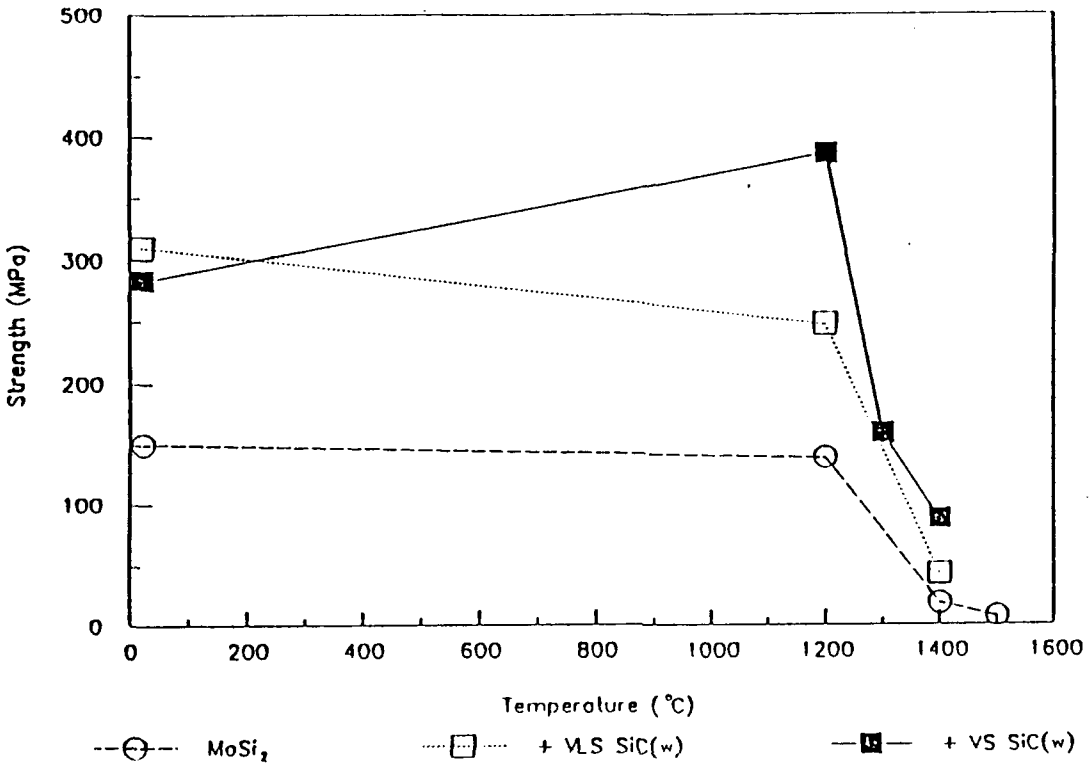

Table 1: Room Temperature Fracture Toughness Data

	$MoSi_2$	$MoSi_2$ + VLS SiC(w)	$MoSi_2$ + VS SiC(w)
$MPa \cdot m^{1}$	5.32	8.20	6.59
$(ksi \cdot in^{1})$	(4.84)	(7.45)	(5.99)

From: D. H. Carter, J. J. Petrovic, R. E. Honnell and W.Scott Gibbs, "Sic - $MoSi_2$ Composites", Los Alamos National Laboratory, LA-11577-MS, June 1989.

Strength of Molybdenum Disilicide

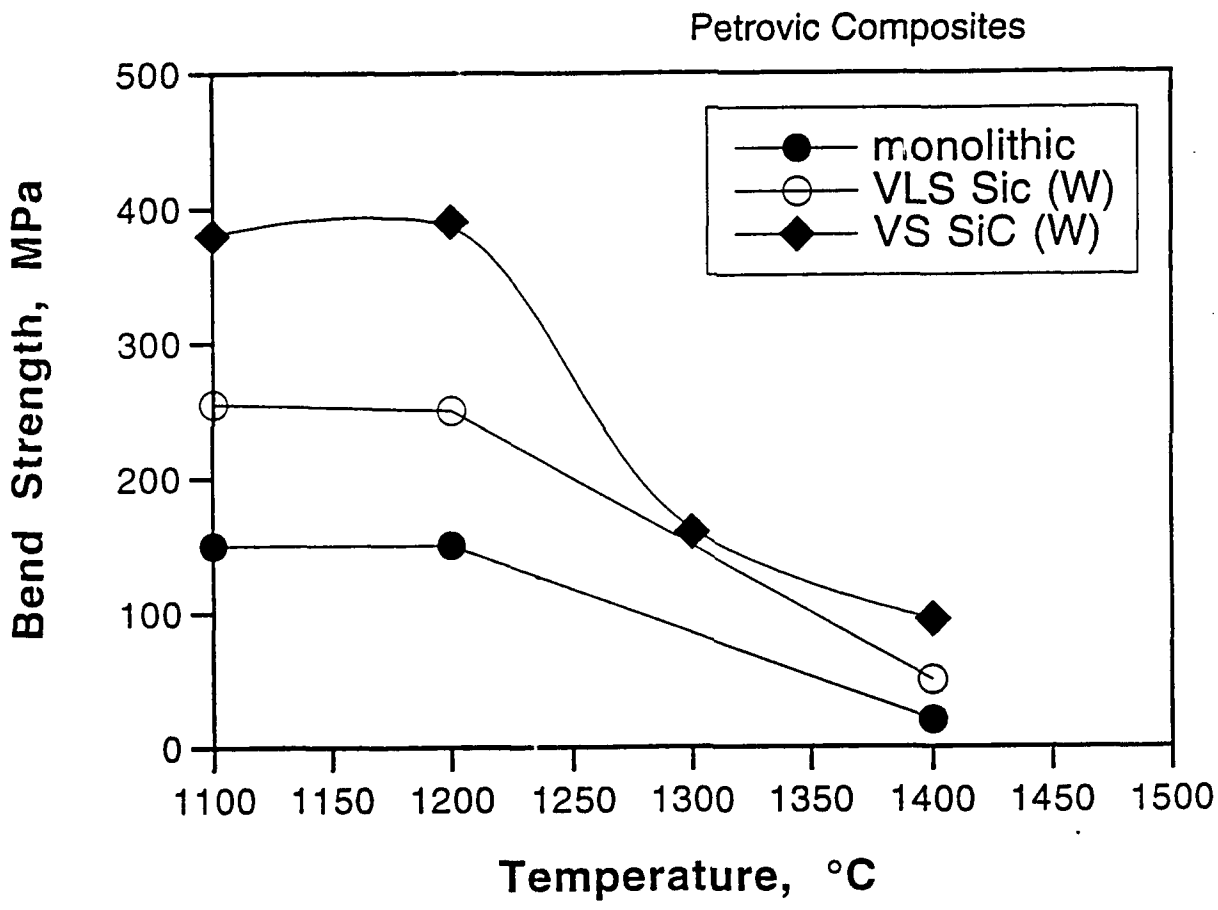

Strength of Molybdenum Disilicide

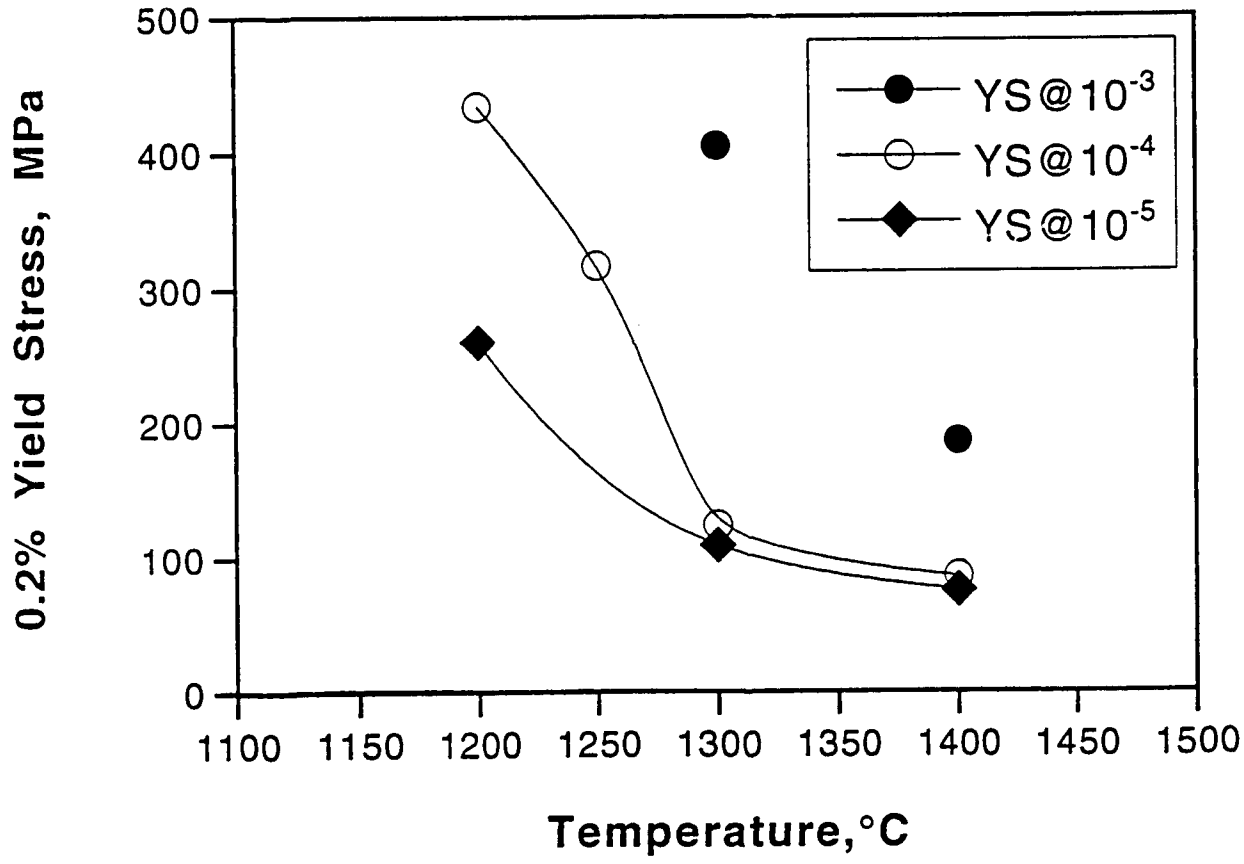

Toughness of Molybdenum Disilicide

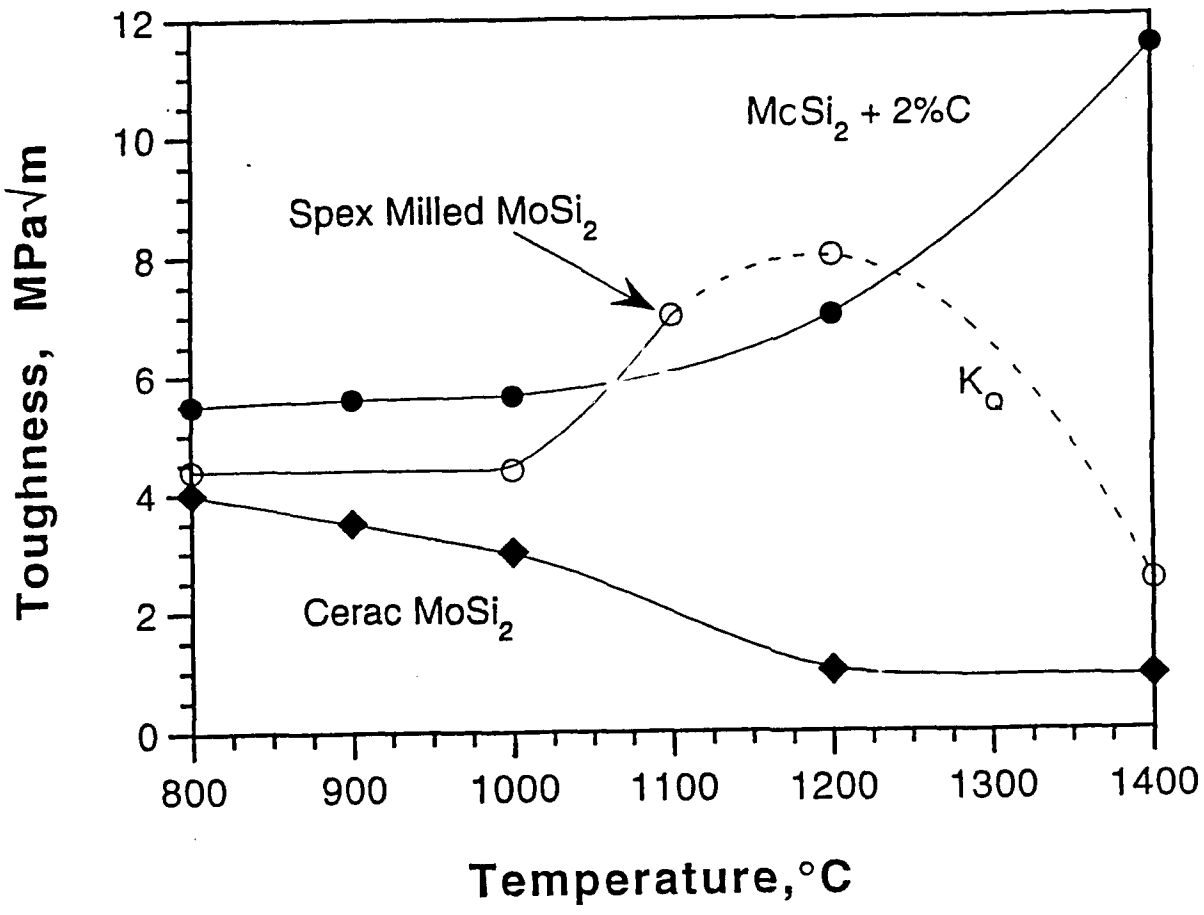

Ductile Phase Toughening by Crack Bridging
(Evans, Ashby, McMeeking, Mehrabian et al)

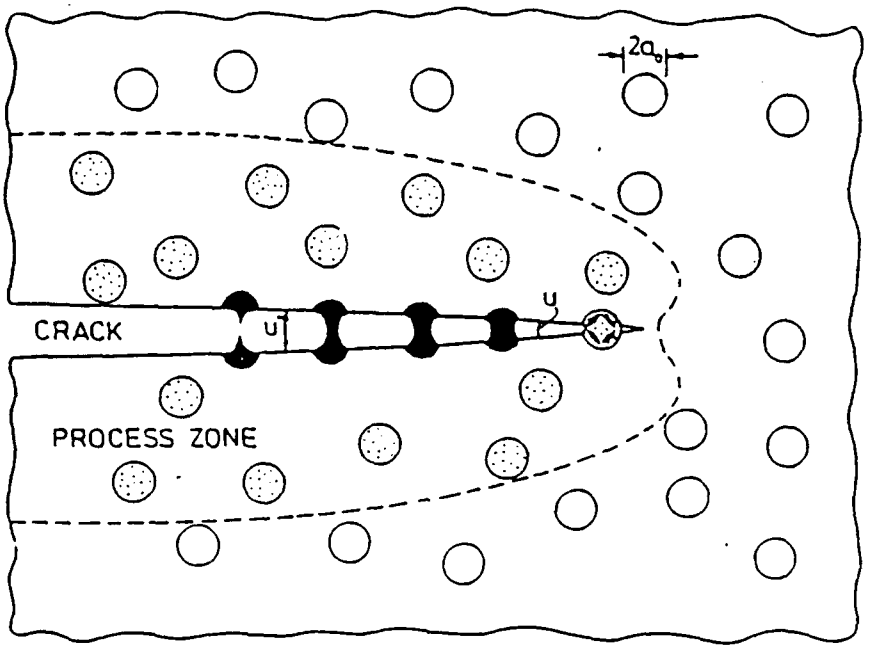

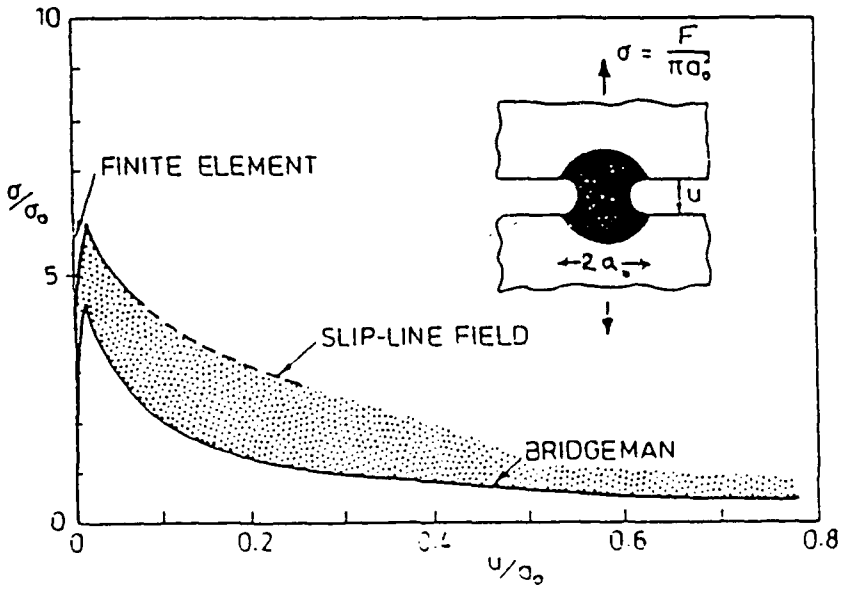

Issues Concerning Ductile Phase Toughening

- Thermodynamic compatibility with $MoSi_2$ matrix
- High temperature strength decrement due to 'soft' refractory metal additions
- Effect of metal additions on physical properties; density, modulus, thermal expansion, oxidation etc.

Nb Wire Reinforced $MoSi_2$

- Hot pressed; ≈95% dense; 5 mm dia. wires; 50 vol%; reaction zone ≈10μm
- Impact resistance increased 700% vs. unreinforced $MoSi_2$
- High Temperature Bend Strength*:

  500 MPa @ 1200°C

  200 MPa @ 1300°C
- Room Temperature Bend Strength**:

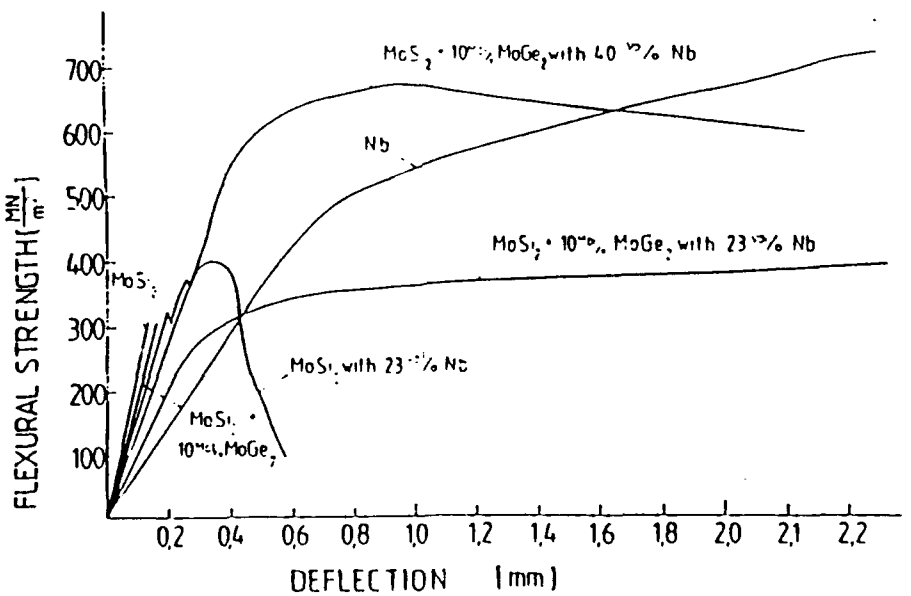

* Ref.: J. Schlichting, *High Temp. - High Pressures*, 10, (1978), 241.

** Ref.: E. Fitzer and W. Remmele, Fifth International Conf. on Composite Materials ICCM-V, (1985), 515.

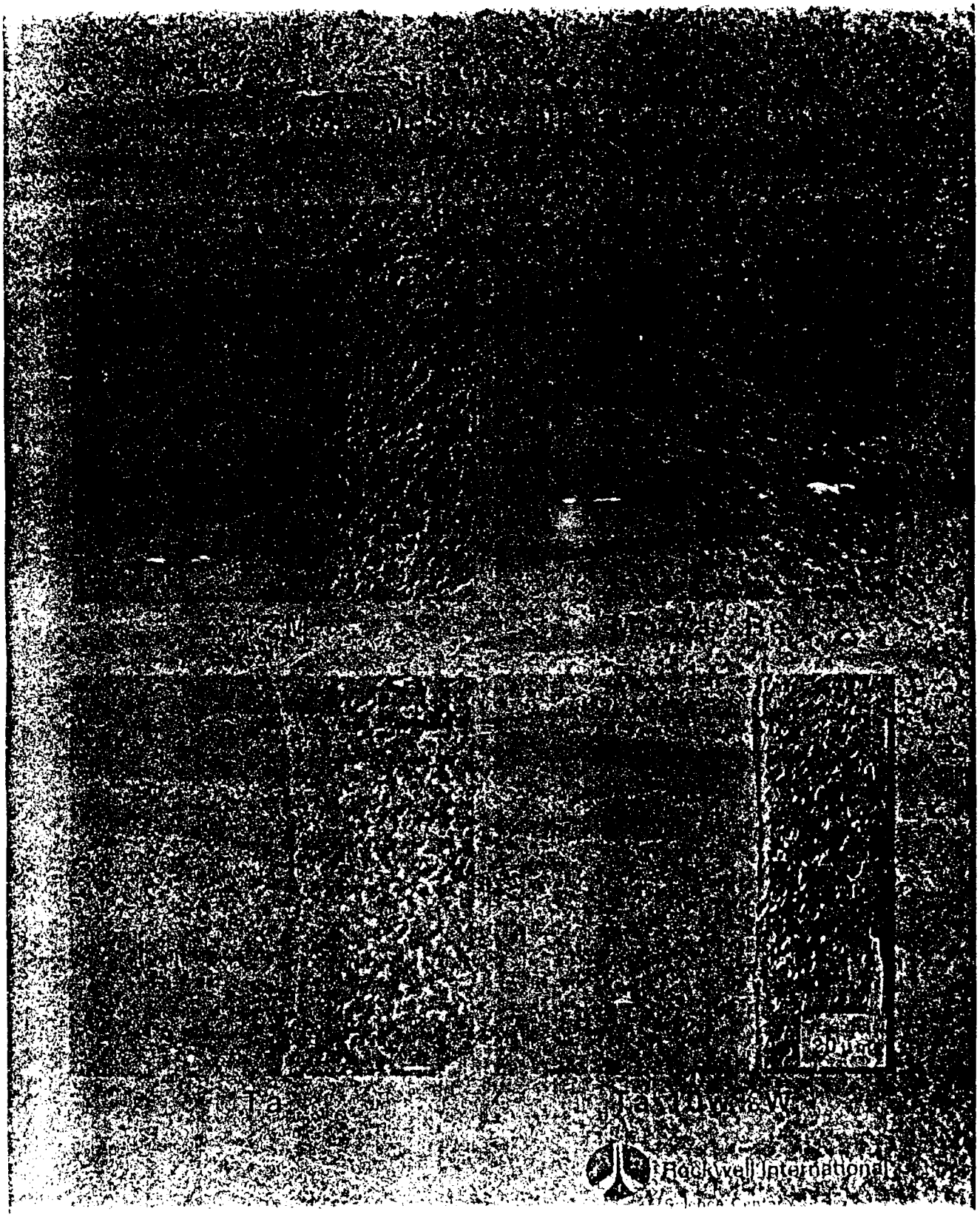
Rockwell International

Parabolic Rate Constant for Growth of M_5Si_3 in Contact with $MoSi_2$

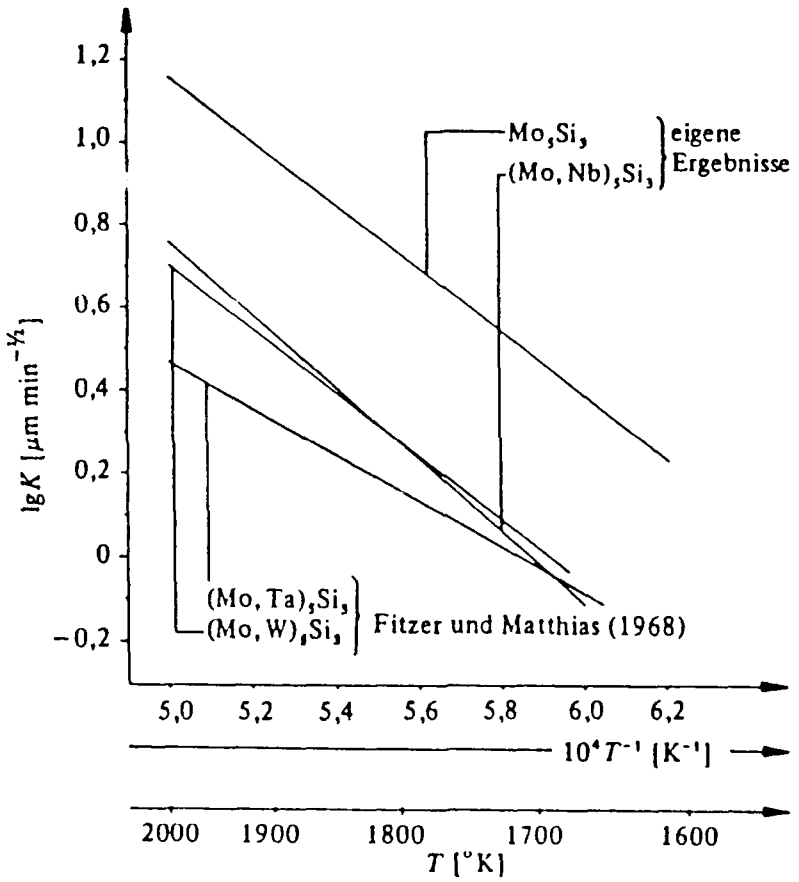

Ref.: E. Fitzer and F. K. Schmidt, *High Temp. - High Pressures*, 3, (1971) 445.

Toughness of Laminated Composites

Table III. Measured Toughness of the Laminated Composites Reinforced with 20 Vol Pct of Nb Foils with a Thickness of 0.25 mm*

Material	Monolithic $MoSi_2$	Uncoated Nb Reinforced	Al_2O_3 Coated Nb Reinforced	ZrO_2 Coated Nb Reinforced	ZrO_2 Coated Nb Reinforced
Hot-pressing temperature	1700 °C	1700 °C and 1400 °C	1400 °C	1400 °C	1700 °C
Damage tolerance ($MPa \cdot m^{1/2}$)	3.3 ± 0.3	15.2 ± 1.3	14.0 ± 1.5	12.8 ± 1.5	8.6 ± 1.3
Work of fracture (J/m^2)	690 ± 30	21,600 ± 3000	28,700 ± 1900	28,700 ± 4600	2800 ± 300
Interfacial fracture energy**	—	high	medium	low	low
Ductility of the reinforcement**	—	high	high	high	low

*Four specimens for each condition were tested except for Al_2O_3 coated Nb system for which eight specimens were tested.
**For details, see Tables I and II.

Xiao & Abbaschian, Met. Trans. 10 (1992)

Thermal Expansion Coefficients

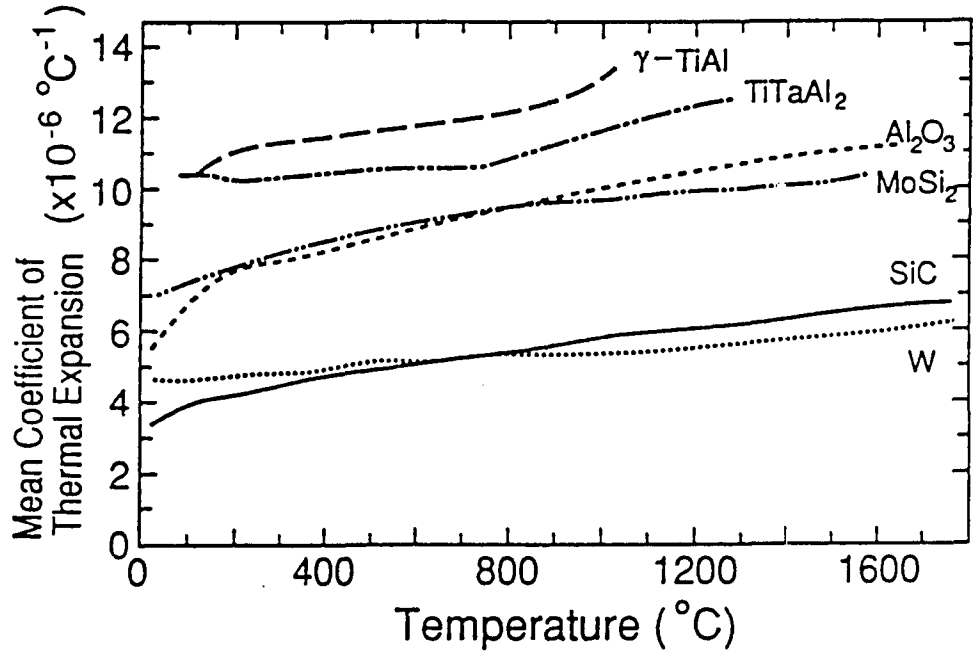

CTE Cracking in Brittle Matrix Composites

radial r-cracks

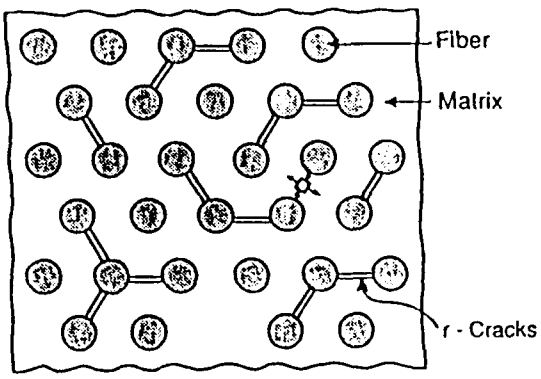

normal z-cracks

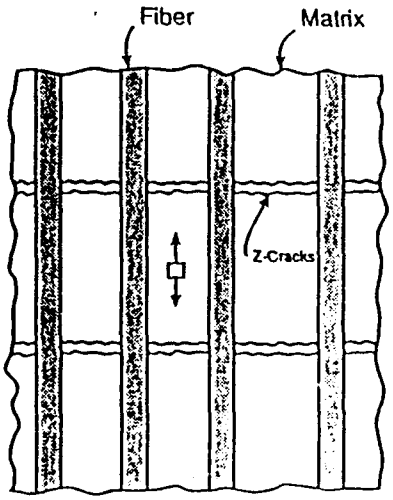

$$\mathcal{R} = R(E_m \varepsilon_T / K_m)^2$$

R = reinforcement size

K_m = matrix toughness

E_m = matrix modulus

ε_T = misfit strain = $f(\Delta\alpha)$

$\mathcal{R}_c$ = critical size below which no cracking occurs

Lu, Evans, Hecht & Mehrabian, Acta Met 8 (1991)

CTE-induced Matrix Cracking

$\mathcal{R}_C$ depends on

f = volume fraction of reinforcement

Σ = ratio of elastic moduli

ν = Poisson's ratio

μ = interface response (friction coefficient)

Trends in cracking coefficent with volume fraction

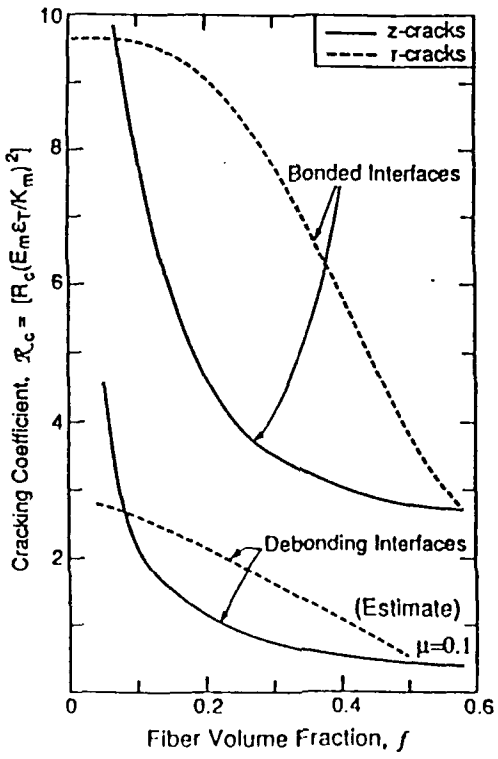

CTE Matrix Cracking - Bonded Interfaces

$MoSi_2$ reinforced with Al_2O_3

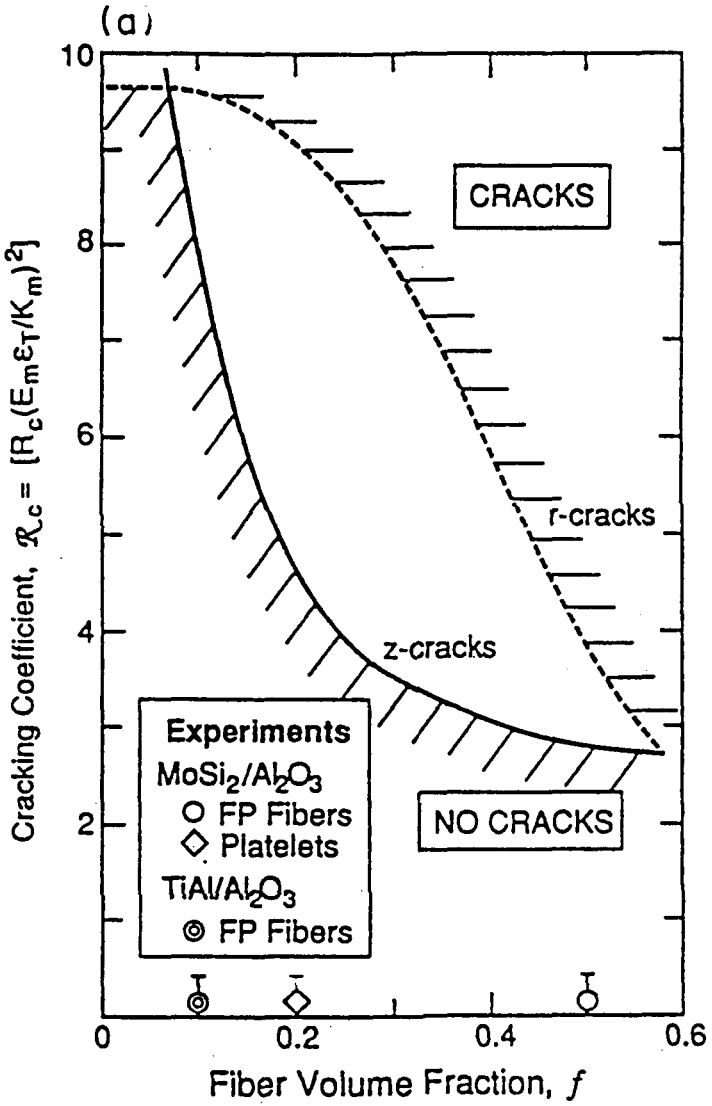

CTE Matrix Cracking - Debonding Interfaces

$MoSi_2$ reinforced with SiC

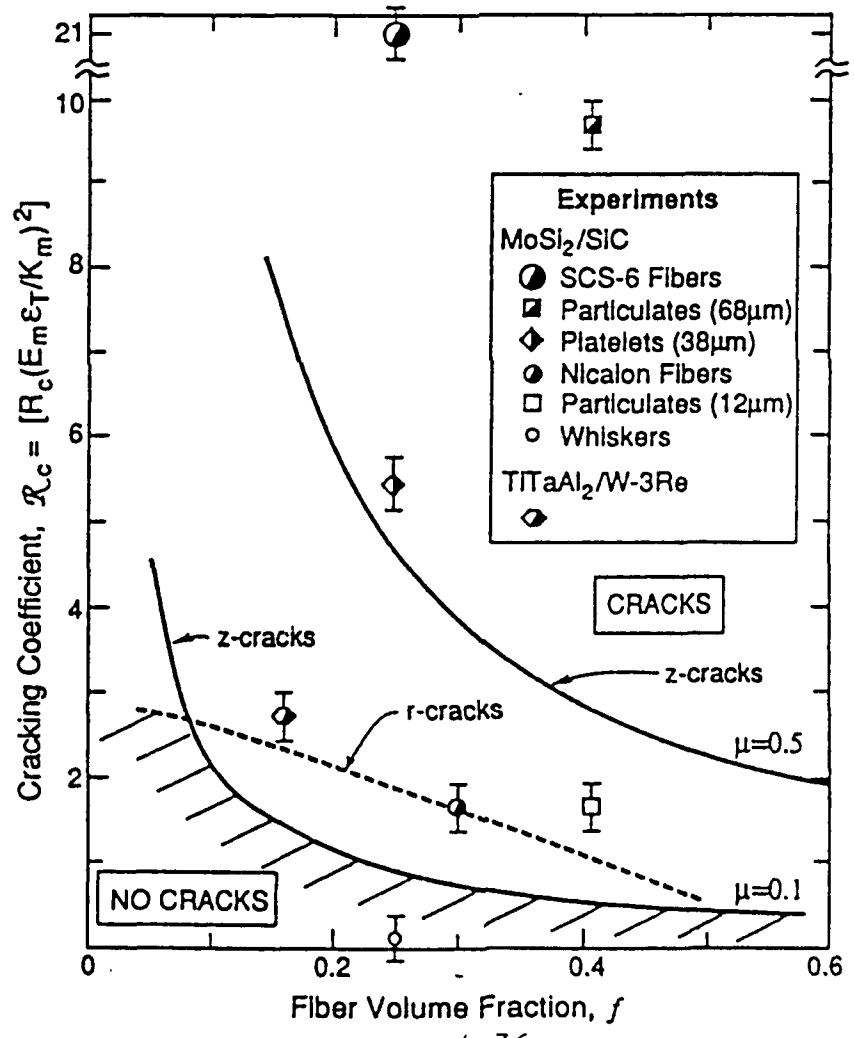

5. Effect of Microstructure on the Creep of Molybdenum Disilicides and their Composites

K. Sadananda and R. Feng
Naval Research Laboratory, USA

EFFECT OF MICROSTRUCTURE ON THE CREEP OF MOLYBDENUM DISILICIDES AND THEIR COMPOSITES

K. SADANANDA AND C.R. FENG
NAVAL RESEARCH LABORATORY
WASHINGTON D.C.

OUTLINE

1. WHY MOLYBDENUM DISILICIDES?

2. MICROSTRUCTURE: MONOLITHIC MATERIAL VS COMPOSITES
   (a) PARTICULATES VS WHISKERS
   (b) DISTRIBUTION OF REINFORCEMENTS AND ASPECT RATIO
   (c) GRAIN SIZE EFFECTS VS REINFORCEMENT EFFECTS
   (d) ALLOYING EFFECTS

3. CREEP PROCESS

4. HOW DO THE MOLYDISILICIDES COMPARE WITH OTHER POTENTIAL CANDIDATE MATERIALS FOR HIGH TEMPERATURE APPLICATIONS

TABLE - 1

CANDIDATE MATERIALS FOR HIGH & LOW TEMPERATURE APPLICATIONS

< 1000°C		> 1000°C
• Nickel base, Superalloys MAR M-246	<-- USE TEMPERATURE 1000 °C -->	• Si-based Ceramics SiC, Si_3N_4, SiC/SiC
• Ni-aluminides		• NiAl, $NbAl_3$, $TaAl_3$
• Ti-aluminides		• $MoSi_2$
• COMPGLAS		

TABLE. 1 List of candidate materials for high (>1000 °C) and low (<1000 °C) temperature applications.

Fig 20

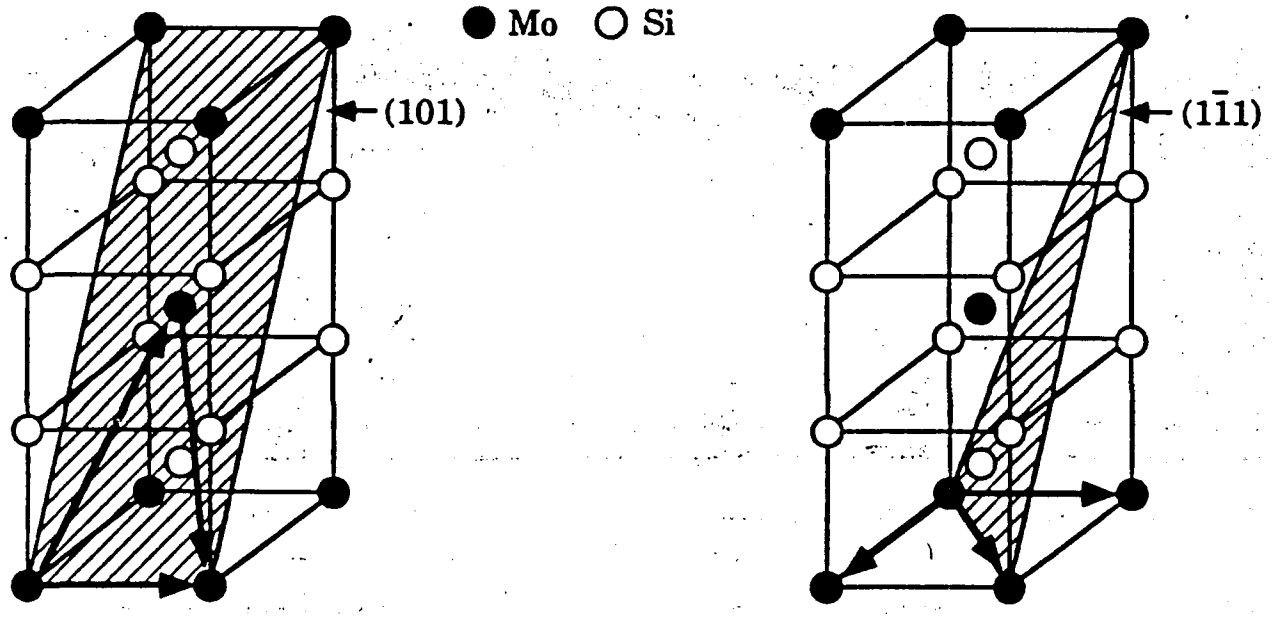

$1/2\,[\bar{1}11] + 1/2\,[11\bar{1}] \rightarrow [010]$

(a)

$[100] + [010] \rightarrow [110]$

(b)

NRL EFFORT ON MOLYBDENUM DISILICIDE COMPOSITES

- √ MONOLITHIC $MoSi_2$
- √ $MoSi_2$ + 20% SiC WHISKERS
- $MoSi_2$ + SiC PARTICULATES
  - 10% VOLUME FRACTION
  - 20% VOLUME FRACTION
  - 30% VOLUME FRACTION
  - √ 40% VOLUME FRACTION
- √ MONOLITHIC $MoSi_2$ + WSi_2 ALLOY
- √ $MoSi_2$ + WSi_2 ALLOY + 20% SiC WHISKERS
- $MoSi_2$ MONOLITHIC - EFFECT OF GRAIN SIZE
- $MoSi_2$ MONOLITHIC + %C (TO ELIMINATE AMORPHOUS SILICA PHASE)

* ALL MATERIALS PROVIDED BY J. PETROVIC OF LOS ALAMOS NATIONAL LABORATORY

Creep Data for $MoSi_2$

Material	Temp., °C	Stress, MPa	n	Act. Eng., kJ/mol	Ref.
$MoSi_2$	1093-1371	8-70	1.3	-	Maxwell
$MoSi_2$	1200	42-130	3.5	-	Suzuki et al
$MoSi_2$	1200	35-70	2.8	-	Bose
$MoSi_2$, HP	1200	35-70	2.8	-	Bose
$MoSi_2$, HIP	1100-1400	10-80	1.7, 4.4	372	Ghosh et al
$MoSi_2$	1100-1300	10-80	2	433	Sadananda et al
$MoSi_2$	1200	70-170	2	-	Bose
$MoSi_2$, single crystal <210>	1200	10-50	2.7	-	Ghosh et al
$MoSi_2$*					
$(Mo,W)Si_2$, HP	1200	35-70	1.6	-	Bose
$(Mo,W)Si_2$	1100-1400	2-200	2.4-3.6	536	Sadananda et al
$MoSi_2$+20v%SiC_w, HP	1200	35-70	3.1	-	Bose
$MoSi_2$+18v%SiC_w, HIP	1200	35-100	3.1	-	Bose
$MoSi_2$+20v%SiC_w	1200	100-250	3.1	-	Ghosh et al
$MoSi_2$+20v%SiC_w	1100-1450	20-200	3.3, 5.2	596	Sadananda et al
$(Mo,W)Si_2$+20v%SiC_w	1100-1400	8-250	2, 4	-	Sadananda et al
$(Mo,W)Si_2$+20v%SiC_w *	1175	30-50	3.2	557	Wiederhorn et al
$(Mo,W)Si_2$+20v%SiC_w*	1225	30-50	2.3	557	Wiederhorn et al
$MoSi_2$+20v%SiC_p, HIP	1200	50-100	2.5	-	Bose
$MoSi_2$+20v%SiC_p+10Nb_p,HIP	1200	65-120	3.5	-	Bose
$MoSi_2$+20v%SiC_p	1100	40-90	5	-	Deve et al
$MoSi_2$+20v%SiC_p/Mo	1100	70-150	3	-	Deve et al
$MoSi_2$+20v%SiC_p	1200	8-100	3.1	-	Ghosh et al
XD $MoSi_2$+30v%SiC_p	1050-1300	35-300	3.5	430	Suzuki et al
$MoSi_2$+20v%$Er_2Mo_3Si_{4p}$	1200-1300	100-280	3.5	-	Patrick et al
$MoSi_2$+20v%CaO_p	1200	100-310	3.5	-	Patrick et al
$MoSi_2$-45v%Mo_5Si_3,HP	1200-1300	10-110	2.5, 3.5	-	Mosan et al
$MoSi_2$-45v%Mo_5Si_3,DS	1100-1300	150-1000	4.5	300	Mosan et al
$MoSi_2$+5v%SiC_p	1100-1200	20-180	1	460	Sadananda et al
$MoSi_2$+10v%SiC_p	1100-1200	20-250	1	460	Sadananda et al
$MoSi_2$+20v%SiC_p	900-1200	15-450	1, 4	460	Sadananda et al
$MoSi_2$+30v%SiC_p	1100-1200	35-300	3, 5.7	460	Sadananda et al
$MoSi_2$+40v%SiC_p	1000-1200	40-400	5	460	Sadananda et al
$MoSi_2$+5v%SiC_p*	1050-1150	10-30	1	815	Wiederhorn et al
$MoSi_2$+10v%SiC_p*	1050-1150	10-30	3	575	Wiederhorn et al
$MoSi_2$+20v%SiC_p*	1050-1150	10-30	5	894	Wiederhorn et al
$MoSi_2$+30v%SiC_p*	1150-1250	30-50	5	684	Wiederhorn et al
$MoSi_2$+40v%SiC_p*	1100-1200	30-50	5, 10	628	Wiederhorn et al
$MoSi_2$+1wt%C	1200-1400	20-250	2, 5	460	Sadananda et al
$MoSi_2$+2wt%C	1000-1400	20-300	3	460	Sadananda et al
$MoSi_2$+4wt%C	1200-1400	20-250	3	460	Sadananda et al

* Tensile Creep Test

100 MICRONS

50/50 MOLE % $MoSi_2/WSi_2$

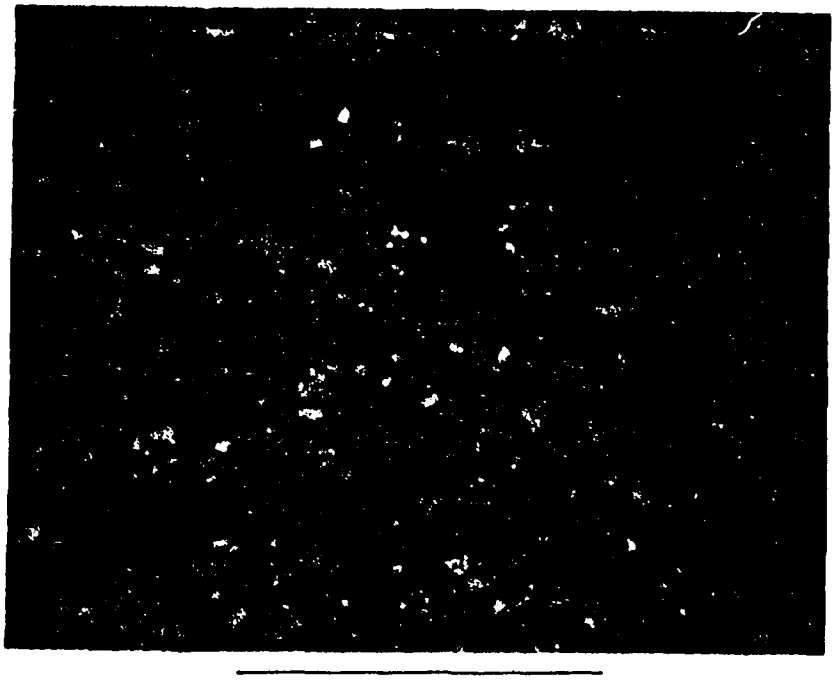

100 MICRONS

30 VOL.% SiC PARTICLE-50/50 MOLE % $MoSi_2/WSi_2$ MATRIX

Fig. 4. K. Sadananda and C.R. Feng

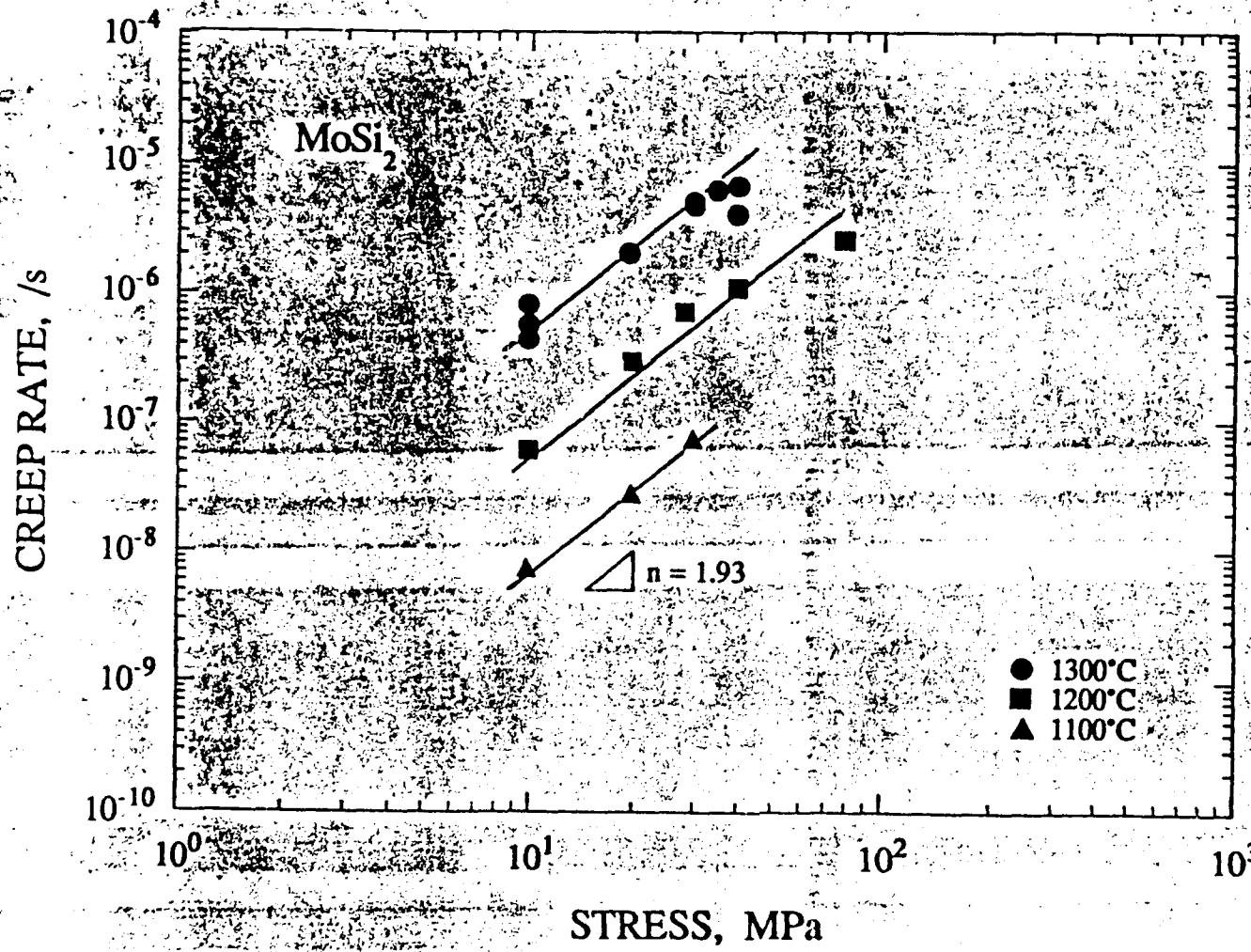

Fig. 5

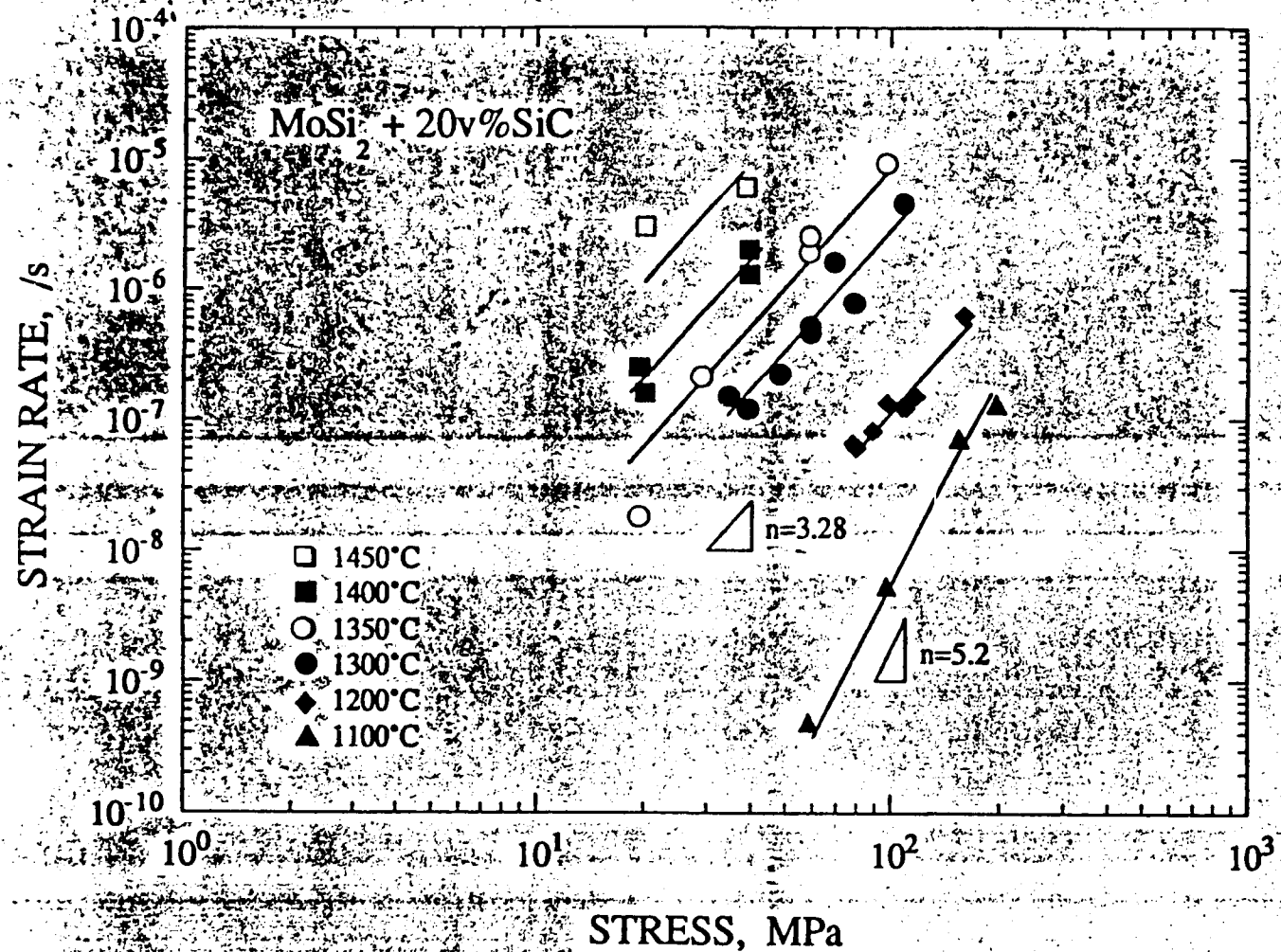
MoSi2 + 20v%SiC
STRAIN RATE, /s
STRESS, MPa
n=3.28
n=5.2
1450°C
1400°C
1350°C
1300°C
1200°C
1100°C

Fig 10c.

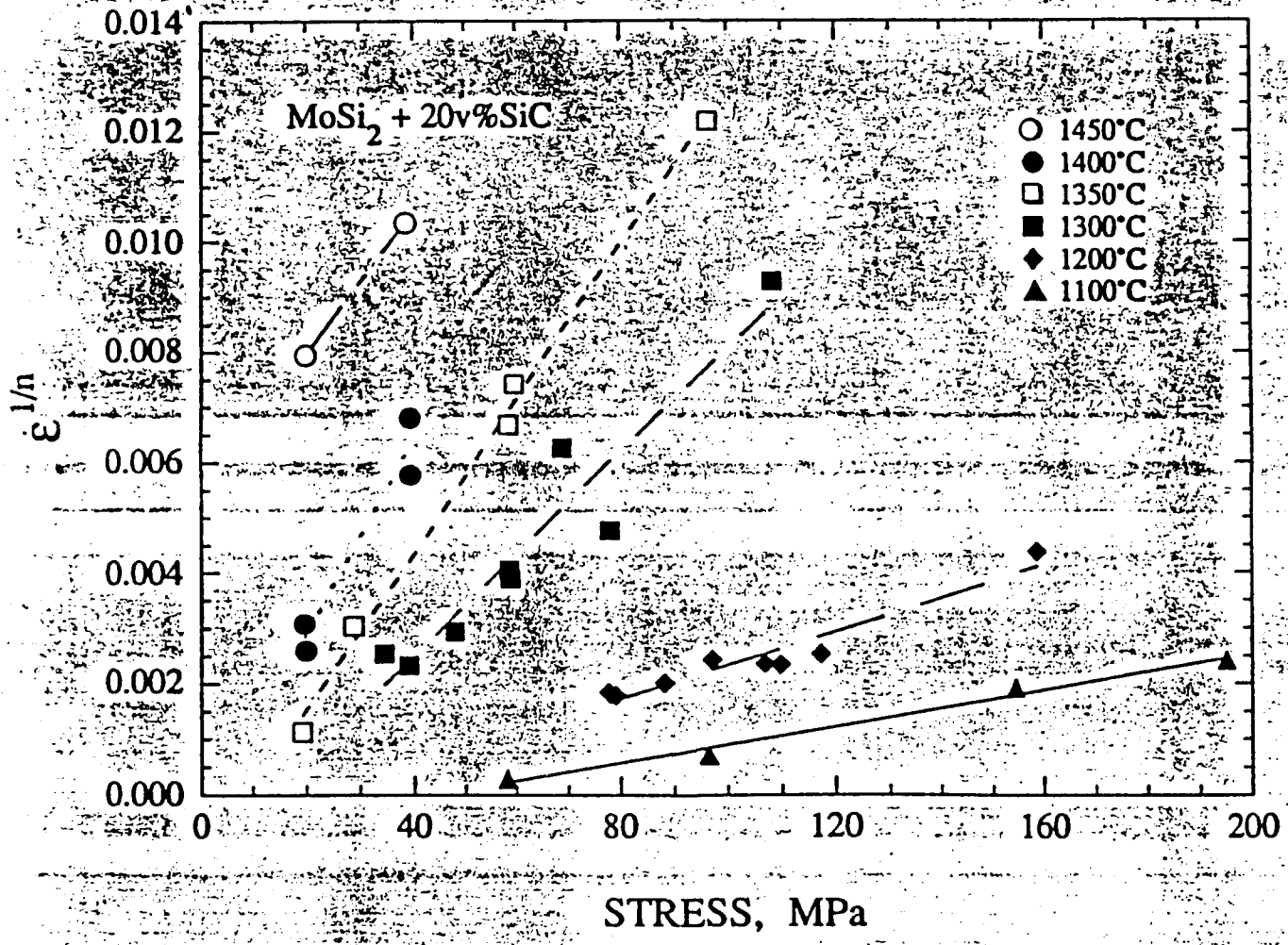
MoSi2 + 20v%SiC
1450°C
1400°C
1350°C
1300°C
1200°C
1100°C
0.014
0.012
0.010
0.008
0.006
0.004
0.002
0.000
ε̇ 1/n
0
40
80
120
160
200
STRESS, MPa

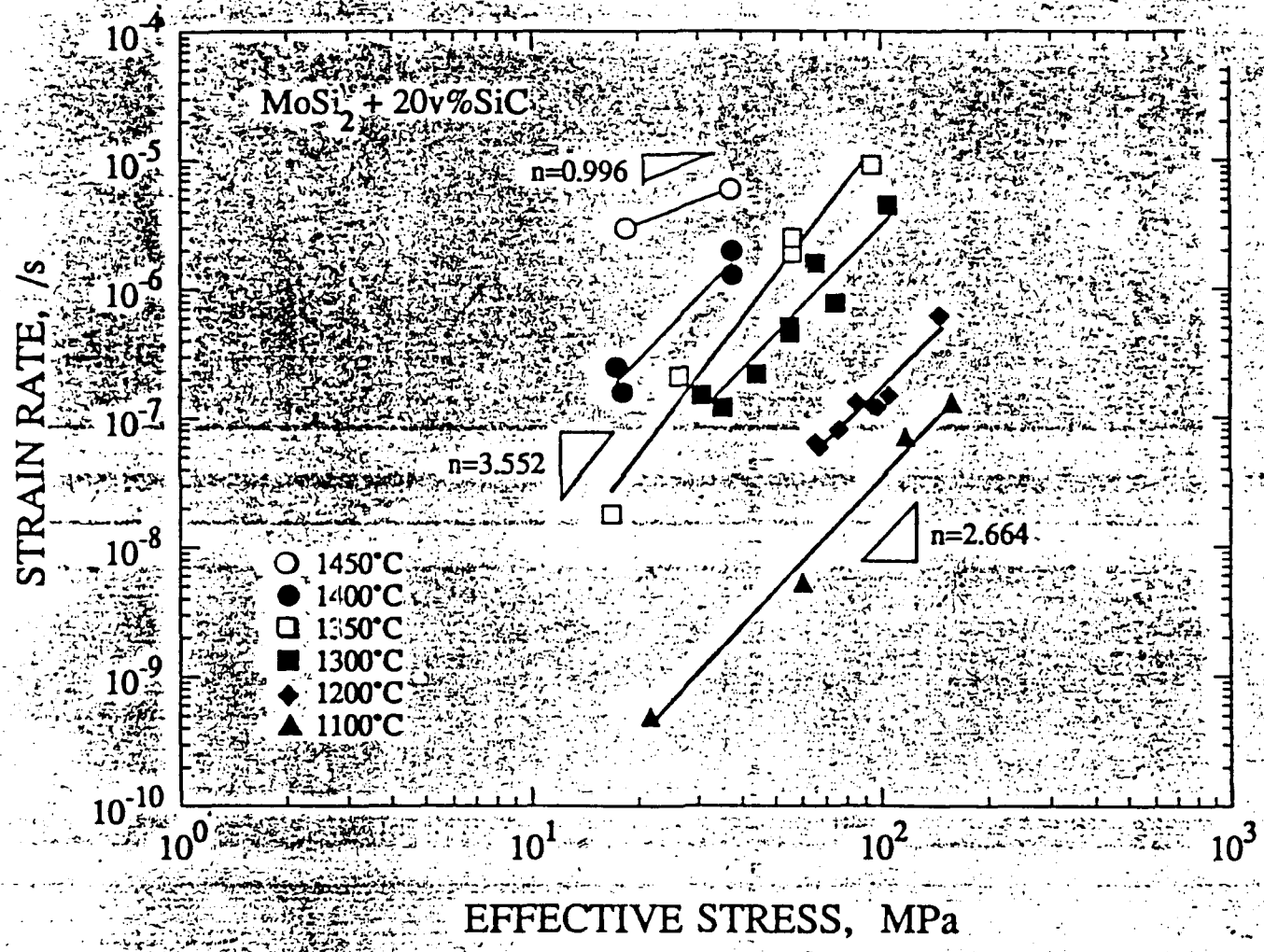
MoSi2 + 20v%SiC
n=0.996
n=3.552
n=2.664
1450°C
1400°C
1350°C
1300°C
1200°C
1100°C
STRAIN RATE, /s
EFFECTIVE STRESS, MPa
10^-4
10^-5
10^-6
10^-7
10^-8
10^-9
10^-10
10^0
10^1
10^2
10^3

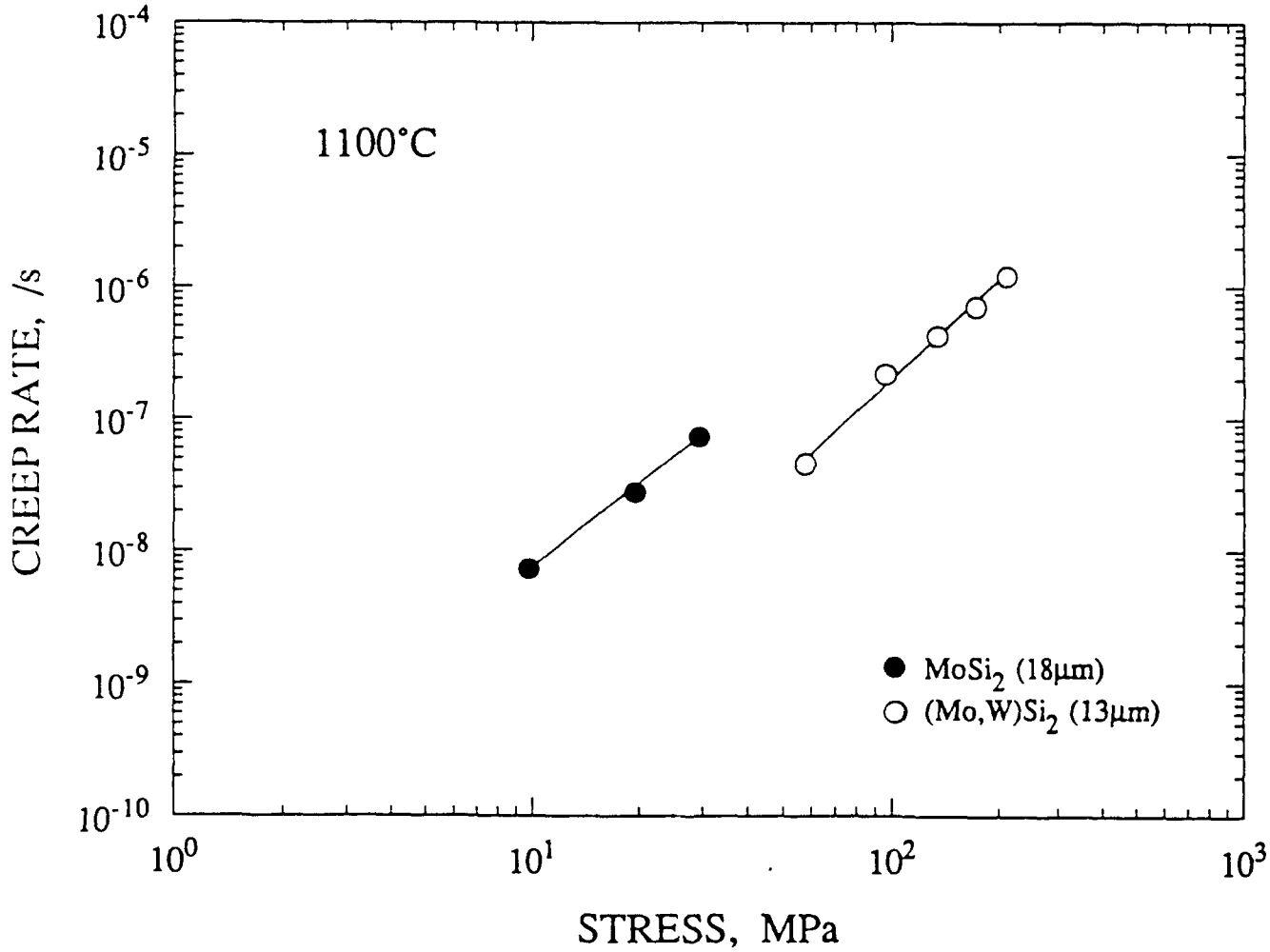
1100°C
CREEP RATE, /s
STRESS, MPa
10^{-4}
10^{-5}
10^{-6}
10^{-7}
10^{-8}
10^{-9}
10^{-10}
10^{0}
10^{1}
10^{2}
10^{3}
$MoSi_2$ (18μm)
$(Mo,W)Si_2$ (13μm)

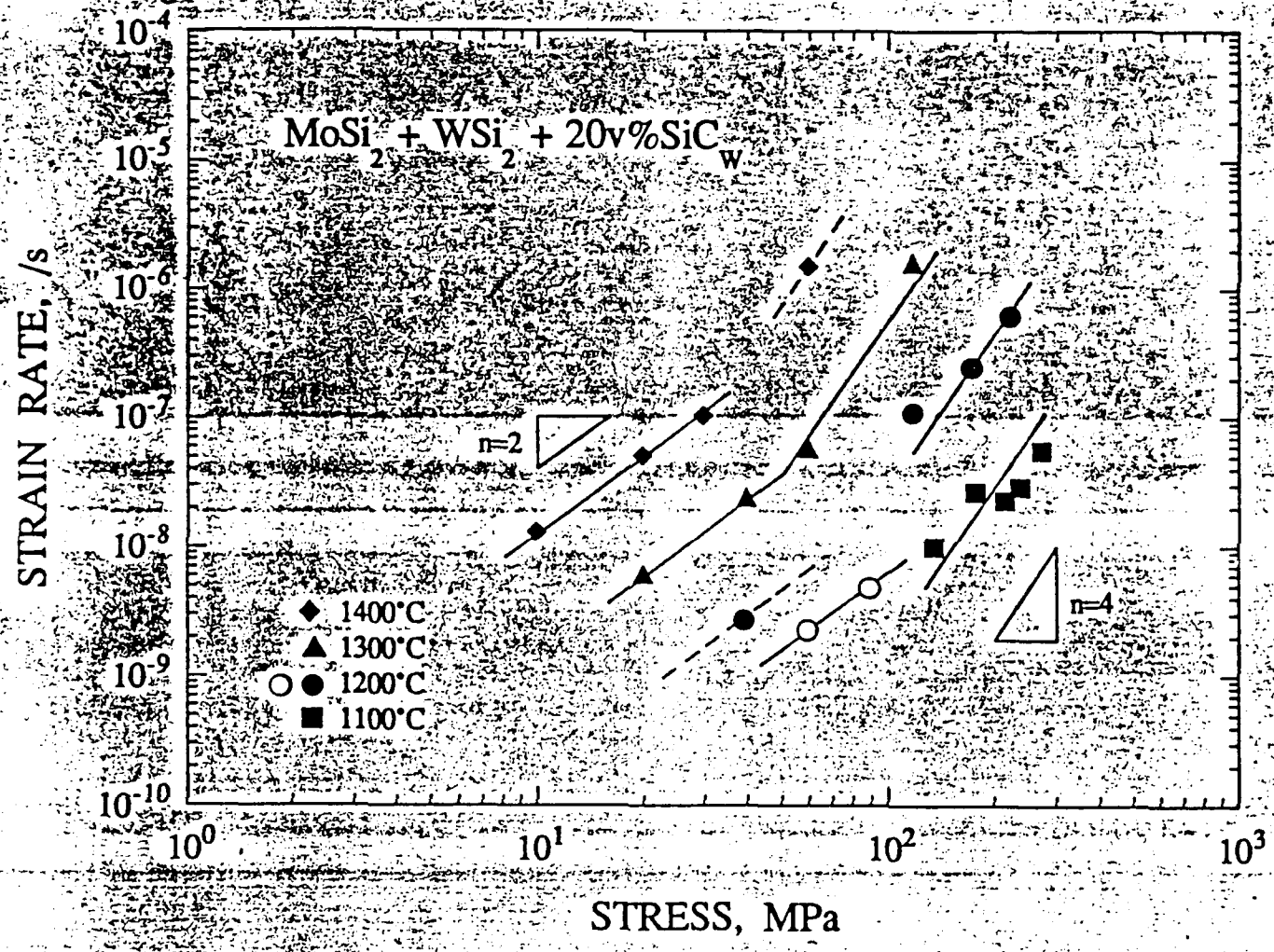
MoSi2 + WSi2 + 20v%SiCw
STRAIN RATE, /s
STRESS, MPa
n=2
n=4
1400°C
1300°C
1200°C
1100°C
10-4
10-5
10-6
10-7
10-8
10-9
10-10
100
101
102
103

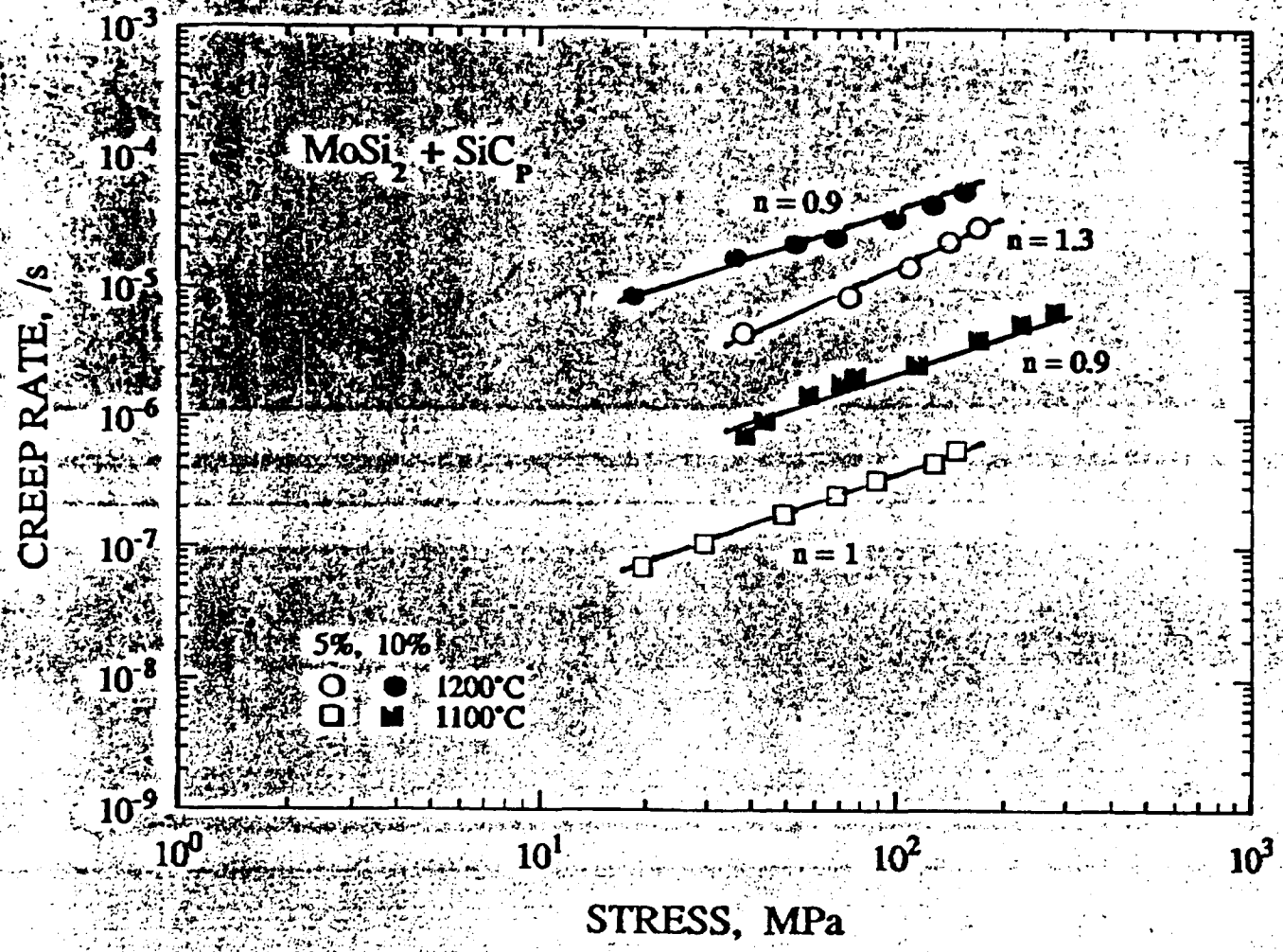
MoSi2 + SiCp
n = 0.9
n = 1.3
n = 0.9
n = 1
5%, 10%
1200°C
1100°C
CREEP RATE, /s
STRESS, MPa
10-3
10-4
10-5
10-6
10-7
10-8
10-9
100
101
102
103

MOLYDISILICIDE WITH SIC PARTICULATES

INCREASE AND THEN DECREASE IN CREEP RATES WITH INCREASE IN VOLUME FRACTION OF SIC

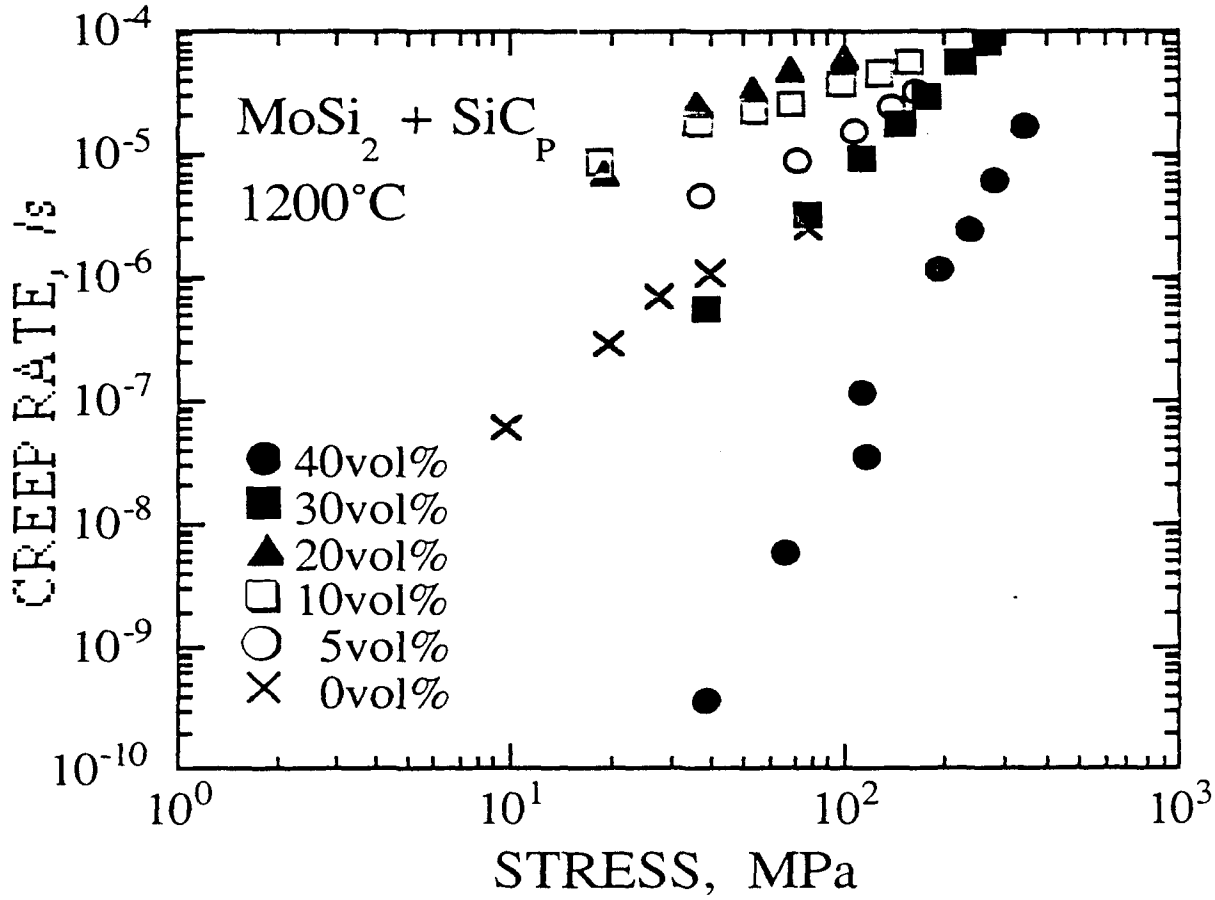

COMBINED EFFECT OF GRAIN SIZE AND VOLUME FRACTION

MODIFIED KELLEY & STREET MODEL CONSIDERING GRAIN SIZE EFFECTS - ARISING FROM COBEL CREEP PROCESS

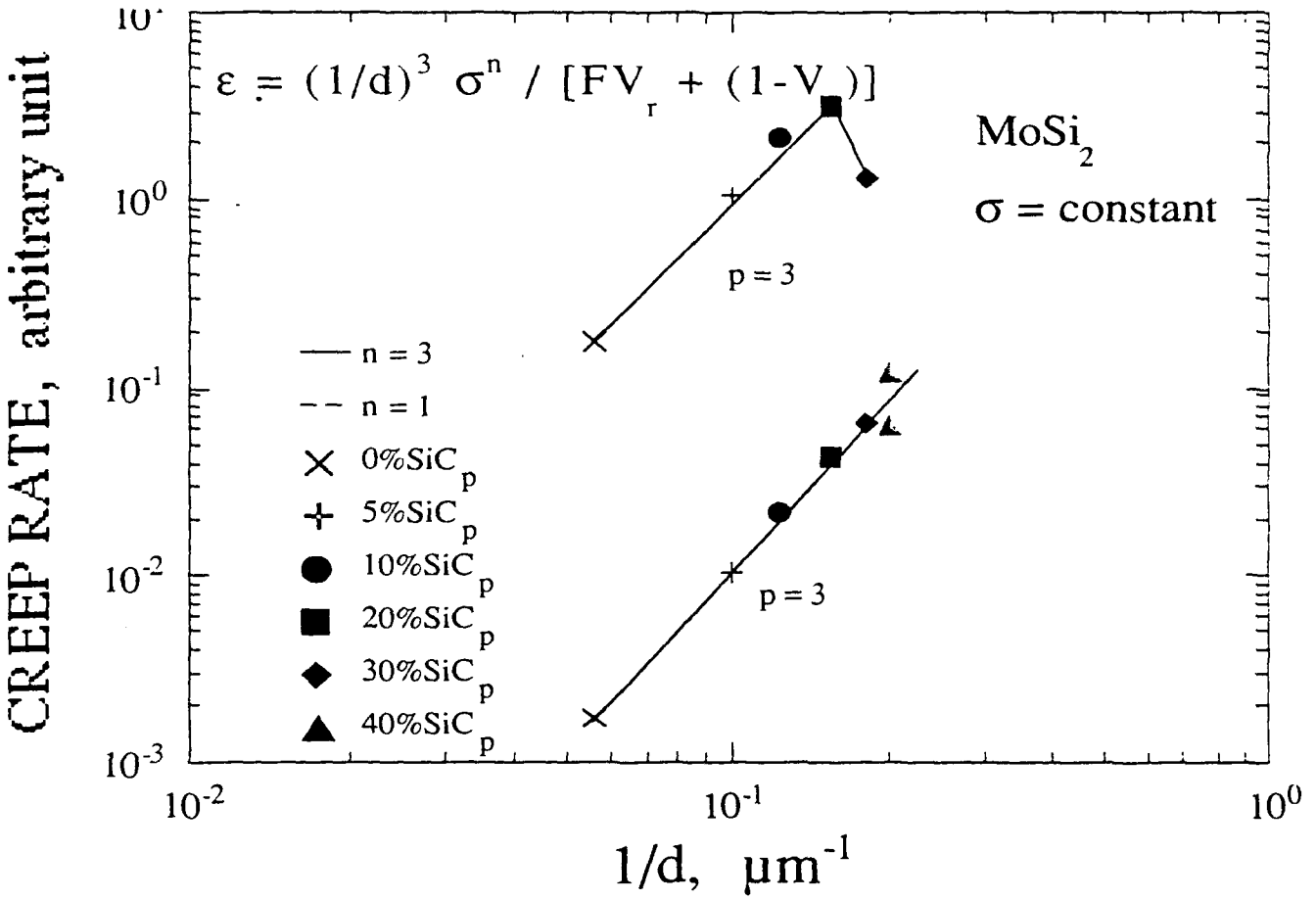

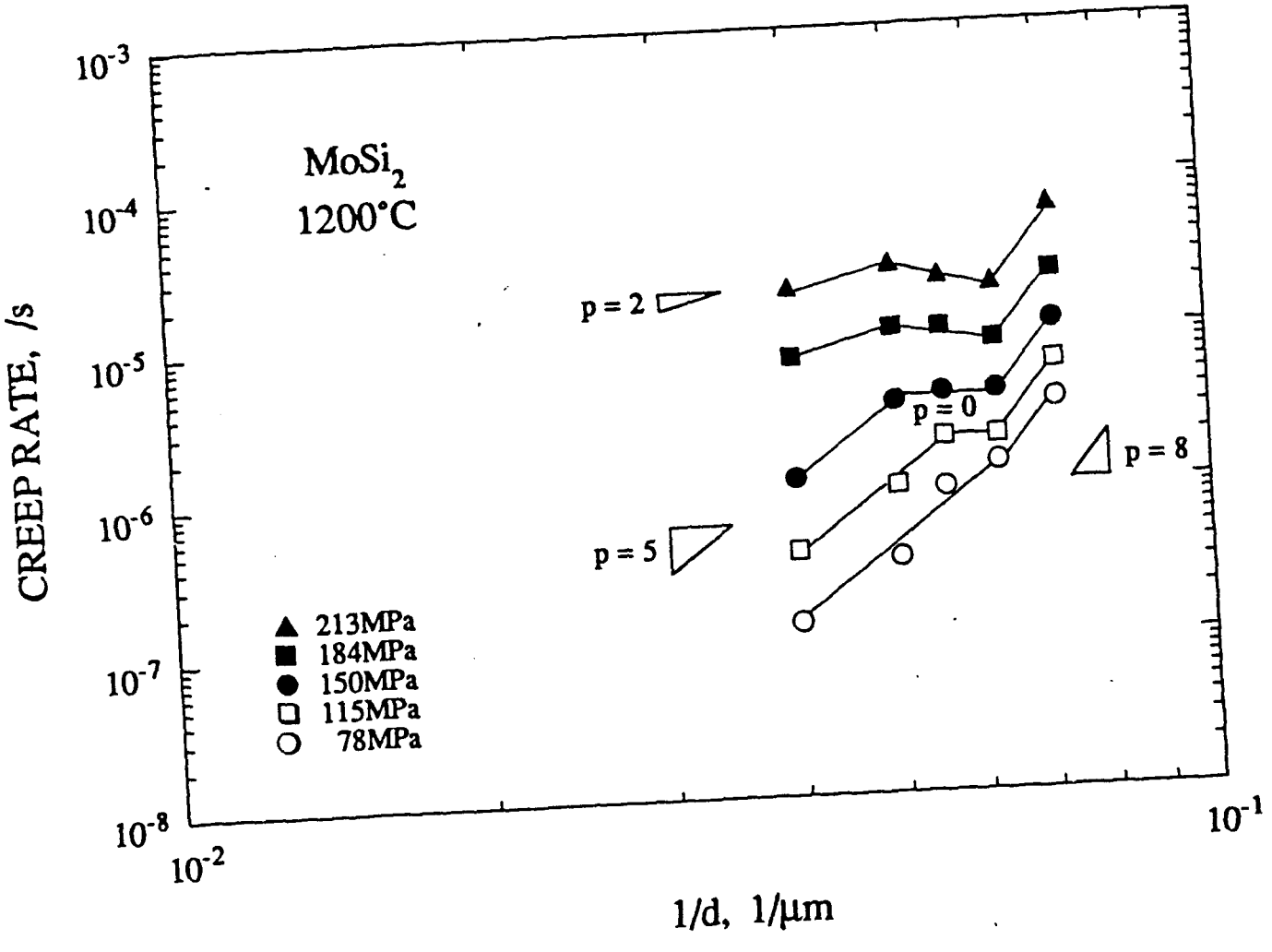
MoSi2
1200°C
CREEP RATE, /s
1/d, 1/μm
10-3
10-4
10-5
10-6
10-7
10-8
10-2
10-1
p = 2
p = 0
p = 8
p = 5
213MPa
184MPa
150MPa
115MPa
78MPa

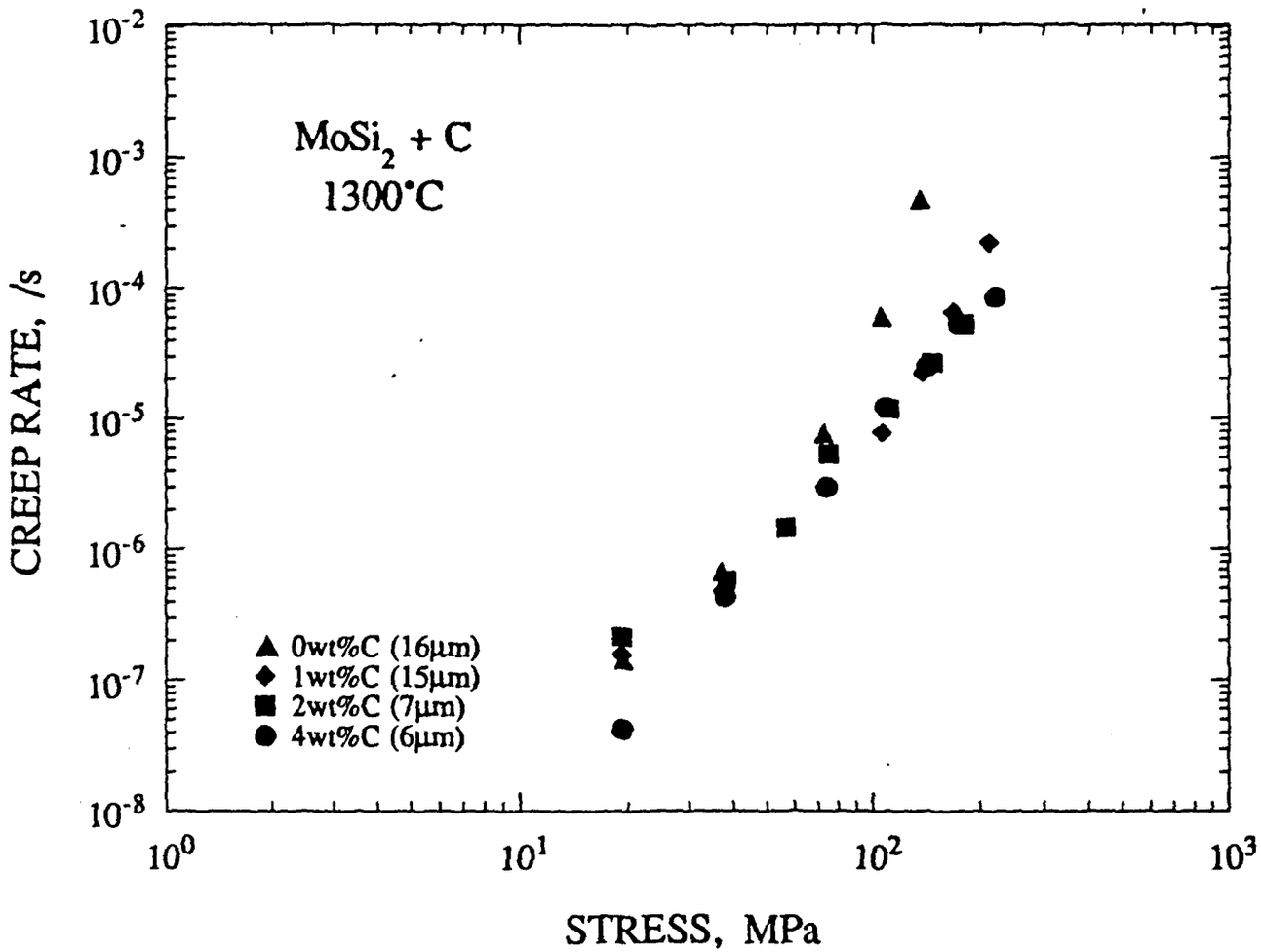
MoSi2 + C
1300°C
CREEP RATE, /s
STRESS, MPa
10-2
10-3
10-4
10-5
10-6
10-7
10-8
100
101
102
103
0wt%C (16μm)
1wt%C (15μm)
2wt%C (7μm)
4wt%C (6μm)

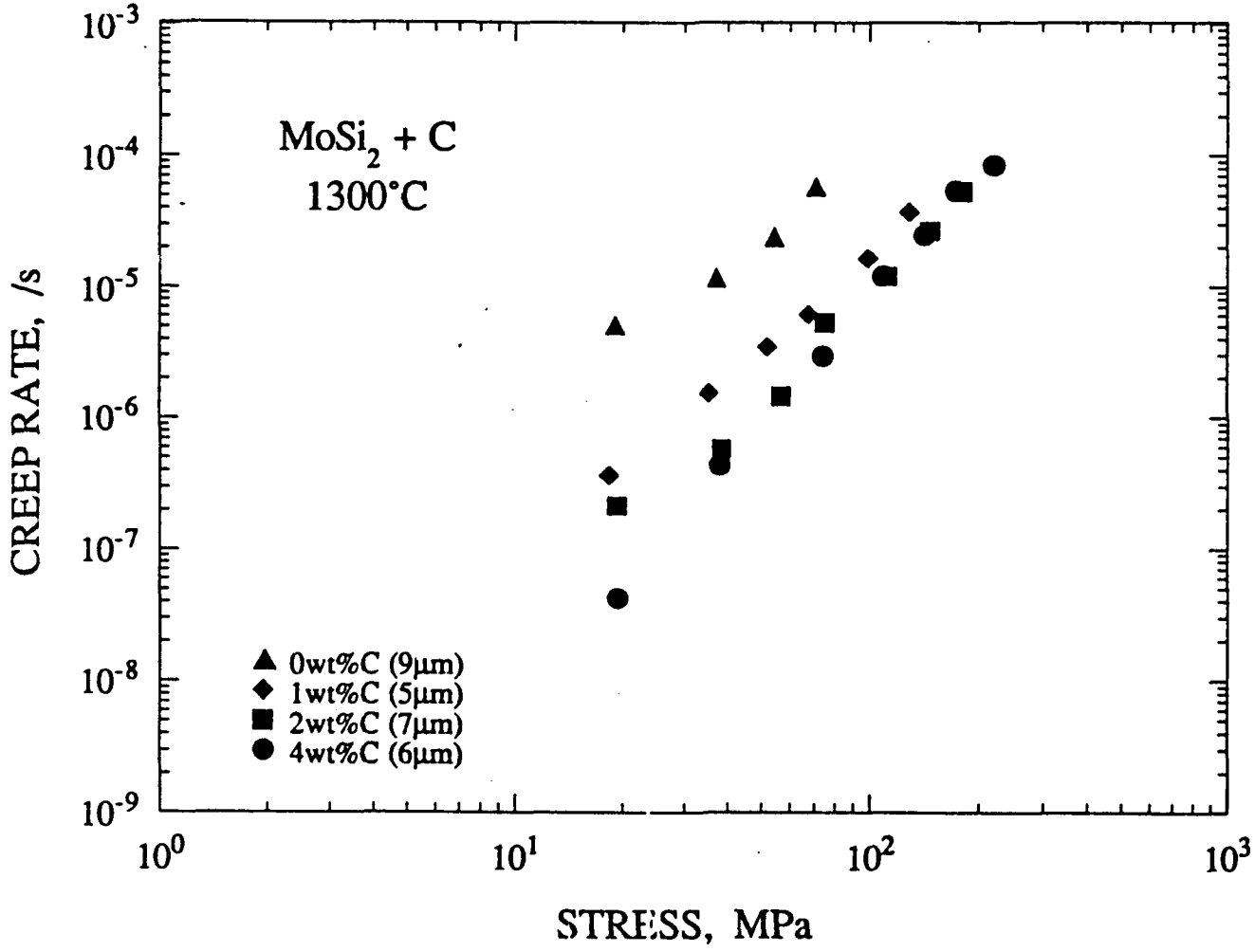
MoSi2 + C
1300°C
0wt%C (9μm)
1wt%C (5μm)
2wt%C (7μm)
4wt%C (6μm)
CREEP RATE, /s
STRESS, MPa
10-3
10-4
10-5
10-6
10-7
10-8
10-9
100
101
102
103

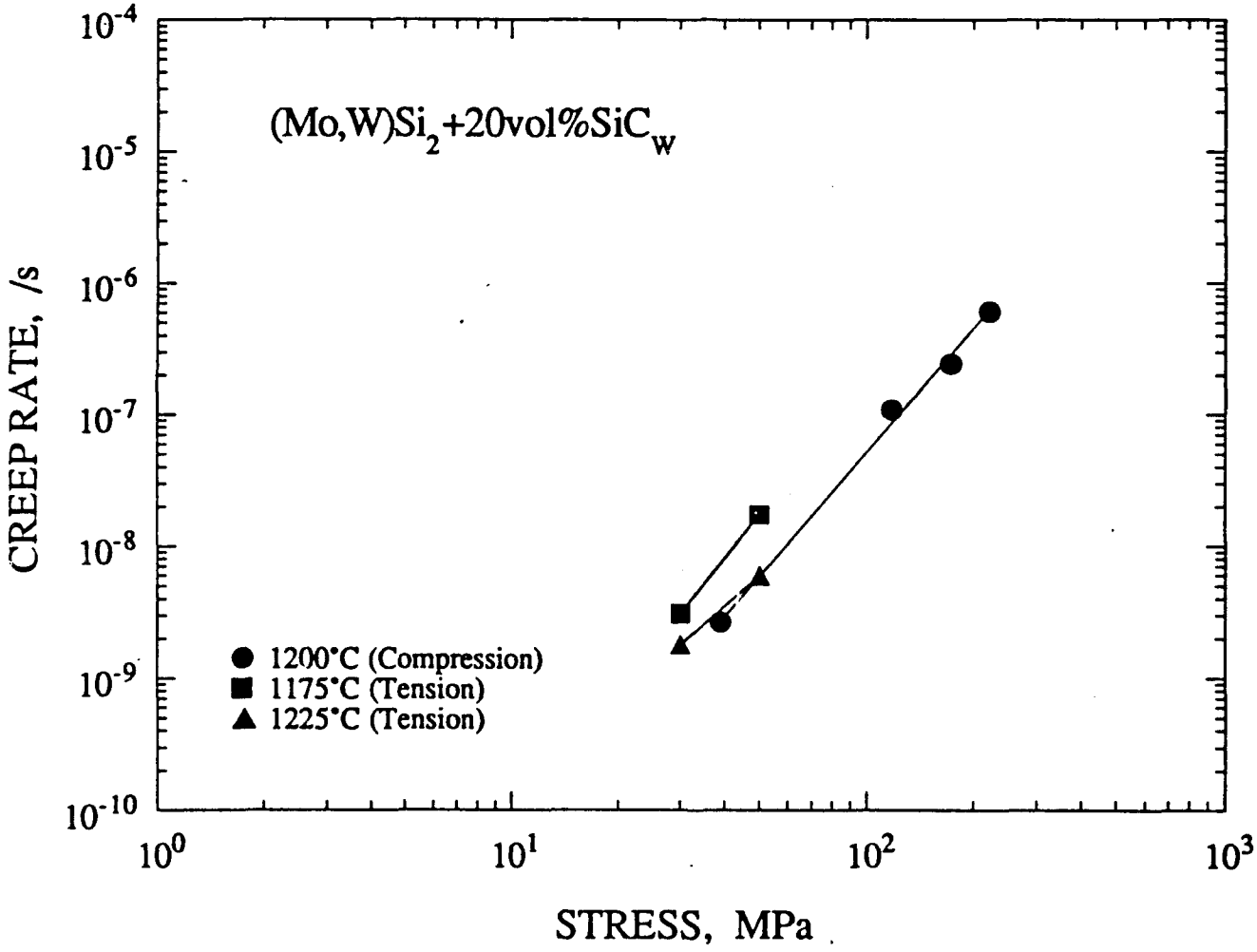
(Mo,W)Si2+20vol%SiCw
CREEP RATE, /s
STRESS, MPa
10-4
10-5
10-6
10-7
10-8
10-9
10-10
100
101
102
103
1200°C (Compression)
1175°C (Tension)
1225°C (Tension)

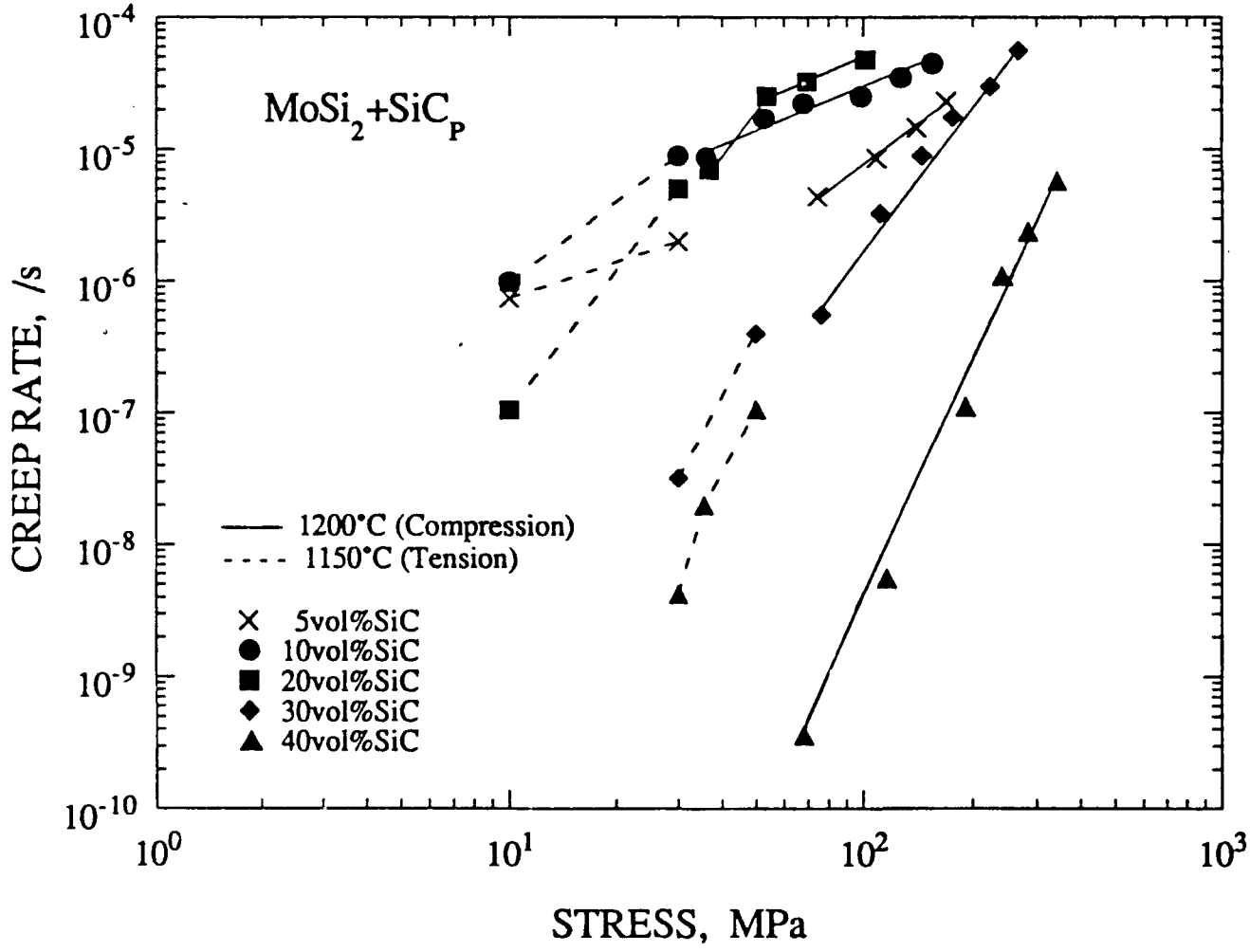
MoSi2+SiCP
CREEP RATE, /s
STRESS, MPa
10-4
10-5
10-6
10-7
10-8
10-9
10-10
100
101
102
103
1200°C (Compression)
1150°C (Tension)
5vol%SiC
10vol%SiC
20vol%SiC
30vol%SiC
40vol%SiC

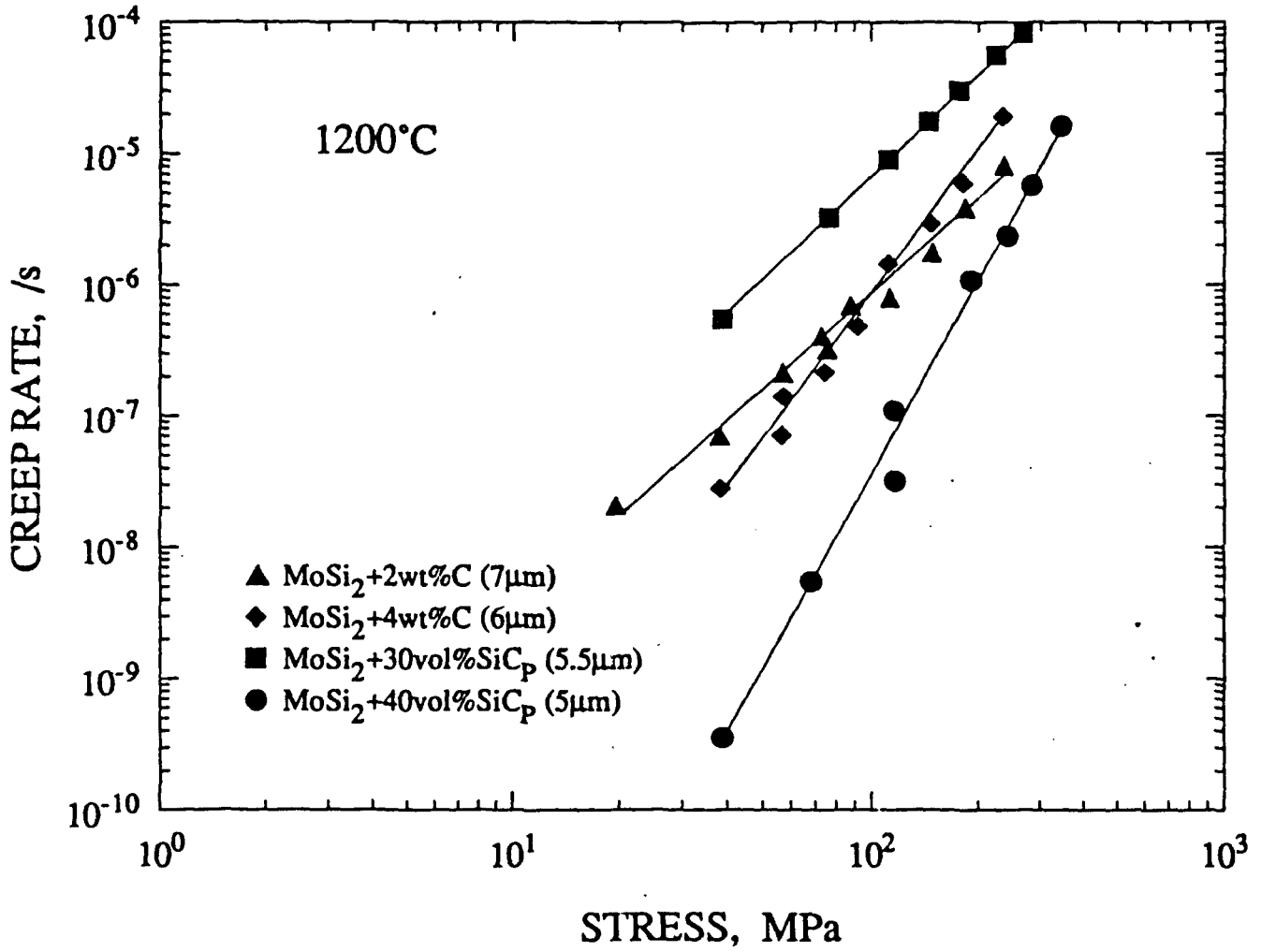
1200°C
CREEP RATE, /s
STRESS, MPa
10^{-4}
10^{-5}
10^{-6}
10^{-7}
10^{-8}
10^{-9}
10^{-10}
10^{0}
10^{1}
10^{2}
10^{3}
▲ $MoSi_2$+2wt%C (7μm)
◆ $MoSi_2$+4wt%C (6μm)
■ $MoSi_2$+30vol%SiC_p (5.5μm)
● $MoSi_2$+40vol%SiC_p (5μm)

CREEP OF NiAl WITH DISPERSOIDS AND REINFORCEMENTS

HIGH VOLUME FRACTION OF REINFORCEMENT REQUIRED TO ENHANCE CREEP RESISTANCE

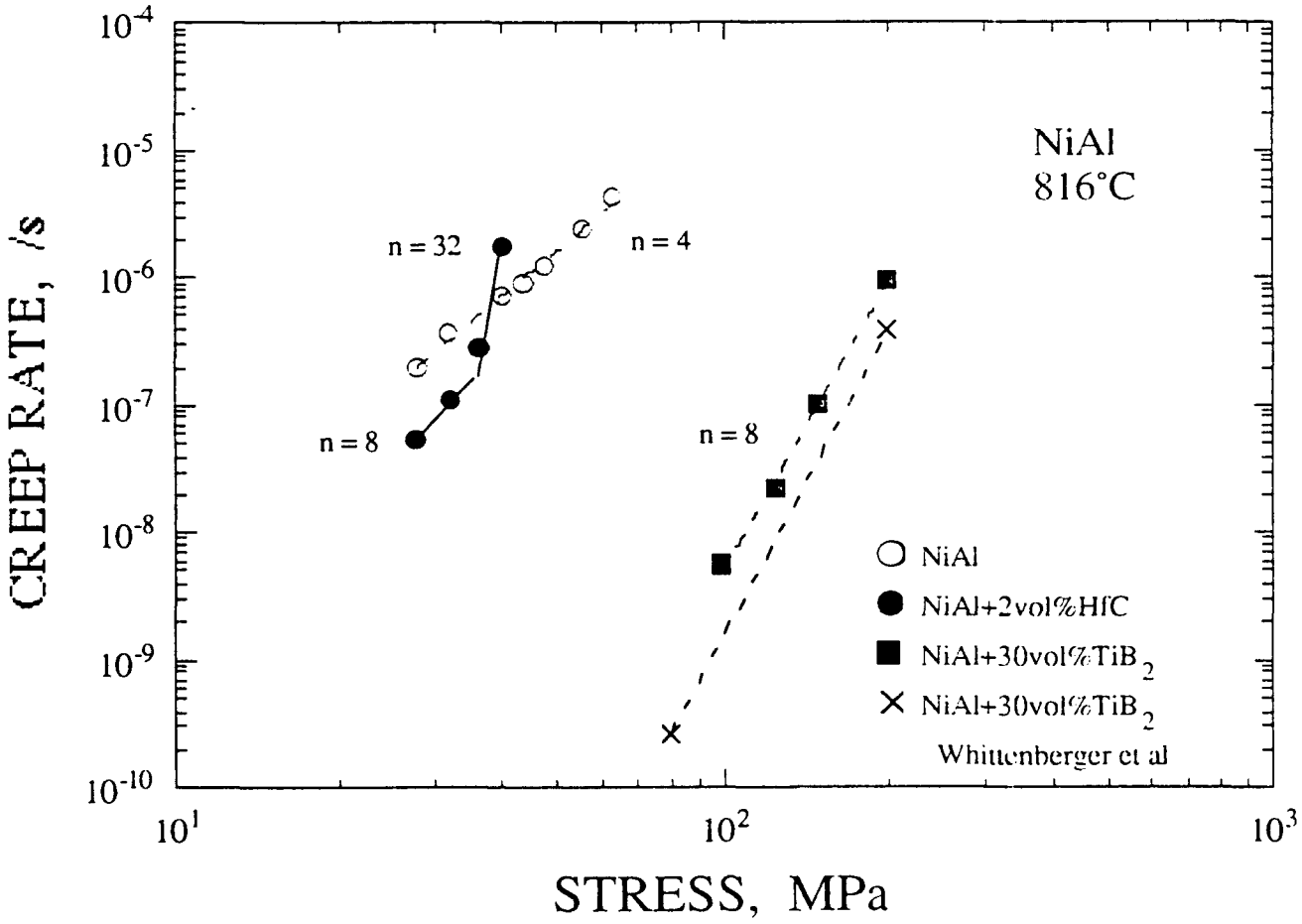

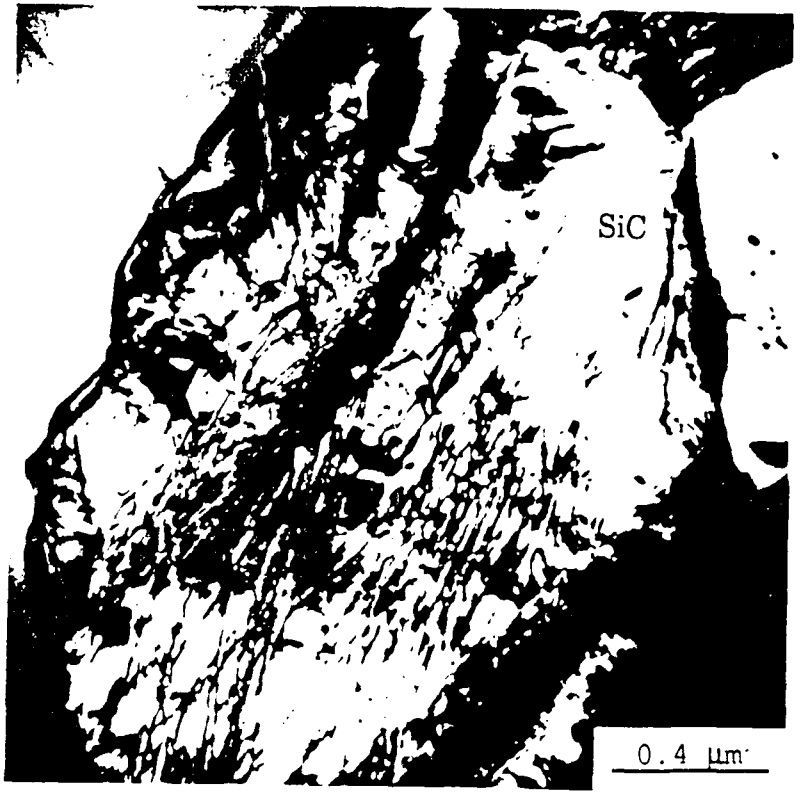

TEM MICROGRAPHS OF $MoSi_2$ + 20vol% SiC
DEFORMED BY CREEP AT 1200°C AND AT 11.5ksi

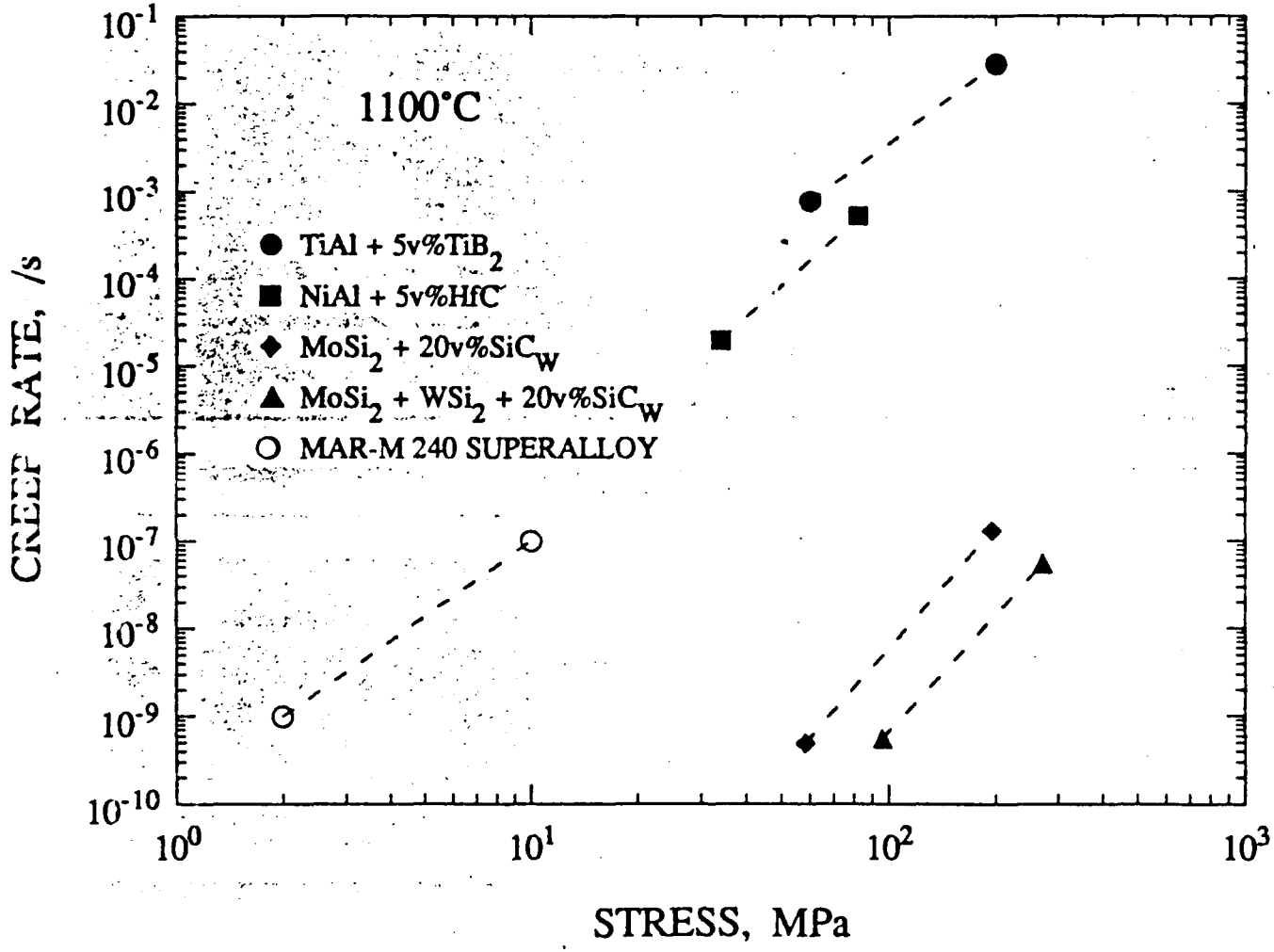
1100°C
TiAl + 5v%TiB2
NiAl + 5v%HfC
MoSi2 + 20v%SiCw
MoSi2 + WSi2 + 20v%SiCw
MAR-M 240 SUPERALLOY
CREEP RATE, /s
STRESS, MPa
10-1
10-2
10-3
10-4
10-5
10-6
10-7
10-8
10-9
10-10
100
101
102
103

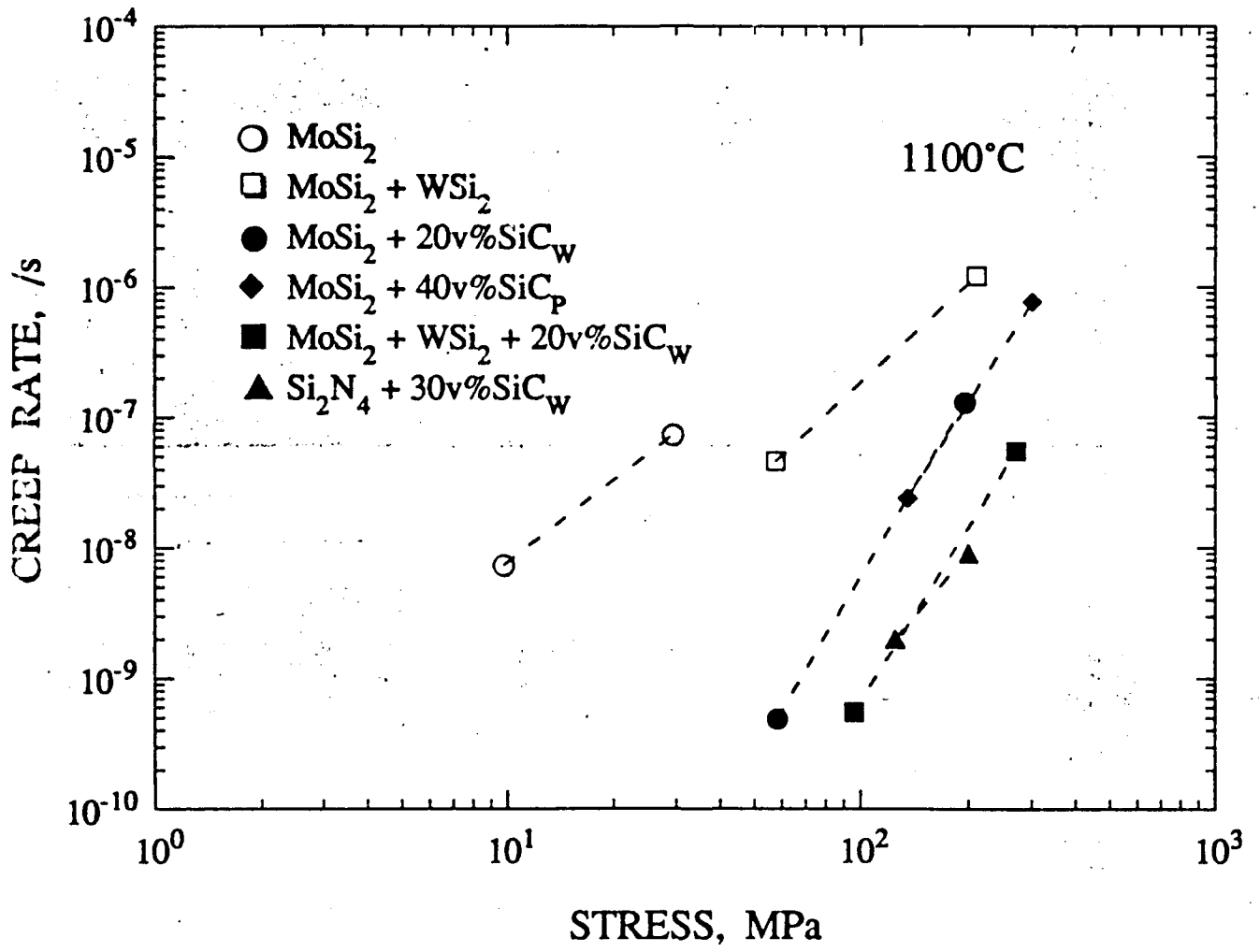
MoSi2
MoSi2 + WSi2
MoSi2 + 20v%SiCw
MoSi2 + 40v%SiCp
MoSi2 + WSi2 + 20v%SiCw
Si2N4 + 30v%SiCw
1100°C
CREEP RATE, /s
STRESS, MPa
10-4
10-5
10-6
10-7
10-8
10-9
10-10
100
101
102
103

TEM MICROGRAPH OF $MoSi_2$
DEFORMED BY CREEP AT 1200°C AND AT 11.5ksi

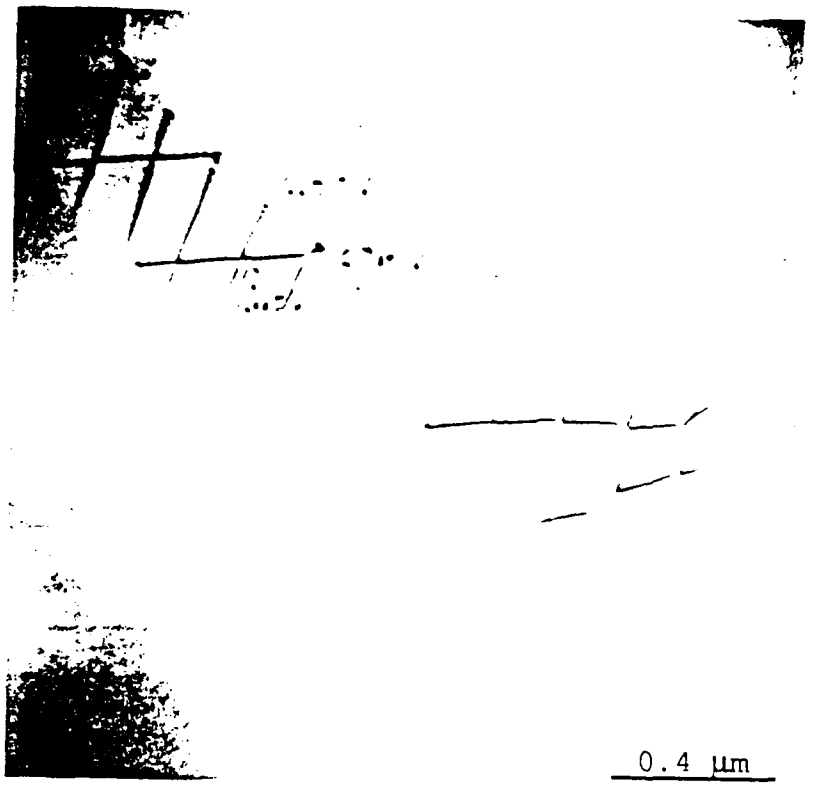

TEM MICROGRAPHS OF $MoSi_2$ + 20vol% SiC
(Undeformed)

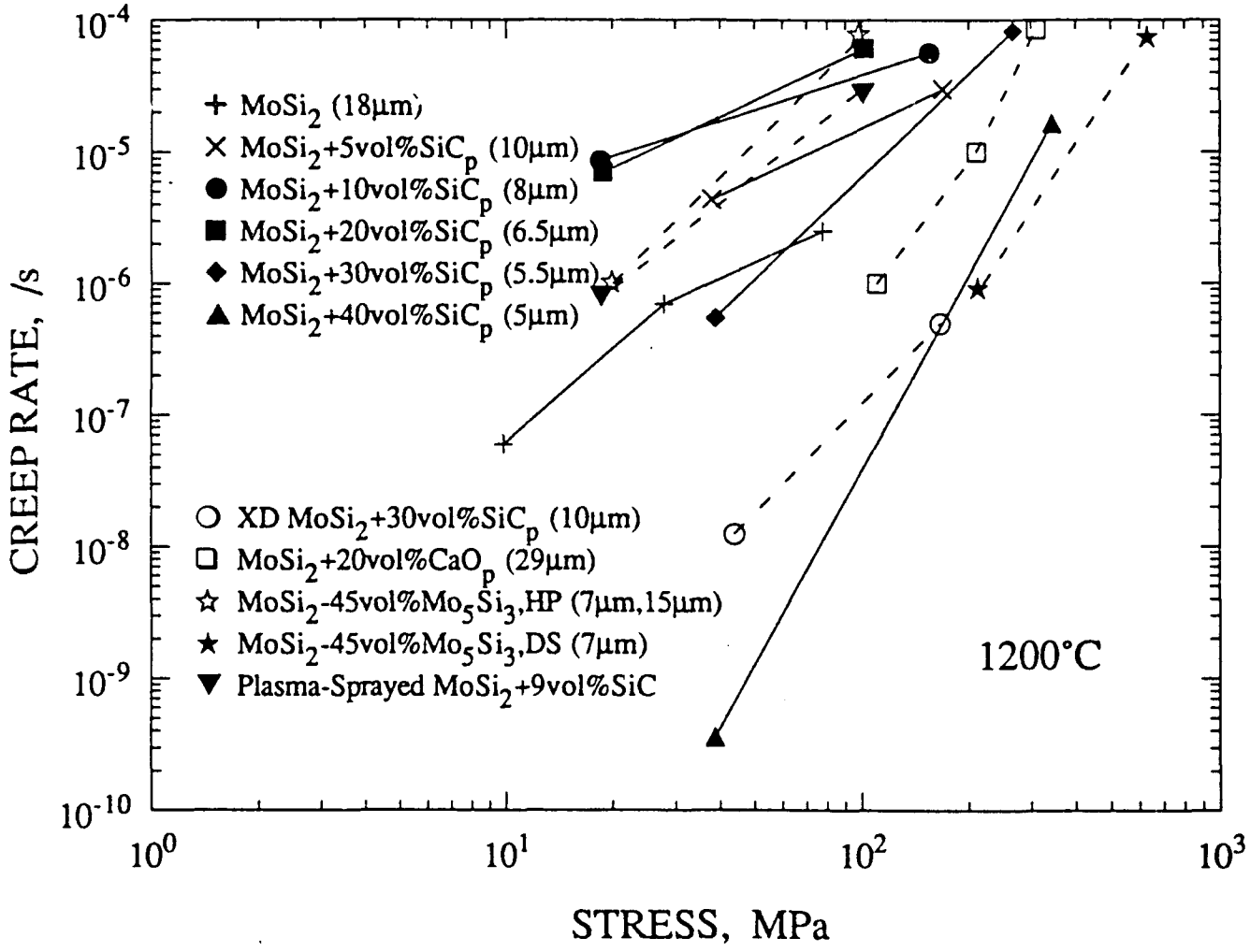
CREEP RATE, /s
STRESS, MPa
10^{-4}
10^{-5}
10^{-6}
10^{-7}
10^{-8}
10^{-9}
10^{-10}
10^{0}
10^{1}
10^{2}
10^{3}
+ $MoSi_2$ (18μm)
× $MoSi_2$+5vol%SiC_p (10μm)
● $MoSi_2$+10vol%SiC_p (8μm)
■ $MoSi_2$+20vol%SiC_p (6.5μm)
◆ $MoSi_2$+30vol%SiC_p (5.5μm)
▲ $MoSi_2$+40vol%SiC_p (5μm)
○ XD $MoSi_2$+30vol%SiC_p (10μm)
□ $MoSi_2$+20vol%CaO_p (29μm)
☆ $MoSi_2$-45vol%Mo_5Si_3,HP (7μm,15μm)
★ $MoSi_2$-45vol%Mo_5Si_3,DS (7μm)
▼ Plasma-Sprayed $MoSi_2$+9vol%SiC
1200°C

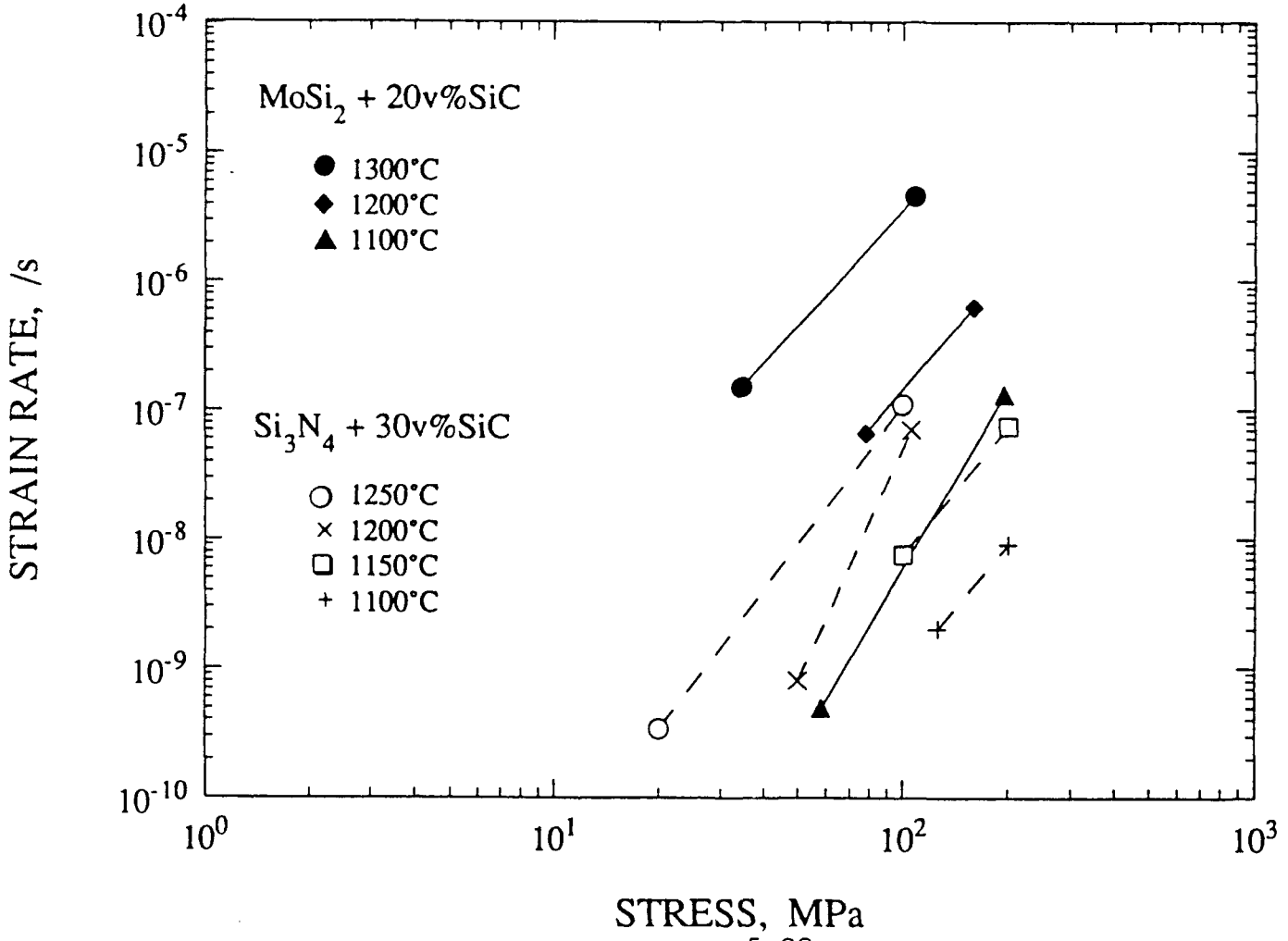
MoSi2 + 20v%SiC
1300°C
1200°C
1100°C
Si3N4 + 30v%SiC
1250°C
1200°C
1150°C
1100°C
STRAIN RATE, /s
STRESS, MPa
10-4
10-5
10-6
10-7
10-8
10-9
10-10
100
101
102
103

5.29

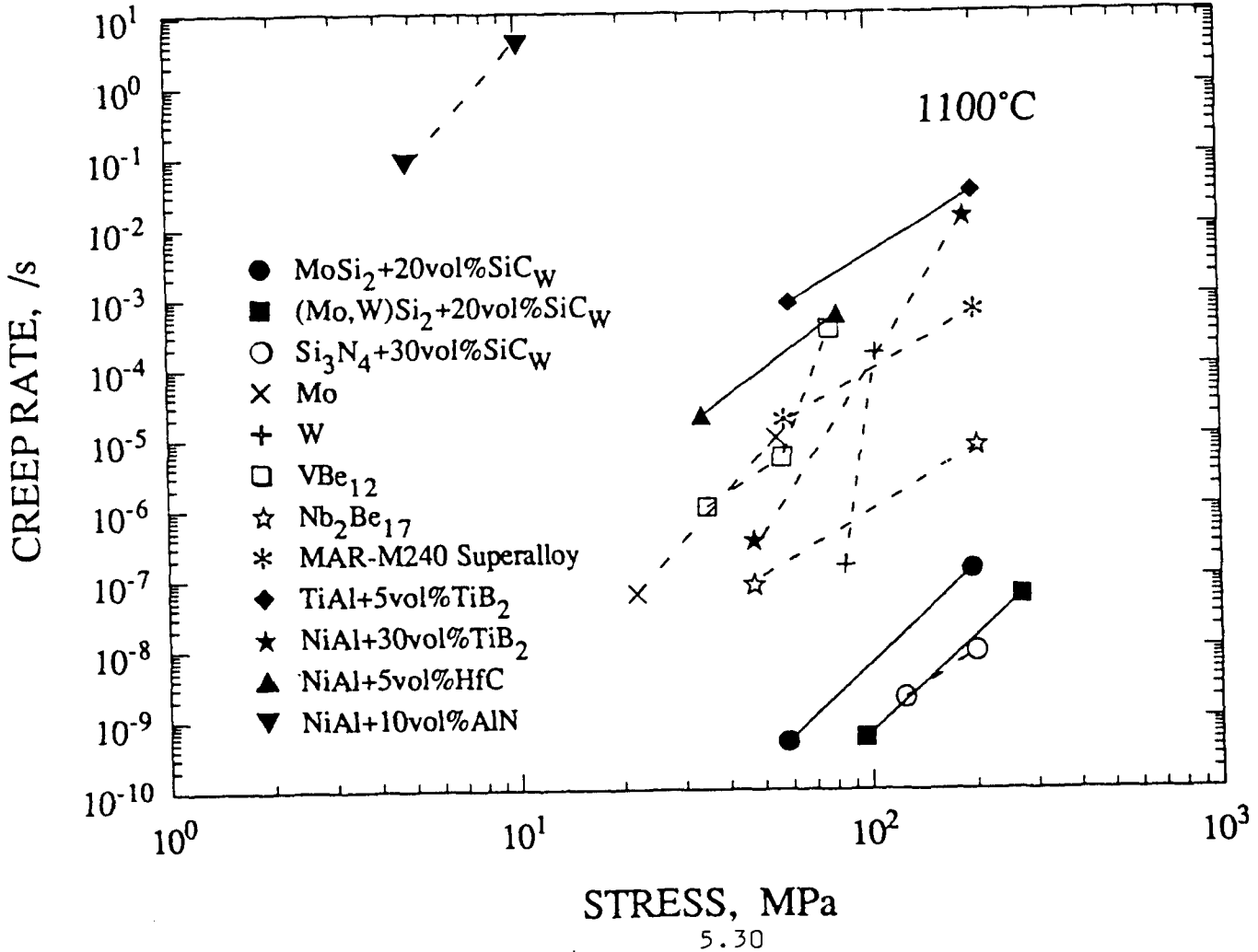
1100°C
CREEP RATE, /s
STRESS, MPa
10^{1}
10^{0}
10^{-1}
10^{-2}
10^{-3}
10^{-4}
10^{-5}
10^{-6}
10^{-7}
10^{-8}
10^{-9}
10^{-10}
10^{0}
10^{1}
10^{2}
10^{3}
$MoSi_2$+20vol%SiC_W
$(Mo,W)Si_2$+20vol%SiC_W
Si_3N_4+30vol%SiC_W
Mo
W
VBe_{12}
Nb_2Be_{17}
MAR-M240 Superalloy
TiAl+5vol%TiB_2
NiAl+30vol%TiB_2
NiAl+5vol%HfC
NiAl+10vol%AlN

5.30

Fig 21

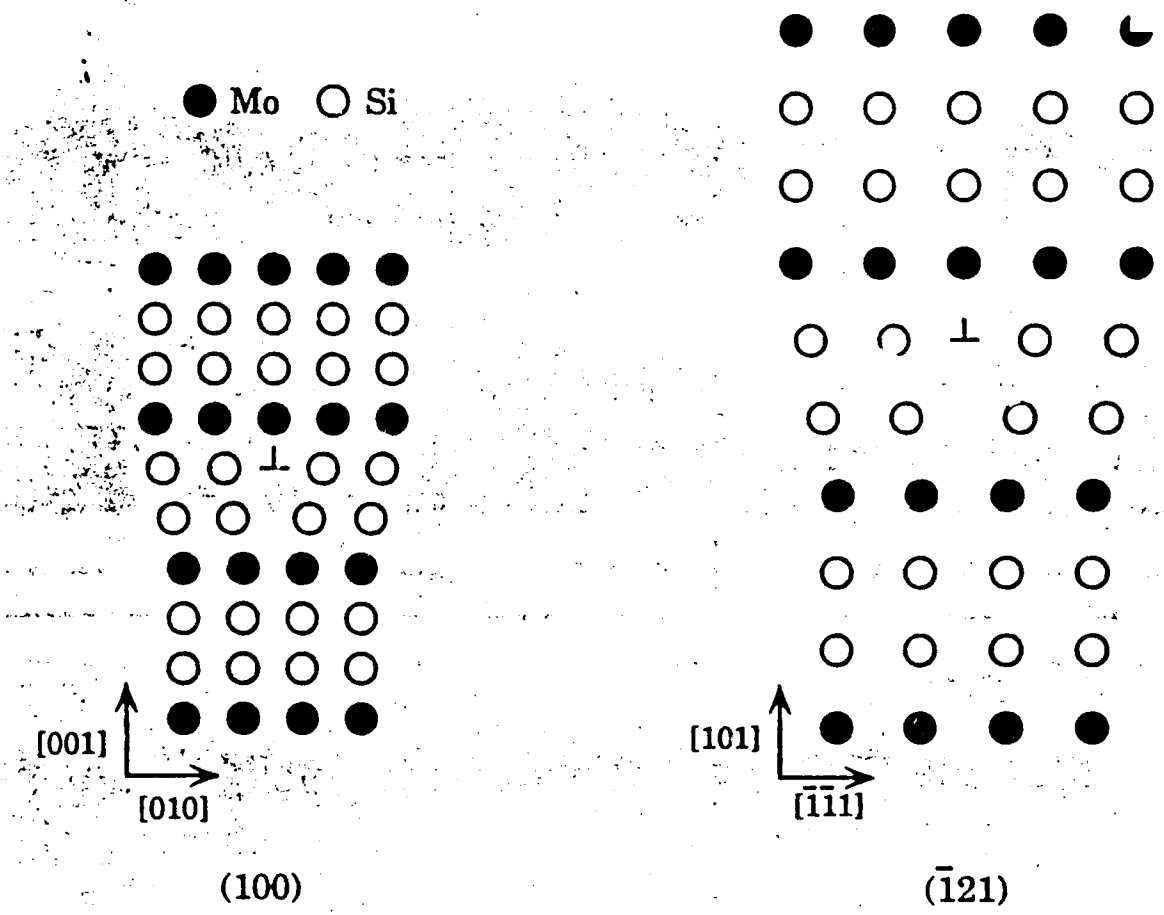

SUMMARY AND CONCLUSIONS

CREEP DEFORMATION BEHAVIOR OF ALUMINIDES AND SILICIDES AND THEIR COMPOSITES.

SIGNIFICANT IMPROVEMENT IN CREEP RESISTANCE BY REINFORCEMENT.

IN ALL CASES THE REINFORCEMENTS DEFORMS MOSTLY ELASTICALLY AT THE TEMPERATURES AND STRESSES INVESTIGATED.

ROLE OF BACK STRESSES OR INTERNAL STRESSES IN THESE MATERIALS ARE INSIGNIFICANT.

RATE CONTROLLING PROCESSES ARE PREDOMINANTLY CLIMB RELATED.

MOLYDISILICIDES ARE FAR SUPERIOR TO ALUMINIDES AND SUPERALLOYS IN TERMS OF CREEP RESISTANCE AT $T > 1000^{\circ}C$.

CONCLUSIONS

* Creep resistance of molydisilicides for superior to superalloys and intermetallic composites

* Grain size effects are very significant even in power-law creep regime

* Creep strengths of $MoSi_2$ Composites comparable to ceramic-ceramic systems

* Efforts should now be concentrated in enhancing low temperature toughness

6. Ordered Ground State Structures in HCP Alloys

A.K. Singh
Defence Metallurgical Research Laboratory,
and
Prof. S.Lele
Banaras Hindu University, India

ORDERED GROUND STATE STRUCTURES IN HCP ALLOYS

A.K.SINGH[1] AND S. LELE[2]

1. Defence Metallurgical Research Laboratory
   P.O. Kanchanbagh, Hyderabad-500258, India

2. Department of Metallurgical Engineering
   Institute of Technology
   Banaras Hindu University
   VARANASI-221005, India

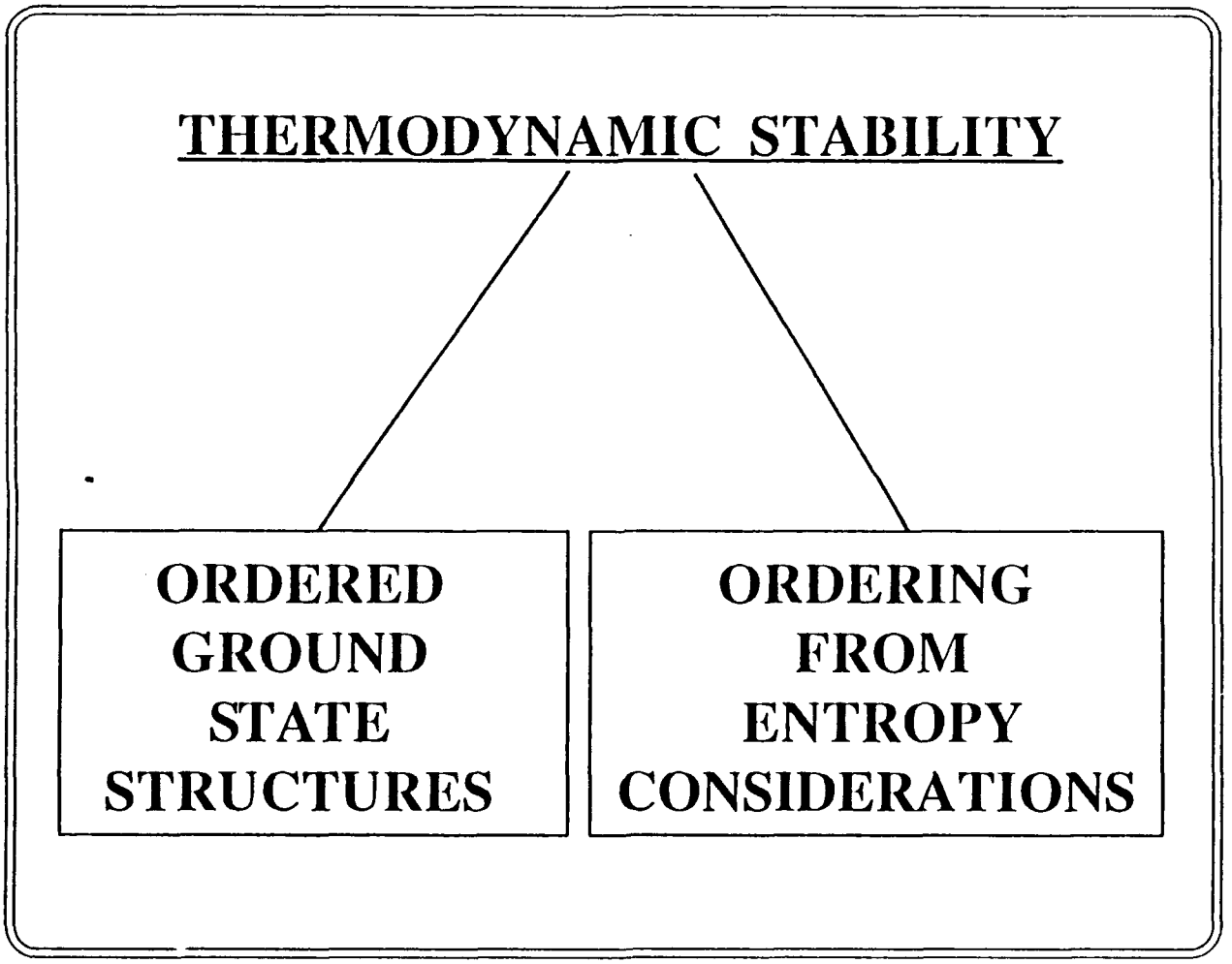
THERMODYNAMIC STABILITY
ORDERED GROUND STATE STRUCTURES
ORDERING FROM ENTROPY CONSIDERATIONS

GROUND STATE STRUCTURES

CONFIGURATION ENERGY

$$E = \sum_j (1/2)\, q_j\, W_j$$

q_j : number of jth neighbour A-B bonds

W_j : $2V^j_{AB} - V^j_{AA} - V^j_{BB}$ = Interchange energy

<u>For third neighbour interaction</u>

$$E = (1/2)\,(q_1W_1 + q_2W_2 + q_3W_3)$$

$$E/W = (1/2)\,(q_1 + q_2v_1 + q_3v_2)$$

where : $v_1 = W_2/W_1$ and $v_2 = W_3/W_1$

- DETAILS OF HCP STRUCTURE

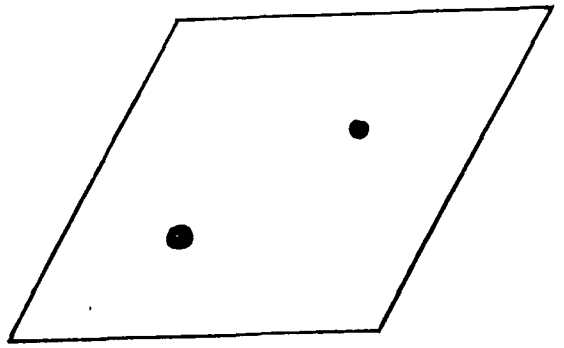

- SPACE GROUP $P6_3/mmc$

- ATOMIC POSITIONS

  2c $\bar{6}m2$ $\frac{1}{3}, \frac{2}{3}, \frac{1}{4}$; $\frac{2}{3}, \frac{1}{3}, \frac{3}{4}$

- CO-ORDINATION NUMBER 6 : 6 : 6

- IDEAL AND NON-IDEAL AXIAL RATIO

GENERAL ASSUMPTIONS:

- BINARY ALLOY

- NON-IDEAL AXIAL RATIO

PAIRWISE INTERACTIONS UPTO THIRD NEIGHBOUR

- ENERGY IS FUNCTION OF PAIRWISE INTERACTIONS ONLY

VIBRATIONAL AND SIZE EFFECTS ARE IGNORED

- VACANT SITES ARE NOT ALLOWED

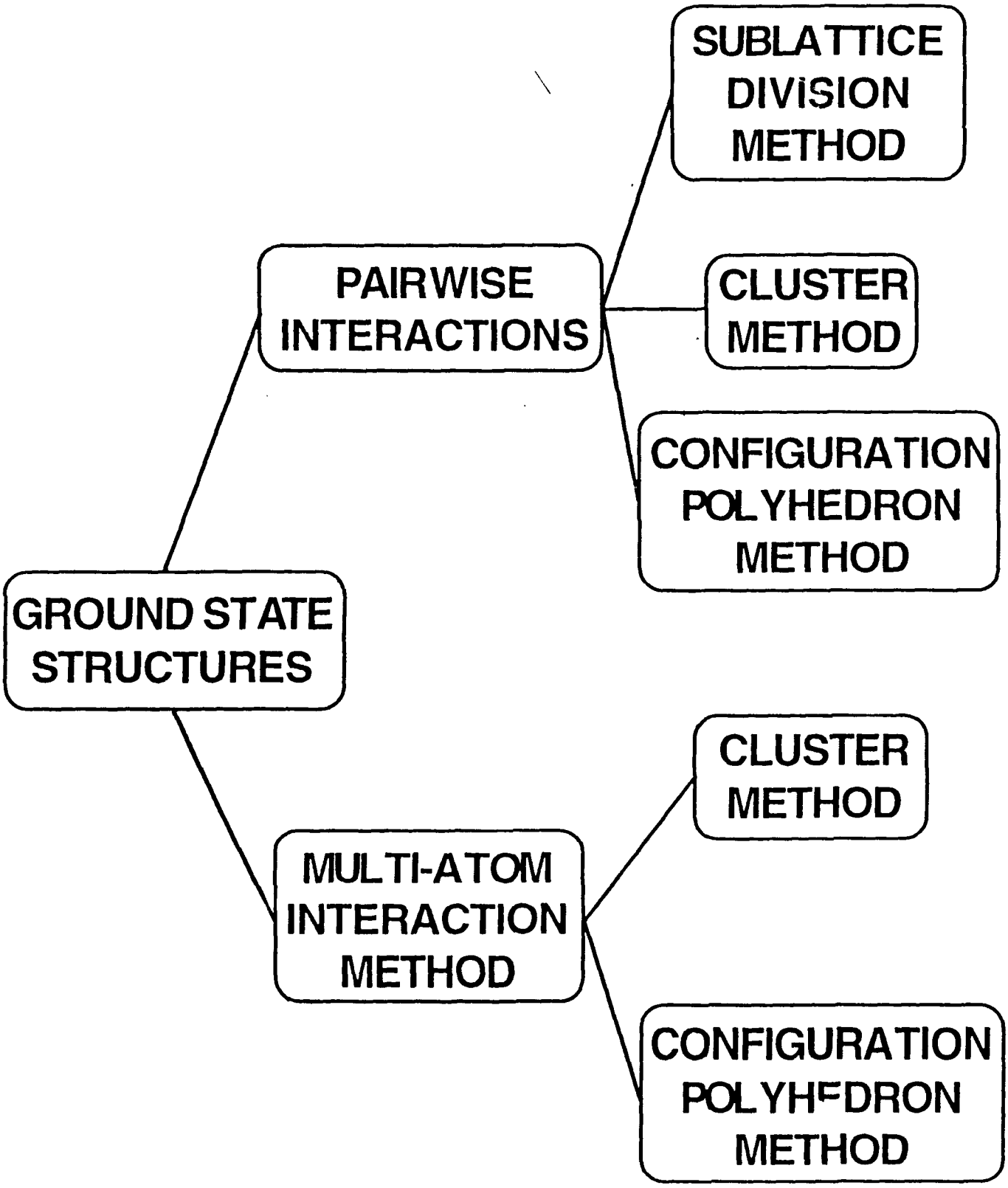
GROUND STATE STRUCTURES
PAIRWISE INTERACTIONS
SUBLATTICE DIVISION METHOD
CLUSTER METHOD
CONFIGURATION POLYHEDRON METHOD
MULTI-ATOM INTERACTION METHOD
CLUSTER METHOD
CONFIGURATION POLYHEDRON METHOD

CLASSIFICATION OF DISTINCT LAYER

(7 SUBLATTICES/LAYER

LAYER DESIGNATION	SITES OCCUPIED BY B ATOMS	FRACTION OF B ATOMS IN LAYER
L1	—	0
L2	1	1/7
L3	1, 2	2/7
L4	1, 2, 3	3/7
L5	1, 2, 4	3/7
L6	4, 5, 6, 7	4/7
L7	3, 5, 6, 7	4/7
L8	3, 4, 5, 6, 7	5/7
L9	2, 3, 4, 5, 6, 7	6/7
L10	1, 2, 3, 4, 5, 6, 7	1

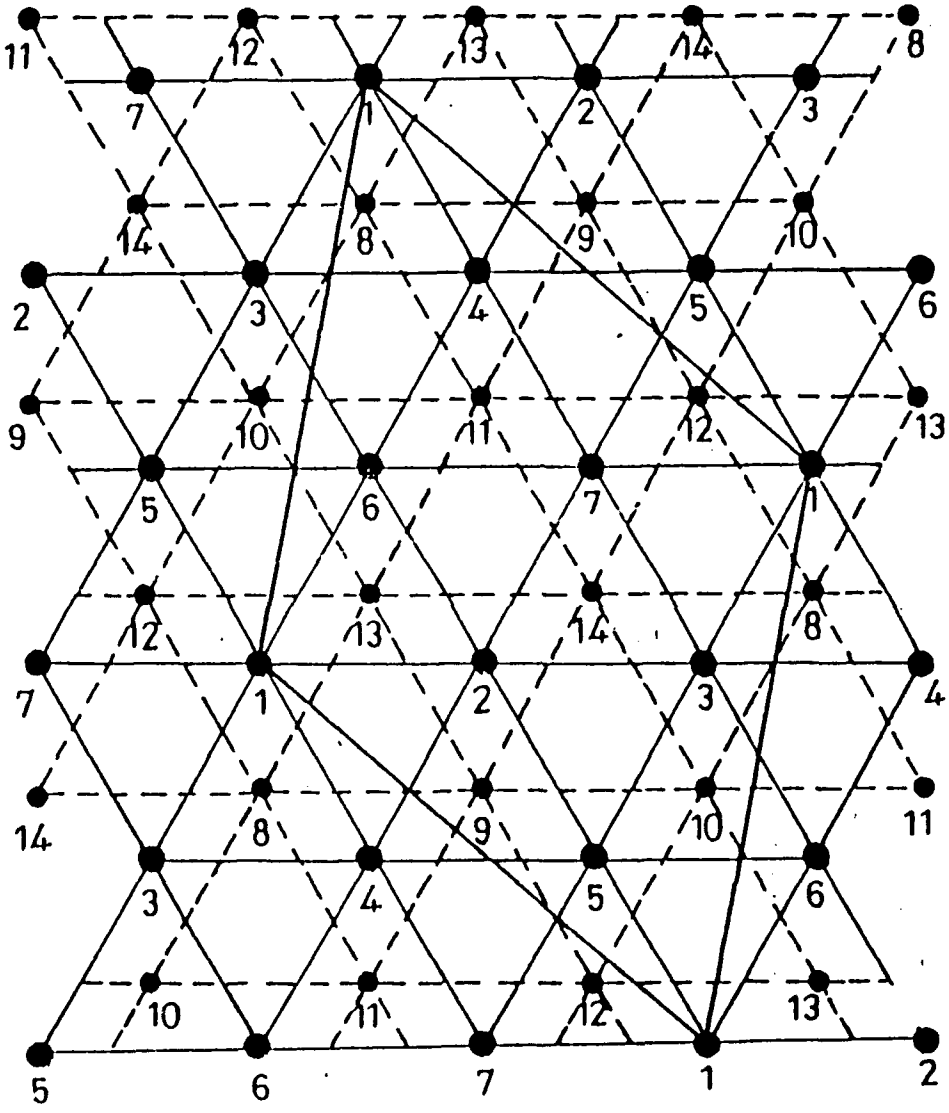
11
12
13
14
8
7
1
2
3
14
8
9
10
2
3
4
5
6
9
10
11
12
13
5
6
7
1
12
13
14
8
7
1
2
3
4
14
8
9
10
11
3
4
5
6
10
11
12
13
5
6
7
1
2

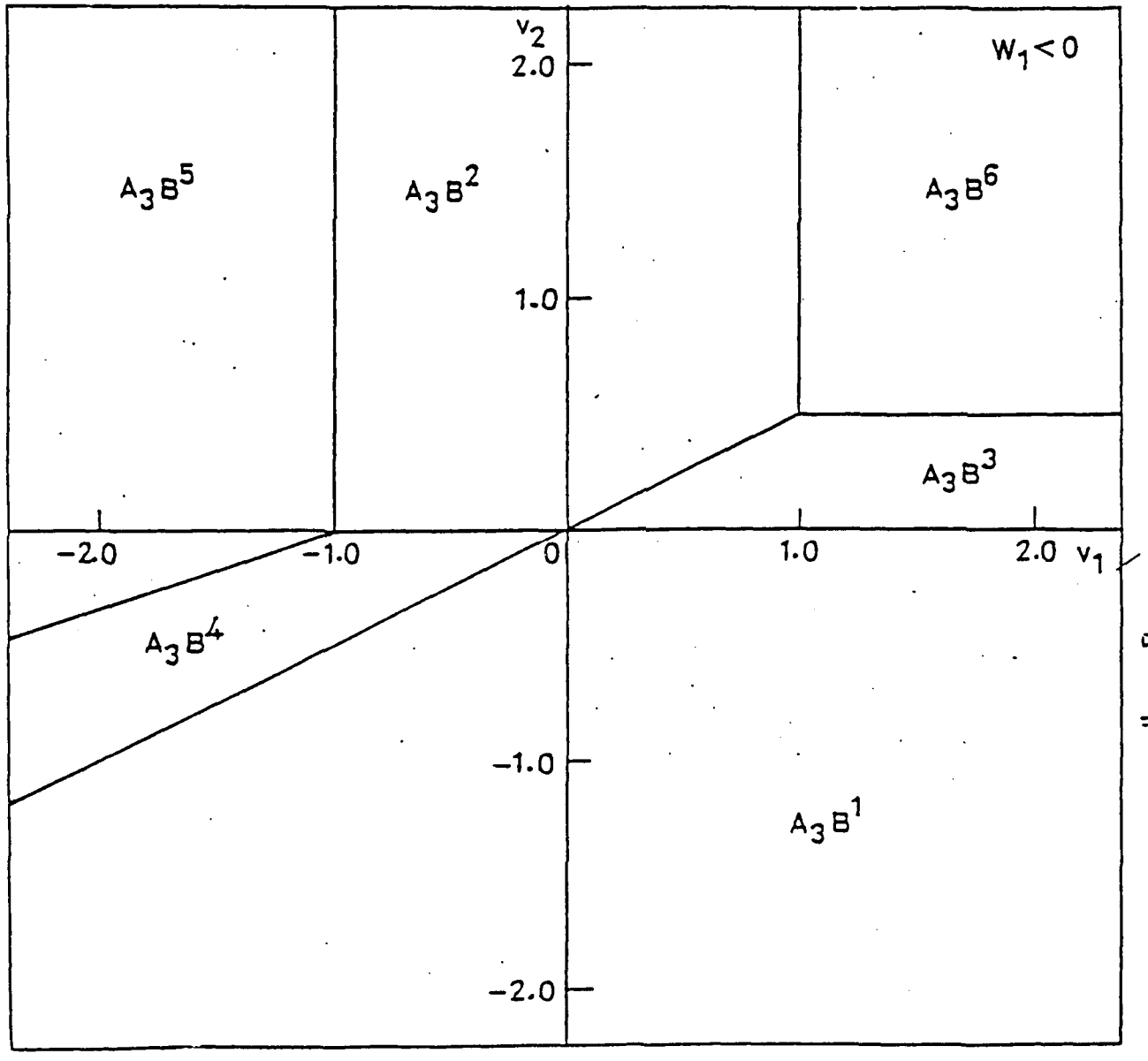

$E(A_3B^1) = E(A_3B$

$\Rightarrow v_2 = 0$

LOW ENERGY ORDERED STRUCTURE

ISO - ENERGY LINE

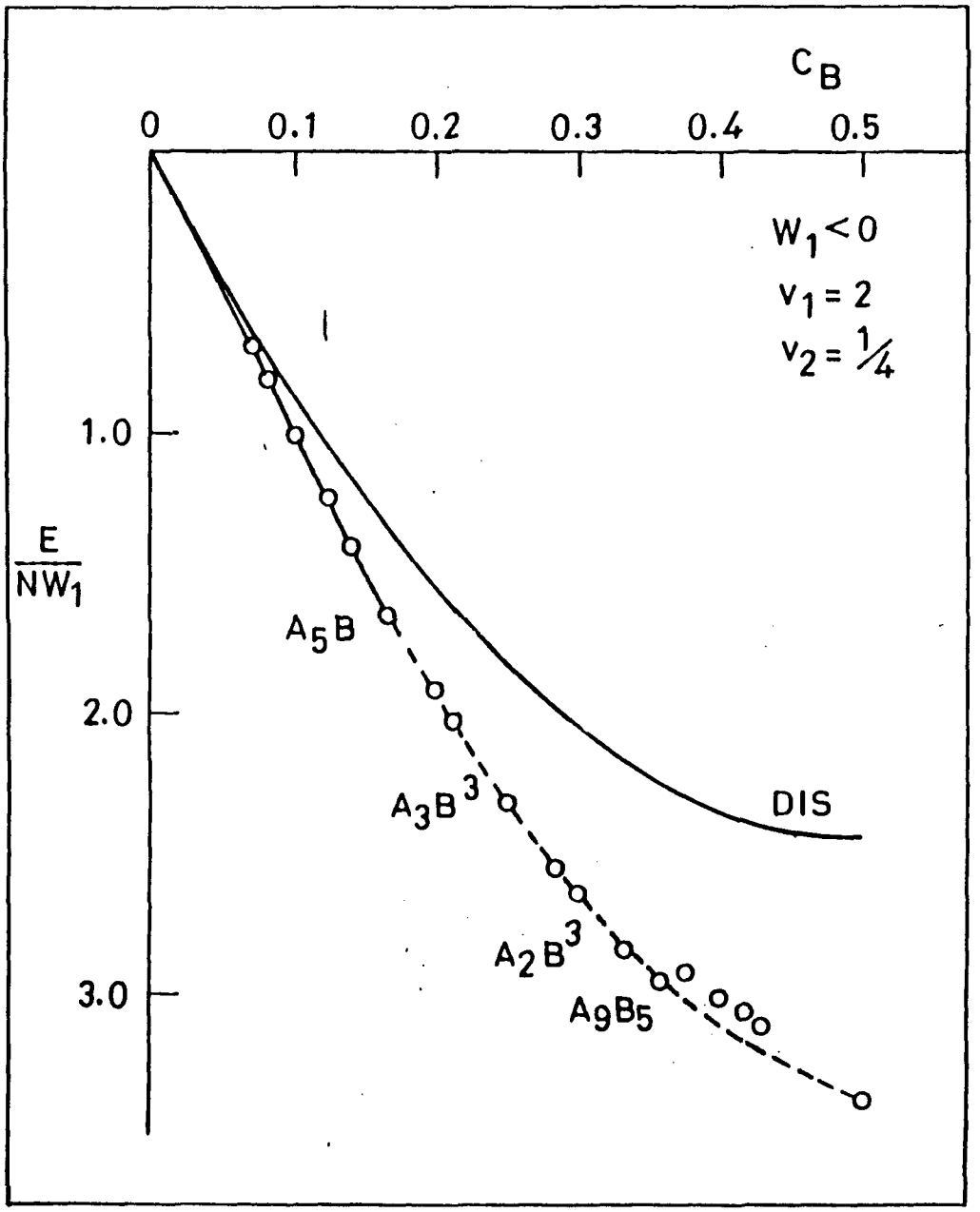
C_B
0
0.1
0.2
0.3
0.4
0.5
$W_1 < 0$
$v_1 = 2$
$v_2 = 1/4$
1.0
2.0
3.0
$\frac{E}{NW_1}$
A_5B
A_3B^3
A_2B^3
A_9B_5
DIS

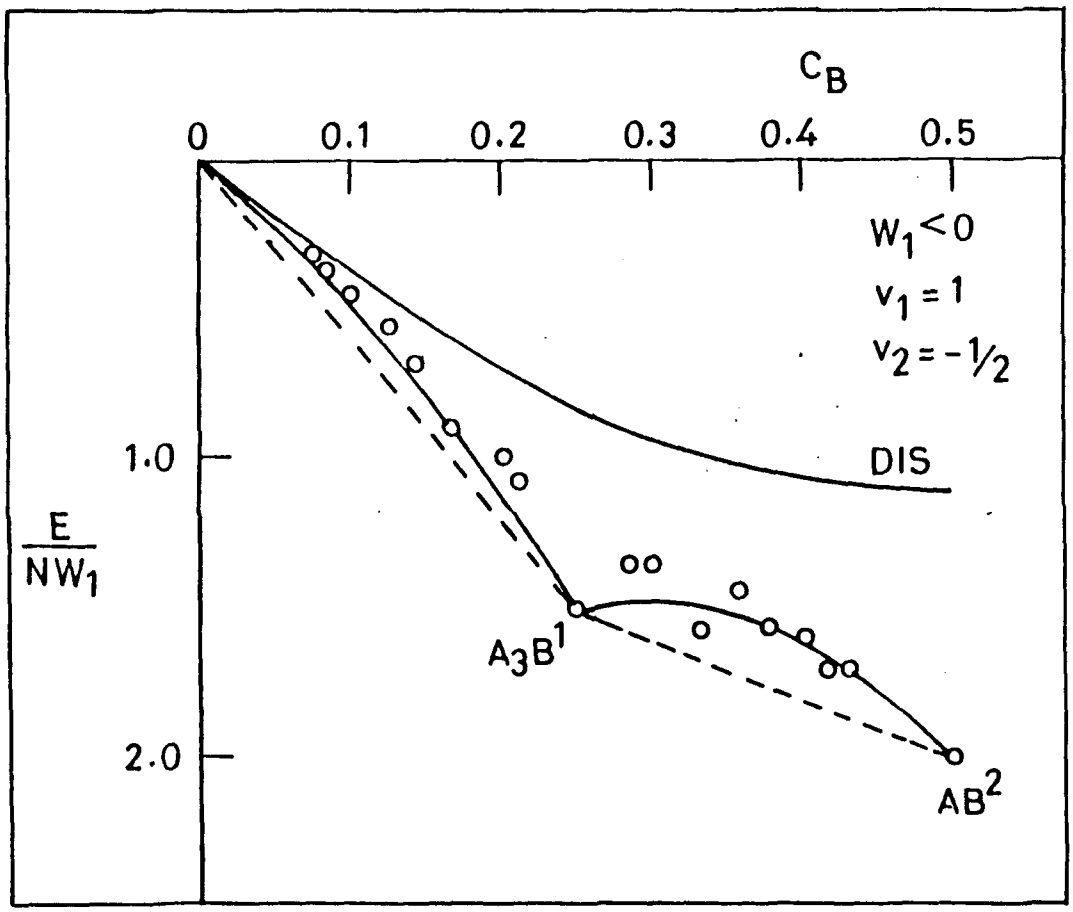
C_B
0
0.1
0.2
0.3
0.4
0.5
$W_1 < 0$
$v_1 = 1$
$v_2 = -1/2$
DIS
1.0
2.0
$\frac{E}{NW_1}$
A_3B^1
AB^2

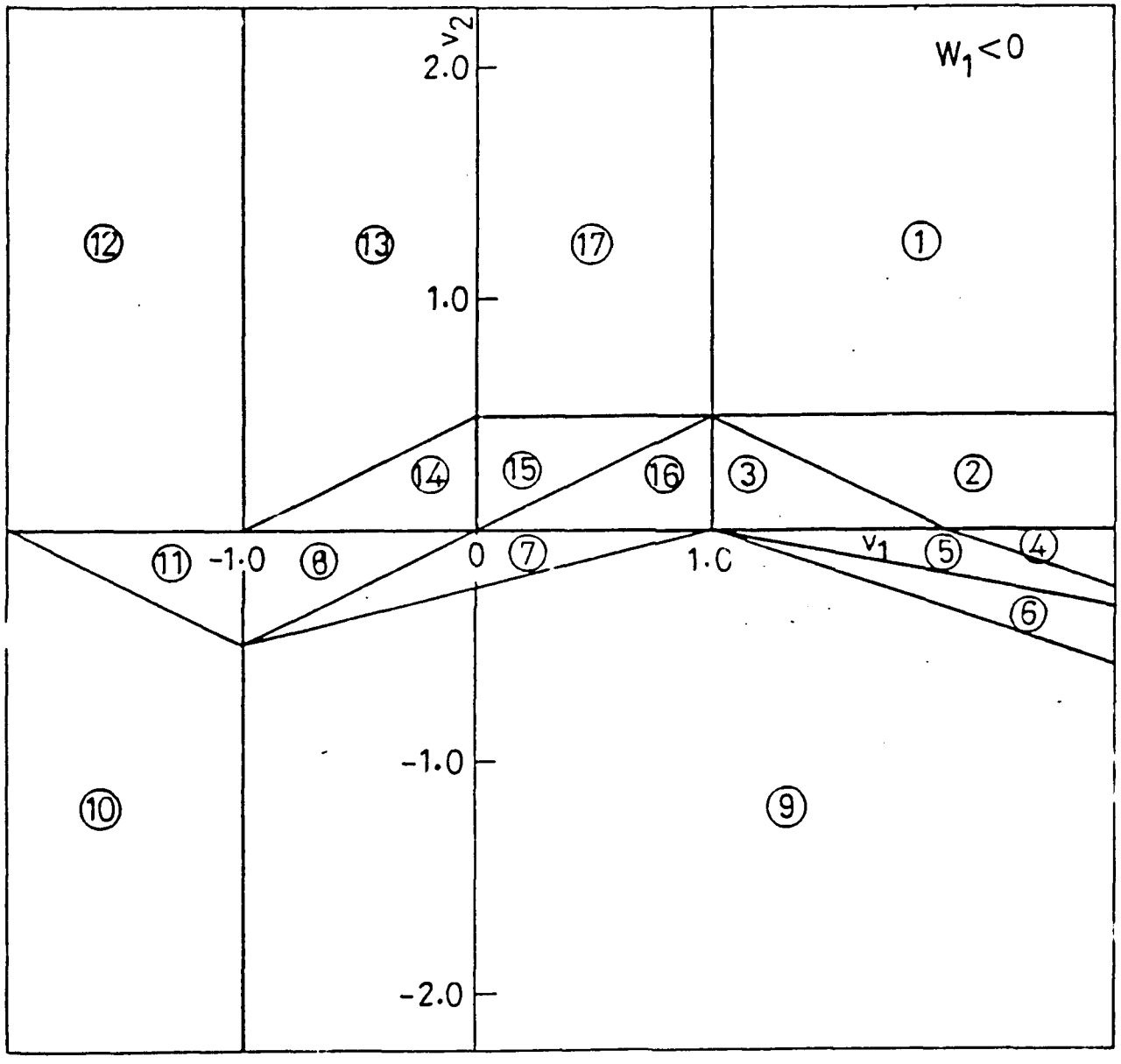
v_2
2.0
1.0
-1.0
-2.0
$W_1 < 0$
v_1
-1.0
0
1.0
1
2
3
4
5
6
7
8
9
10
11
12
13
14
15
16
17

SUBLATTICE DIVISION METHOD

- ATOMIC SITES OF HCP STRUCTURE CAN BE DIVIDED INTO 6, 8, 10, 16, 20, 24 AND 28 SUBLATTICES
- SUBLATTICE / LAYER
- POPULATE LAYERS : ALL POSSIBLE A & B ATOMS
- STRUCTURES : STACKING OF LAYERS
- RELATIVE STABILITY OF STRUCTURES
- STABILITY DOMAINS
- COMPOSITE MAP

RESULTS : 15 STRUCTURES

A_5B, A_3B (3), A_2B (1), A_9B_5, A_7B_5, AB (5)

CRYSTALLOGRAPHIC DETAILS :

BRAVAIS LATTICE
SPACE GROUP
No OF ATOMS PER UNIT CELL
PEARSON SYMBOL
LATTICE PARAMETERS
COORDINATES OF EQUIVALENT POSITIO

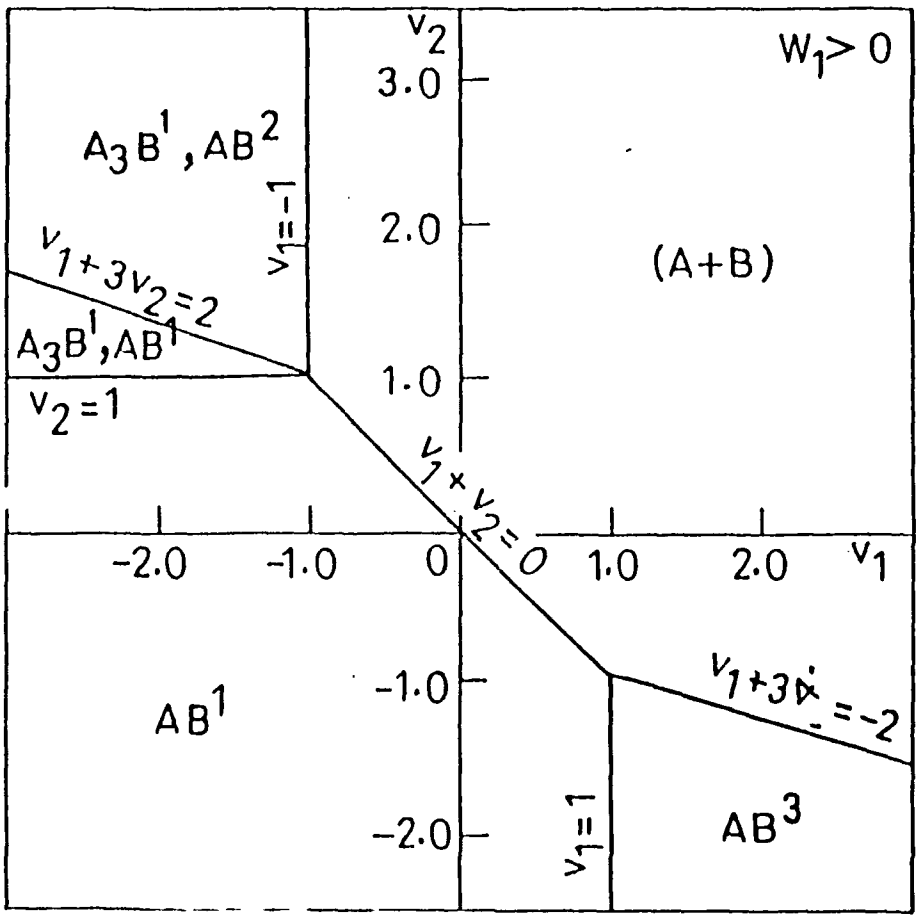
v_2
$W_1 > 0$
3.0
A_3B^1, AB^2
$v_1 = -1$
2.0
(A+B)
$v_1 + 3v_2 = 2$
A_3B^1, AB^1
1.0
$v_2 = 1$
$v_1 \times v_2 = 0$
-2.0
-1.0
0
1.0
2.0
v_1
$v_1 + 3v_2 = -2$
AB^1
-1.0
-2.0
$v_1 = 1$
AB^3

- RESULTS

- SUBLATTICES 6, 8(2), 10, 12(2), 14(2), 16(2), 20, 24(2), 28(2)

  FOR GROUND STATE 6, 8(2), 10, 12(2), 14(2)

- $W_1 < 0$

- 15 GROUND STATE STRUCTURES

  A_5B, A_3B (3), A_2B (4), A_9B_5, A_7B_5, AB (5)

- $W_1 > 0$

  4 GROUND STATE STRUCTURES OUT OF ABOVE 15

- DEGENERATE STRUCTURES

1. A_5B (I) A_5B (II) A_5B (III)

   HEXAGONAL ORTHORHOMIC MONOCLINIC

2. A_7B PARTIAL ORDERD 6 SUBLATTICES

   ORDERED 8 SUBLATTICES

- SOLID SOLUTION

  MISCIBILITY GAP

  ADJACENT STOICHIOMETRIC STRUCTURES BASED ON SAME SUBLATTICES (TWO SITES PARTIALLY OCCUPIED)

CLUSTER METHOD

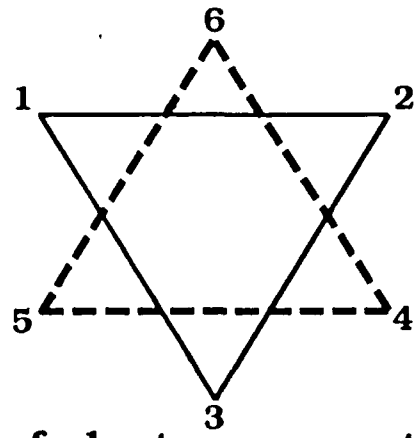

- MOTIF
- CLUSTER
- WEIGHT
- ENERGY: Linear function of cluster concentration
- MINIMISATION OF ENERGY: Linear programming method (Two cluster solution)
- Realisation of solution on hcp atomic sites in a consistent manner
- RESULT : 9 structures
  A_5B, $A_3B(3)$, A_2B, $AB(4)$
- LIMITATIONS

- CLUSTER METHOD

- MOTIF $X_k w_k = Y_k$ (WEIGHTED FRACTION
- CLUSTER 13 POSSIBLE CLUSTES
- WEIGHT

$$Y_1 + Y_2 + Y_3 + Y_4 + Y_5 + Y_6 + Y_7 + Y_8 + Y_9 + Y_{10} + Y_{11} + Y_{12} + Y_{13} = 1 \quad (1)$$

$$Y_2 + 2Y_3 + 2Y_4 + 2Y_5 + 3Y_6 + 3Y_7 + 3Y_8 + 4Y_9 + 4Y_{10} + 4Y_{11} + 5Y_{12} + 6Y_{13} = 6C \quad (2)$$

- ONE CAN WRITE NO OF AB BOND (q_j) AS

$$\frac{q_j}{N} = \frac{1}{2} \sum_k q_{jk} Y_k \qquad \text{FOR } j = 1, 2$$

$$= \sum_k q_{jk} Y_k \qquad \text{FOR } j = 3$$

- ONE CAN OBTAIN THE CONFIGURATIONAL ENERGY

$$E = \frac{1}{2} N W_1 [Y_2 (1 + v_1 + v_2) + Y_3 (1 + 2v_1 + 2v_2) + Y_4 (2 + v_1 + 2v_2) + Y_5 (2 + 2v_1) + Y_6 (3v_1 + 3v_2) + Y_7 (2 + v_1 + 3v_2) + Y_8 (2 + 2v_1 + v_2) + Y_9 (2 + 2v_1) + Y_{10} (2 + v_1 + 2v_2) + Y_{11} (1 + 2v_1 + 2v_2) + Y_{12} (1 + v_1 + v_2)]$$

- SOLUTIONS : LINEAR PROGRAMMING METHOD

RESULTS

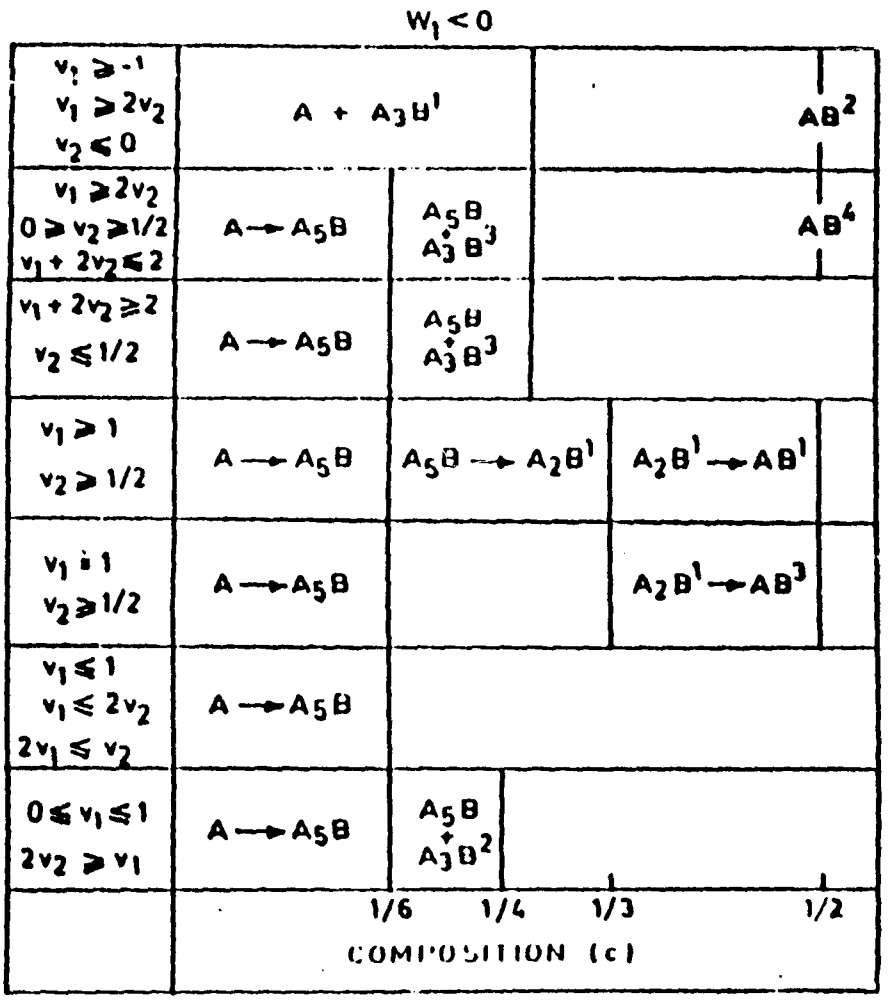

Fig. 7. Different structures obtained by cluster method as a function of composition

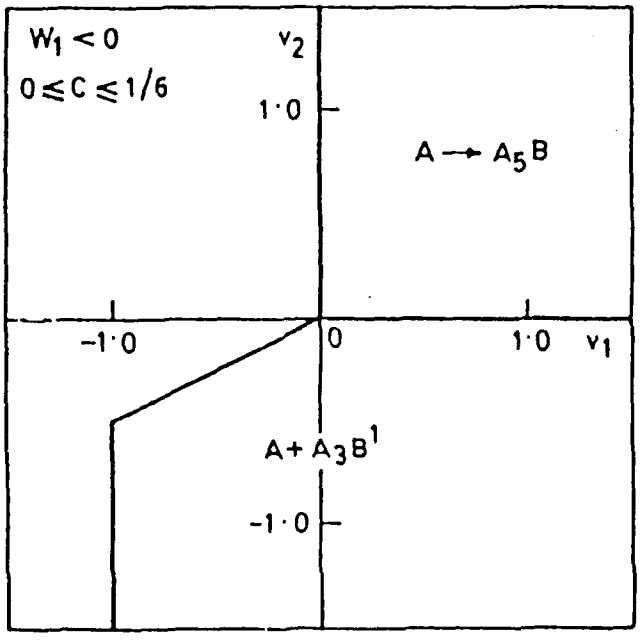

Fig. 3. Stability regions of structures obtained by cluster method as a function of interchange energy ratios v_1 and v_2 for $W_1 < 0$ and $0 \leq C \leq 1/6$. Arrows indicate stable solid solution at intermediate composition while the plus sign corresponds to a miscibility gap.

CONFIGURATION POLYHEDRON METHOD

- MOTIF
- Structural inequalities:
  half space (r_1, r_2, r_3, C)
- Convex polyhedron: Configuration polyhedron
- Realisation of solution on hcp atomic sites in a consistent manner
- RESULTS
  - 15 structures
  - Series of long period APB modulated superstructures with stoichiometries $A_{n+3}B_{n+1}$
  - Entire surface of the configuration polyhedron corresponds to ground state structures
- LIMITATIONS

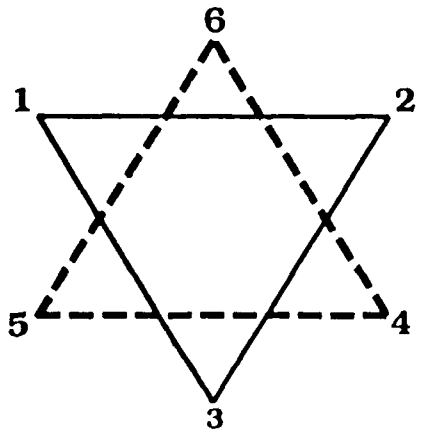

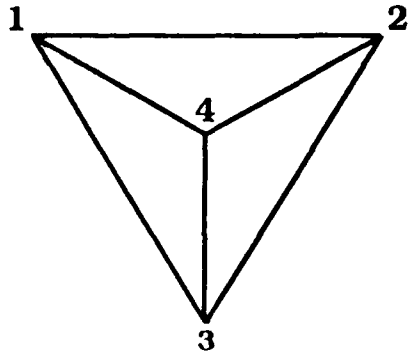

CONFIGURATION POLYHEDRON METHOD

- MOTIF

$$E/NW_1 = \left(3c - \frac{r_1}{N}\right) + \left(3c - \frac{r_2}{N}\right)u_1 + \left(3c - \frac{r_3}{N}\right)u_2$$

STRUCTURAL INEQUALITIES $(M = 14)$

r_1, r_2, r_3, c

EACH INEQUALITY REPRESENTS A HALF SPACE BOUNDED BY A HYPERPLANE ON WHICH THE INEQUALITY BECOMES EQUALITY

- SOLUTION : 4 INEQUALITIES FROM THE SET OF M ARE SELECTED AND TREATED EQUALITY

<u>POSSIBILITIES</u> (i) SOLUTION DOES NOT EXIST

(ii) A SOLUTION EXISTS BUT DOES NOT SATISFY ONE OR MORE REMAINING INEQUALITIES

(iii) A SOLUTION EXISTS THAT SATISFIES THE REMAINING INEQUALITIES

ONLY CASE (iii) CORRESPONDS TO A VERTEX OF CONFIGURATION POLYHEDRON

REALISATION OF STRUCTURE ON HCP ATOMIC SITES

RESULTS

LIMITATIONS (i) VIRTUAL STRUCTURE

(ii) STRUCTURAL REALISATION

One can write a general expression for the number $r_1, \ldots, r_3$ of B–B bonds, concentration Y_1, Y_5, Y_6 and energy of the nth member of the series as follows:

$$r_1 = \frac{3n(n+1)}{2(n+2)^2}, \tag{18}$$

$$r_2 = 0, \tag{19}$$

$$r_3 = \frac{3(n+1)}{(n+2)^2}, \tag{20}$$

$$C_n = \frac{n+1}{2(n+2)}, \tag{21}$$

$$Y_1 = \frac{1}{(n+2)^2}, \tag{22}$$

SPACE GROUP
P 6₃/mmc

$$Y_5 = \frac{3(n+1)}{(n+2)^2}, \tag{23}$$

$$Y_6 = \frac{n(n+1)}{(n+2)^2} \tag{24}$$

and

$$\frac{E_n}{NW_1} = \frac{3}{2}\frac{n+1}{(n+2)^2}[2+(n+2)v_1+nv_2]. \tag{25}$$

$a = a_d[n+2]$ [100]

Fig. 3

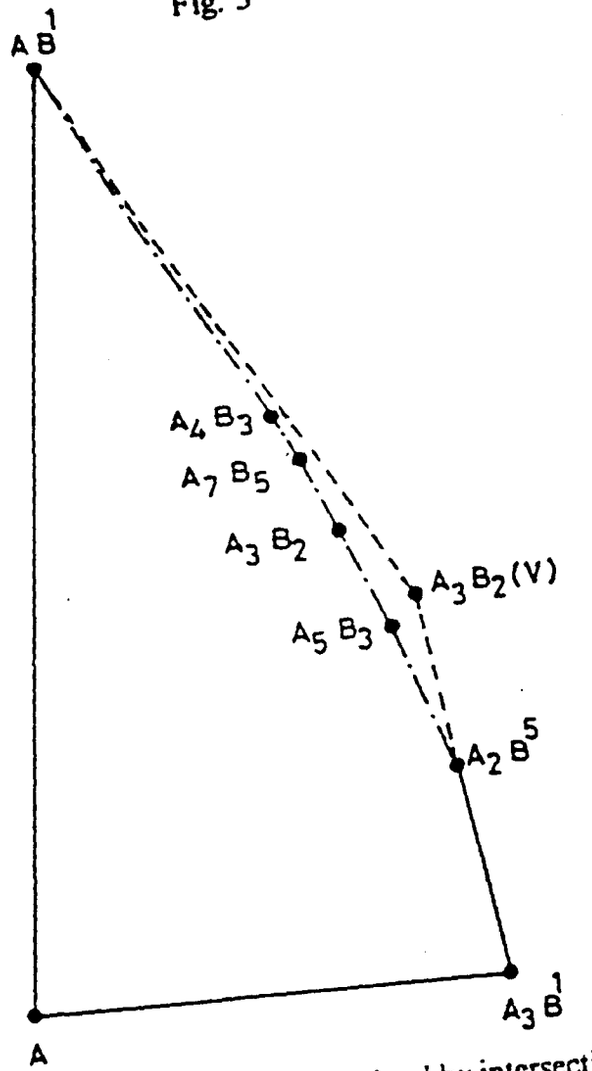

2D planar surface of configuration polyhedron obtained by intersection of hyperplanes 2 and 8. The solid lines join the vertices corresponding to real structures. The broken lines join the vertices which correspond to real and virtual structures while the chain lines join the points which correspond to the structures obtained by appropriate cluster combinations. The structures succeeding A_4B_3 ($n > 5$) are not shown in the figure, since the points [illegible] such structures) are very close.

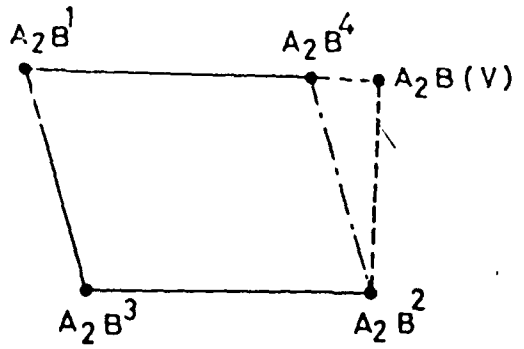

(*a*)

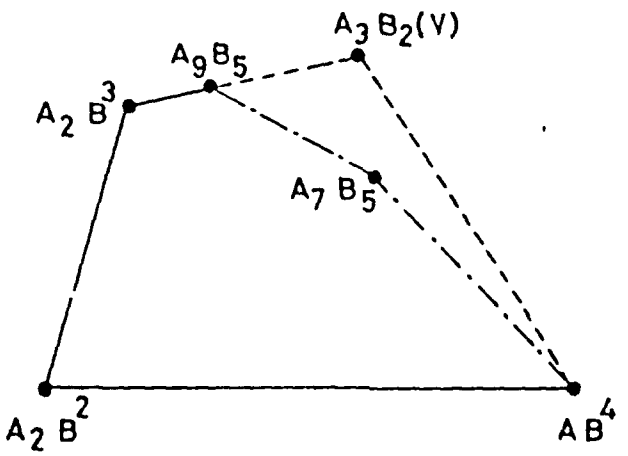

(*b*)

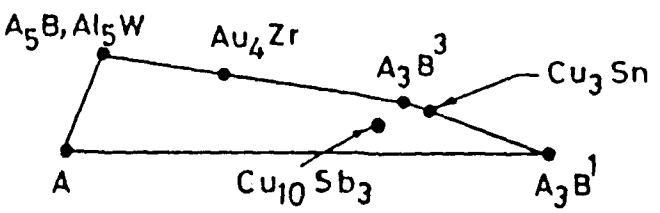

(*c*)

2D planar surface of configuration polyhedron obtained by intersection of hyperplanes (*a*) 4 and 5, (*b*) 5 and 9 and (*c*) 1 and 2.

MULTI-ATOM INTERACTION METHOD

- CLUSTER METHOD
- MOTIF [Tetrahedron]
- Multi-atom interaction parameters
  [4 body force]
- Look for minimum number of variables
- MINIMISE ENERGY IN PARAMETER SPACE
- RESULTS

  A_3B, A_2B, AB, AB_2 and AB_3

Table 1. Possible cluster configurations on the motif (Fig. 1) and their energies.

cluster type i	cluster configuration/ sites occupied by B atoms	weight of the cluster w_i	composition of the cluster c_i	first neighbour unlike pairs n_i^{I}	second neighbour unlike pairs n_i^{II}	cluster energy ε_i
0	-	1	0	0	0	0
1	1	3	1/4	2	1	$3/2W(1+\alpha)$
2	4	1	1/4	0	3	$3/2W(1+\beta)$
3	1,2	3	1/2	2	2	$2W$
4	1,4	3	1/2	2	2	$2W$
5	1,2,3	1	3/4	0	3	$3/2W(1+\gamma)$
6	1,2,4	3	3/4	2	1	$3/2W(1+\delta)$
7	1,2,3,4	1	1	0	0	0

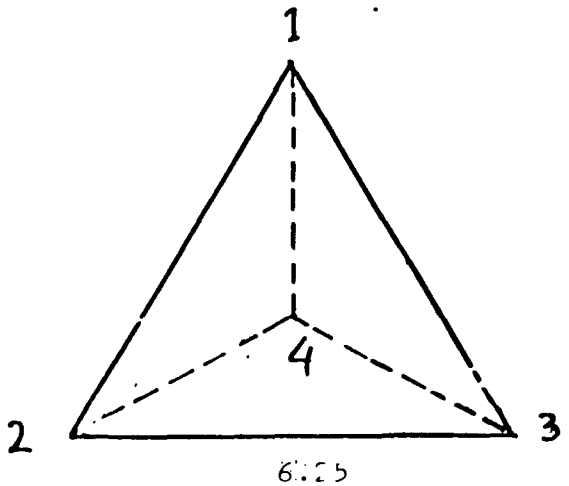

Table 3. Crystallographic data for the structures pertinent to the ground state ordered h.c.p. alloys.

Phase	Space group	Pearson symbol	Lattice vector in units of a_d and c_d			M/K	Sublattice type occupied by B atoms
			a	b	c		
A_5B(I)	$P\bar{6}2m$ D^1_{3h}	hP6	[210]	[$\bar{1}$10]	[001]	6 2	1
A_5B(II)	Pnmm (Pmmn) D^{13}_{2h}	oP12	[$\bar{1}$10]	[330]	[001]	12 2	1,9
A_5B(III)	Pm C^1_s	mP12	[$\bar{1}$20]	[220]	[001]	12 3	1,9
A_3B^1	$P6_3/mmc$ D^4_{6h}	hP8	[200]	[020]	[001]	8 3	1,5
A_3B^2(I)	C2mm (Amm2) C^{14}_{2v}	oC16	[420]	[020]	[001]	8 3	1,6
A_3B^2(II)	Pm C^1_s	mP8	[$\bar{1}$10]	[220]	[001]	8 2	1,5
A_3B^3	Pnmm (Pmmn) D^{13}_{2h}	oP8	[210]	[020]	[001]	8 3	1,6
A_2B^1	$P\bar{6}2m$ D^1_{3h}	hP6	[210]	[$\bar{1}$10]	[001]	6 2	1,2
A_2B^2	Ccmm (Cmcm) D^{17}_{2h}	oC12	[120]	[300]	[001]	6 2	1,4
A_2B^3(I)	$Pn2_1m$ ($Pmn2_1$) C^7_{2v}	oP12	[$\bar{1}$10]	[330]	[001]	12 2	1,2,9,10
A_2B_3(II)	Ccmm (Cmcm) D^{17}_{2h}	oC12	[3$\bar{3}$0]	[110]	[001]	12 3	1,4,9,12
A_2B^4(I)	Pnmm (Pmmn) D^{13}_{2h}	oP12	[$\bar{1}$10]	[330]	[001]	12 2	1,3,5,1
A_2B^4(II)	Pm C^1_s	mP12	[$\bar{1}$20]	[220]	[001]	12 3	1,3,9,1[illegible]
A_9B_5	Pm C^1_s	mP14	[310]	[230]	[001]	14 3	1,2,3,5,11
A_7B_5	Pm C^1_s	mP12	[$\bar{1}$20]	[220]	[001]	12 3	[illegible],2,4,9,12
AB^1	$P\bar{6}m2$ D^1_{3h}	hP2	[100]	[010]	[001]	8 3	1,2,3,4
AB^2	Pcmm (Pmma) D^5_{2h}	oP4	[210]	[010]	[001]	8 3	1,2,5,6
AB^3	Pnmm (Pmmn) D^{13}_{2h}	oP4	[210]	[010]	[001]	8 3	1,2,7,8
AB^4	Pnam (Pnma) D^{16}_{2h}	oP8	[$\bar{1}$10]	[220]	[001]	8 2	1,2,6,7
AB^5	Pcam (Pbcm) D^{11}_{2h}	oP8	[$\bar{1}$10]	[220]	[001]	8 2	1,2,5,8

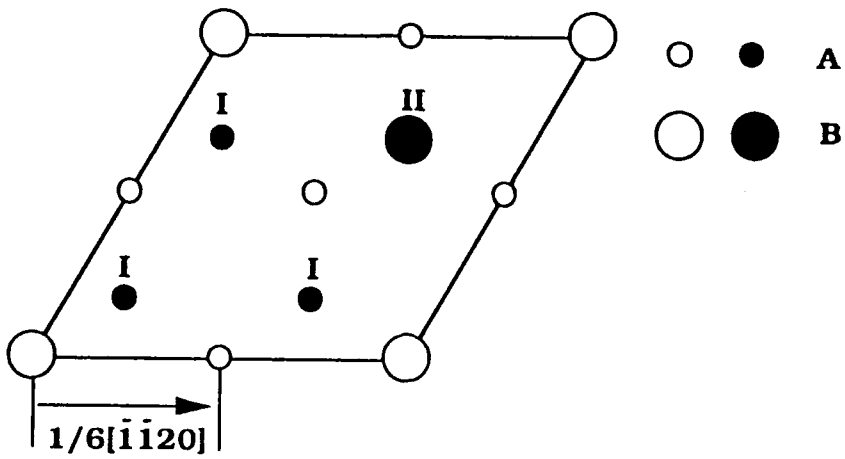

SPACE GROUP : $P6_3/mmc$

NO OF ATOMS PER UNIT CELL : 8

PEARSON'S SYMBOL : hP8

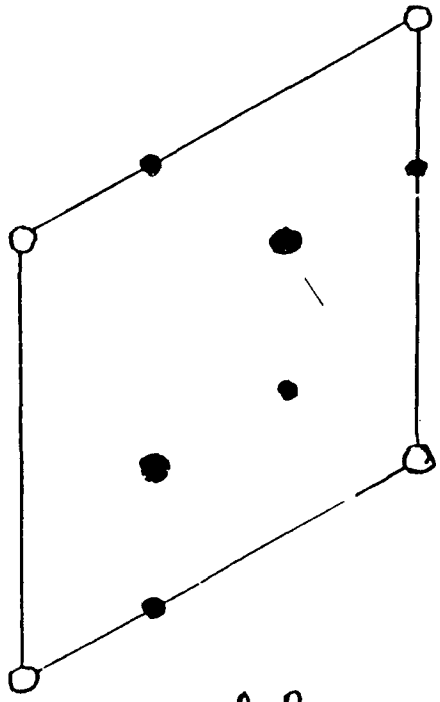

AsB

$E_{AsB} = \frac{1}{2}(1 + v_1 + v_2)$

AsB : HEXAGONAL

$P\bar{6}2m$ OR D_{3h}^{3} ; 6 ATOMS PER UNIT CELL

$hP6$

$a = a_d[210]$, $b = a_d[\bar{1}10]$ and $c = c_d[001]$

co-ordinates of equivalent positions

(1) 1 B atom at $(0,0,0)$ $(\bar{6}2m)$

(2) 2 A atoms at $(\frac{1}{3}, \frac{2}{3}, 0)$; $(\frac{2}{3}, \frac{1}{3}, 0)$ $(\bar{6})$

(3) 3 A atoms at $(\frac{1}{3}, 0, \frac{1}{2})$; $(0, \frac{1}{3}, \frac{1}{2})$; $(\frac{\bar{1}}{3}, \frac{\bar{1}}{3}, \frac{1}{2})$ (m2

STABILITY OF OBSERVED HCP SUPERSTRUCTURE

Ti_3Al, Mn_3Sn, Mg_3Cd — A_3B^1
(DO_{19})

WC & LiRh — AB^1

Mg Cd — AB^2

Cu_3Sn — E(TWO PHASE MIXTURE of $A_3B^1 + A_3B^3$)

Sb_3Cu_{10} — E(TWO PHASE MIXTURE $A + A_3B^3$)
OR
E(POLY PHASE MIXTURE $A_5B + A_3B^1 + A_3B^3$)

$ZrAu_4$ — E($A_5B + A_3B^3$)

Al_5W — E(A_5B)

STABILITY OF EXPERIMENTALLY OBSERVED HCP SUPERSTRUCTURES

A_3B^1:	Ni_3Sn, Mg_3Cd, Ti_3Al	$W_1 < 0$, $v_1 > -1$, $v_2 < 0$
A_2B^2:	Pt_2Ta	$W_1 < 0$, $0 < v_1 < 1$, $v_2 < 0$, $v_1 - v_2 > 0$
AB^1:	WC, LiRh	$W_1 < 0$, $v_1 > -1$, $v_2 > 1/2$
AB^2:	MgCd	$W_1 < 0$, $v_1 > -1$, $v_2 < 0$
$A_5B + A_3B^3$:	Au_4Zr	$W_1 < 0$, $v_1 > 1$, $0 < v_2 < 1$
$A_3B^1 + A_3B^3$:	Cu_3Sn	$W_1 < 0$, $v_1 > 0$, $v_2 = 0$
$A + A_5B + A_3B^1 + A_3B^3$:	$Cu_{10}Sb_3$	$W_1 < 0$, $v_1 > 0$, $v_2 > 0$

7. Stability

S. Raju, E.Mohandas and V.S.Raghunathan
Indira Gandhi Centre for Atomic Research, India

STABILITY

S. Raju
E. Mohandas
V.S.Raghunathan

Indira Gandhi Centre for Atomic Research
Kalpakkam-603102, India

STABILITY OF INTERMETALLICS

A Metallurgical Physics Perspective

S. Raju
Indira Gandhi Centre for Atomic Research
Kalpakkam-603102, India

PHYSICAL METALLURGY

EMPIRICAL EXPLANATION OF ALLOYING

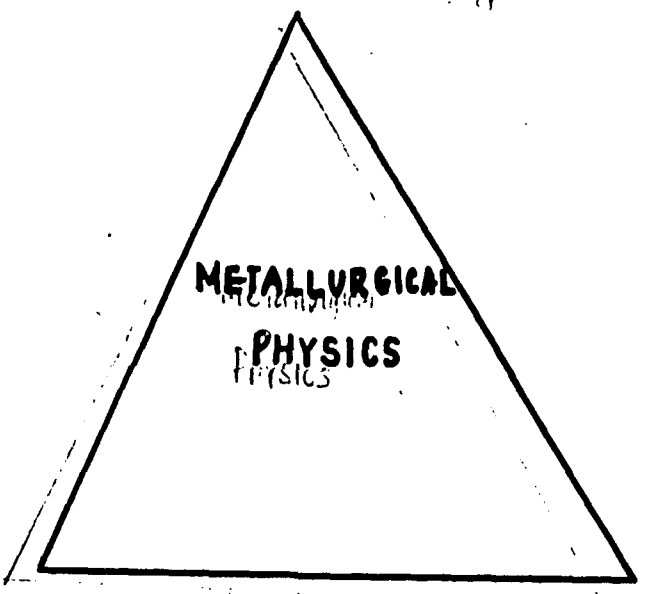

CONDENSED MATTER PHYSICS

SOLID STATE CHEMISTRY

QUANTUM THEORY OF STRUCTURE & BONDING

DOES THIS ALLOYING MODEL VALID?

No	Acceptable
Tight binding, DFT Protagonists	Pseudopotential theorists
Pettifor, Williams, Watson & Bennett ?	Chelikowsky & Phillips, Hafner ? Alonso & Girifalco Hodges & Stott
↓	↓
Such basic splitting is not warranted for transition metal Cohesion	ρ, ϕ, have well defined quantum physical status.
Better numerical agreement	Rather poor agreement.

STRUCTURAL STABILITY

FIRST PRINCIPLES APPROACH

EMPIRICAL SCHEMES

UNDERSTANDING ALLOYING

PREDICTION

THEORY/MODEL FOR COHESION

STRUCTURAL SYSTEMATICS

SEMIEMPIRICAL METHODS

- Establish the trend using appropriate alloy theory parameters
- Setup a microscopic model in terms of these parameters.

- Pseudopotential & Tight binding methods
- Pair potential analysis (Machlin)
- Macroscopic Atom model (Miedema)
- Interstitial electron density model (Schubert, Johnson)

PAIR POTENTIALS

$$E = \tfrac{1}{2}(N) \sum_{R_{ij} \neq 0} \phi(R_{ij})$$

- Absence of volume dependence
- Ordering Energy may be represented

$$E = F(\rho) + \tfrac{1}{2} \sum \phi(R)$$

Volume dependence
(structural term)

EMBEDDED ATOM MODEL

MIEDEMA'S MODEL

ALLOY ≡ ASSEMBLY OF NEUTRAL W-S CELLS

PARAMETERS :

- electron density (ρ ; $\rho^{1/3}$)
- Chemical potential due to electronic charge (ϕ^*)
- Molar volume

$$\Delta^{o}H_f \equiv \{-P(\Delta\phi^*)^2 + Q(\Delta\rho^{1/3})^2 \pm R\} * f(c)$$

MIEDEMA MAPS

$$\langle \Delta\phi^{*}, \ \Delta\rho^{1/3} \rangle$$

$$U_d = \text{No. of } d\, e^{-\Delta s} \times \text{energy of } d \text{ electron}$$

$$U_d = \int_0^{E_F} N(E)\, dE \cdot E - N_d E_d^{at}$$

$$= -\frac{W_d}{20}\left(10 - N_d\right) N_d \qquad \text{FRIEDEL}$$

W_d : width of d-band

N_d : No. of d-electrons

For an $A_x B_{1-x}$ alloy

$x = 1/2$

$$\int_0^{E_F} E\, N(E)_{AB}\, dE - 1/2 \int_0^{E_F^A} E\, N(E)\, dE - 1/2 \int_0^{E_F^B} E\, N(E)\, dE$$

$$= \frac{-W_{AB}}{20}\, \bar{n}\,(10 - \bar{n}) + \frac{W_A}{40}\, n_A (10 - n_A) + \frac{W_B}{40}\, n_B (10 - n_B)$$

$$- 1/4\, \Delta\delta n$$

$$\bar{n} = (n_A + n_B)/2$$

$$\delta n = n_A - n_B$$

PETTIFOR'S MODEL

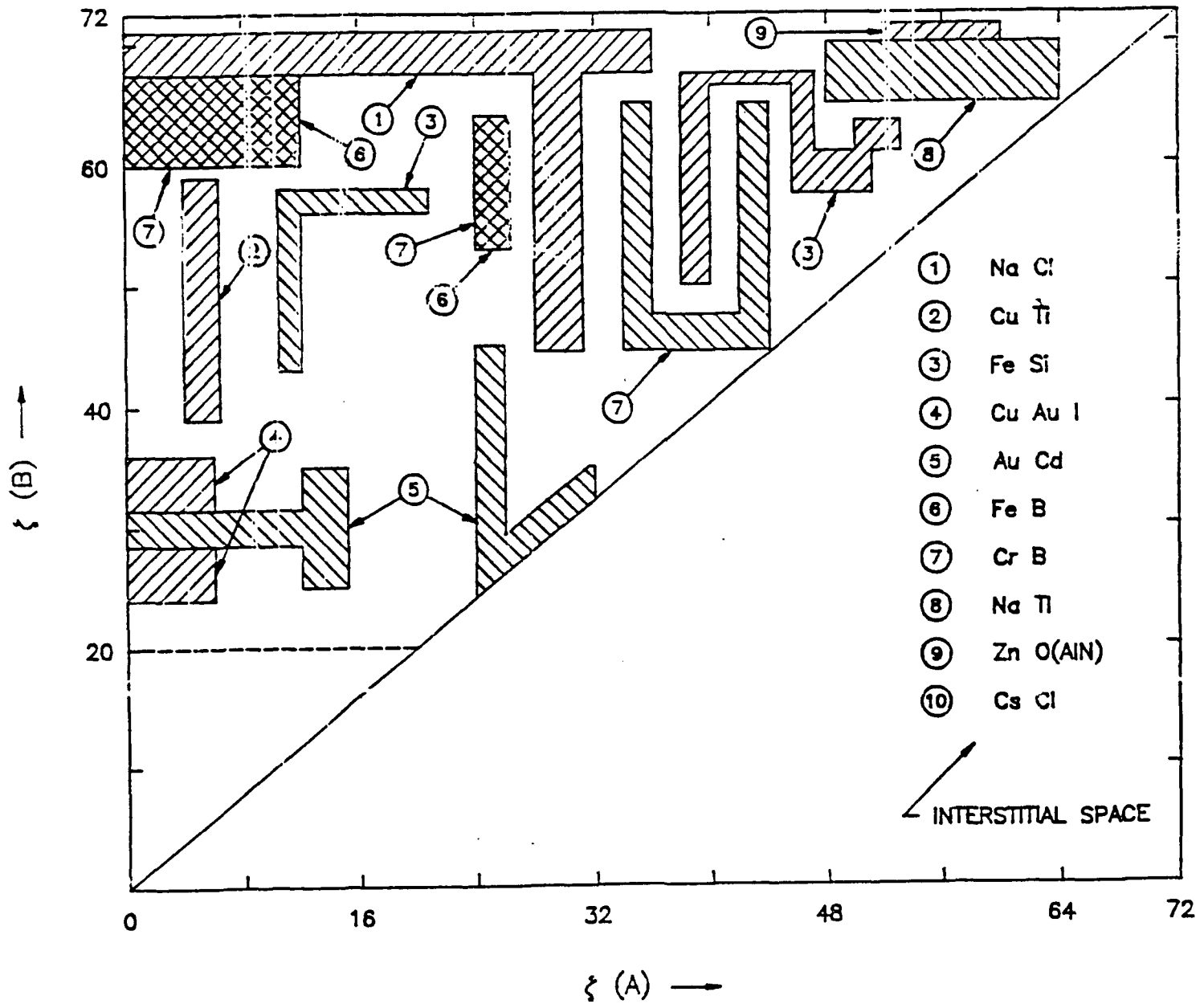
72
60
40
20
0
16
32
48
64
72
ζ (B) ⟶
ζ (A) ⟶
1 Na Cl
2 Cu Ti
3 Fe Si
4 Cu Au I
5 Au Cd
6 Fe B
7 Cr B
8 Na Tl
9 Zn O(AlN)
10 Cs Cl
INTERSTITIAL SPACE

Fig. 2

2: Stringing up the periodic table

THE QUANTUM character of the chemical elements is reflected directly in the periodic table. This two-dimensional arrangement of the elements is a consequence of Schrödinger's equation. Each element in the periodic table is characterised by two co-ordinates, namely its period and group. To classify the structures of binary compounds, I have reduced this to a single co-ordinate, as described in the main text by arranging the elements along a one-dimensional axis, their relative ordering being given by what I have called the Mendeleev number.

The arrangement of the periodic table shown here is slightly different from usual (*New Scientist*, 7 March 1985, p 32). This arrangement places the group IIA elements beryllium and magnesium with group IIB and separates the divalent rare earths or lanthanides (those that have two valence electrons) from the trivalent. The way I have ordered the elements in group IVA reflects the so-called lanthanide contraction: hafnium has a smaller core size than zirconium. My arrangement of group VA leads to a marginally better separation of structures of compounds than running the string straight from nickel to palladium to platinum. The anomalous ordering of gallium with respect to aluminium arises because gallium has a full core of *d* electrons. Chemists well know that the second row elements boron, carbon, nitrogen, oxygen and fluorine behave differently from the other elements in their respective groups. They are much more electronegative due to the absence of *p* electrons in the core. □

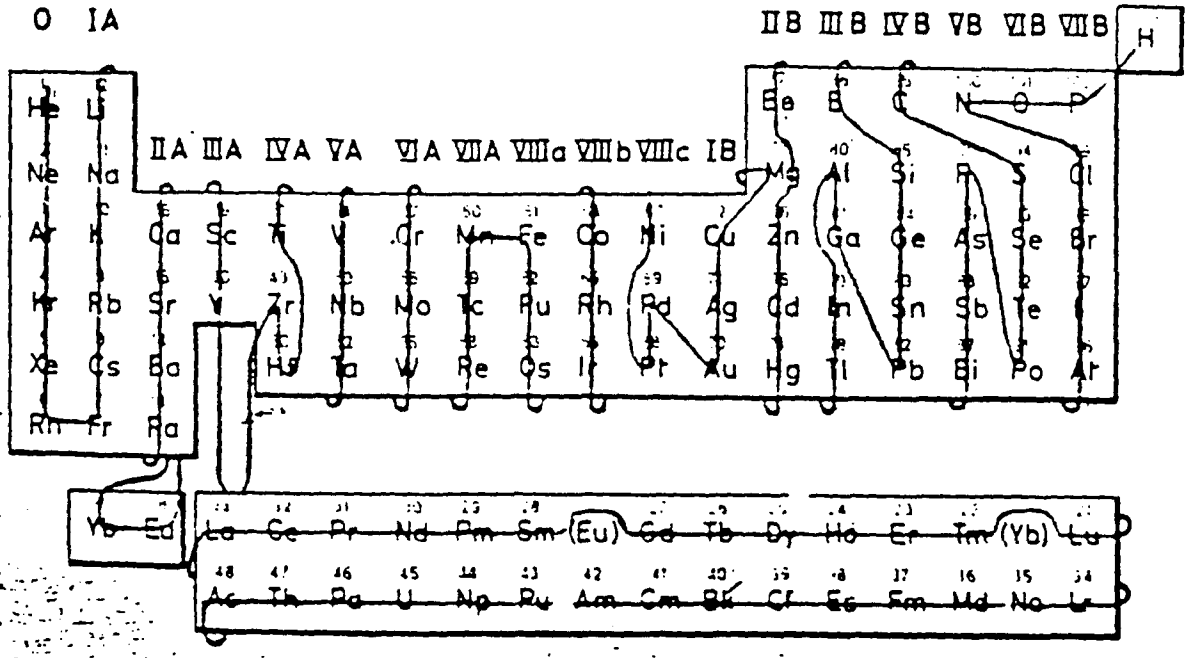

The string running through this modified periodic table puts all the elements in sequential order, given by the Mendeleev number

Typically What do the Material Scientists want from systematization studies?

- Under What conditions do two elements A & B Combine and if so
- Do they form compounds or Solid / liquid Solutions?

More Specifically they look for

- Number of compounds
- Crystal Structure information
- Stability of compounds (polymorphic & other transition, Cohesive energy, Lattice Stability Parameters etc.)
- Extent of solid solubility
- Type of solid Solubility
  - isomorphous
  - eutectic
  - peritectic & a host of others

- If they are insoluble then why?

- Basically, these are the primary information, which together form a comprehensive physical Metallurgical data base. No doubt, one can take other properties like
  - thermodynamic
  - electrical, magnetic
  - transport properties

  but in my opinion they do not form a simple & minimal basis.

- CRITICAL APPRAISAL

  - In its core the model is empirical.
  - Subtle effects like magnetic contribution to stability is neglected
  - Alloys with Si, Ge etc are not satisfactorily represented.
  - The physics of alloying as advanced by this model is strictly incorrect, although its numerical agreement with precise first principle calculations is surprisingly good.

- APPLICATIONS

  - Extrapolation/ Interpolation for limited ΔH_f data bank.
  - Calculation of interfacial energies
  - Prediction of glass formation ranges
  - Assessing the relative stability trends
  - Analysing solid solubility data

* USE OF BASIC COORDINATES TO CRYSTAL STRUCTURE SYSTEMATICS

- An algorithm to generate probable structural alternatives
  - Structure maps
  - Simple phenomenological correlations
  - A truly first principles approach is a non starter by itself

- Effect of various approximations on the output!

- Is there a UNIVERSAL THEORY?

SIMPLE METAL ALLOYS	TRANSITION METAL ALLOYS
• Pseudo potential	• Tight binding • LMTO(ASA)

HYBRID VARIETIES

DFT (LDA); ?
ASW

STABILITY ?

$$F = -\beta^{-1} \ln \mathcal{Z} \qquad 1$$

$$\mathcal{Z} = \mathrm{Tr}\,\{\exp(-\beta H)\} \qquad 2$$

$\beta = 1/k_B T$

$Z =$ Partition function

$H =$ a (ground state) energy function

$$H = \sum H_{e-e} + H_{i-i} + H_{i-e}$$

$H = E_k + E_p$ (Schröedinger equation, Virial theorem, ...)

SIMPLE METAL ALLOYS

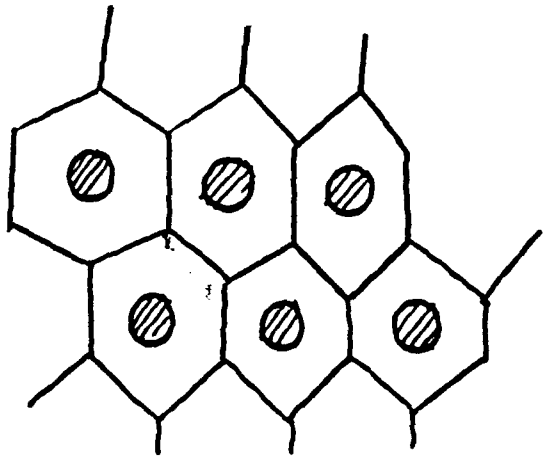

METAL = SCREENED ION CORE + DELOCALIZED CONDUCTION ELECTRONS

$$\Delta^{\circ}H_f = x\,\Delta\bar{H}_A + (1-x)\,\Delta\bar{H}_B$$

$$\Delta^{\circ}\bar{H}_A = (E_A - E^{\circ}_A)$$

$$E = E(r_s)$$

r_s = volume/electron , electron density

$$E = \underbrace{\sum E_k + E_{el} + E_{ex} + E_c}_{E_{eg}} + \mathcal{U}_{Pot.} + \mathcal{U}_{Madelung}$$

$E = E_{eg}$ + Structure dependent contribution.

Depending on the sophistication, plug in appropriate E_i

$\left.\frac{dE}{dr_s}\right|_{r=r_s}$, $\frac{\partial^2 E}{\partial r_s^2}$, give equilibrium conditions.

For a binary $A_x B_{1-x}$, the final expression

$$E\,(\text{Per atom}) = Z^*\left(\frac{2.21}{r_s^2} - \frac{0.916}{r_s} - 0.115 + 0.031 \ln r_s\right)$$

$$+ \frac{1}{4/3\,\pi r_s^3}\left[x\mu_A + (1-x)\mu_B\right] - \frac{\alpha}{r_s} Z^{*\,5/3}$$

$$Z^* = x Z_A + (1-x) Z_B$$

$$\alpha = 1.792 \quad (\text{fcc})$$

$$\mu_\alpha = 2\pi e^2 Z_\alpha \left(r_c^\alpha\right)^2$$

$$\Delta F_{mix} = \Delta E_{mix} - T\Delta S_{mix}$$

The present study attempts to devise a Single Coordinate structure map.

Why one parameter?

Periodic table has one dimension, namely Z

Is it possible by just providing one extra parameter to correctly account for the bonding trend.?

Secondly is it possible to combine a few other independent parameters to get a single one which represents a compromise of competing tendencies?

Ans (i). Yes - one parameter

(ii) No - not truly independent

PRESENT PARAMETER

$$\chi \equiv \frac{\phi^*}{\eta_{ws} \cdot V} = \text{Volt} \,|\, \text{electrons}$$

- ϕ^* = Work function related Electronegativity ($\propto E_F$)

η_{ws} = electron density at W-S cell surface

V = Volume / mole ..

χ AS A STRUCTURE MAP PARAMETER

- Prediction of Solid Solubility
- Prediction of compound formation
- AB Structure type sorting

- The range of χ is increased by artificially stringing it in the decreasing order.

  Ce : 1
  H : 72 (actinide omitted)

- Predicts reasonably solid solution exclusion and compound formation exclusion zone.

- Sort AB structure type only as good as any other single coordinate Map.

- The χ VARIATION FOR TRANSITION METAL PERIODS IS RATHER IRREGULAR

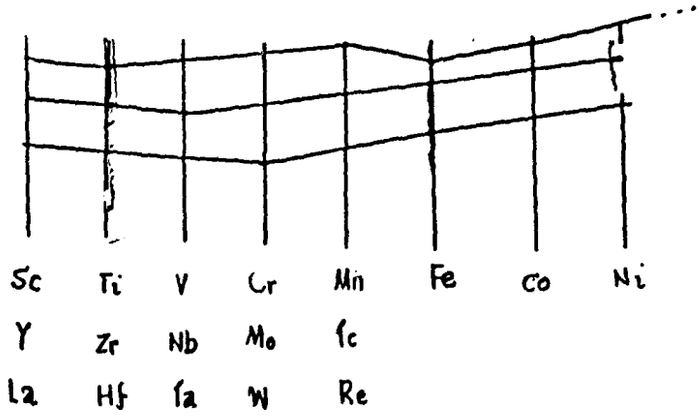

- Also there is a drop in χ in going from IA → IIA
  ie. Li → Be : Na → Mg etc.
  $1s^1 - 1s^2$ $2s^1 - 2s^2$

- χ does not appear to be a smooth function of Z.

- $\chi \not\equiv$ Electronegativity ?

  $\cong$ an energy parameter, characteristic of the Condensed state, not the <u>elemental state</u>

  ∴ It may not therefore obey the trends of an atomic coordinate.

- If we propose χ ≈ measure of electronegativity then the high electronegative elements on the extreme right has no option other than covalent bond.

- Low χ values of metals indicates that electron redistribution is rather easy upon homopolar bond formation. Low electronegativity suggests that transfer and delocalization of atomic valence shell in to conduction band is energy in-expensive

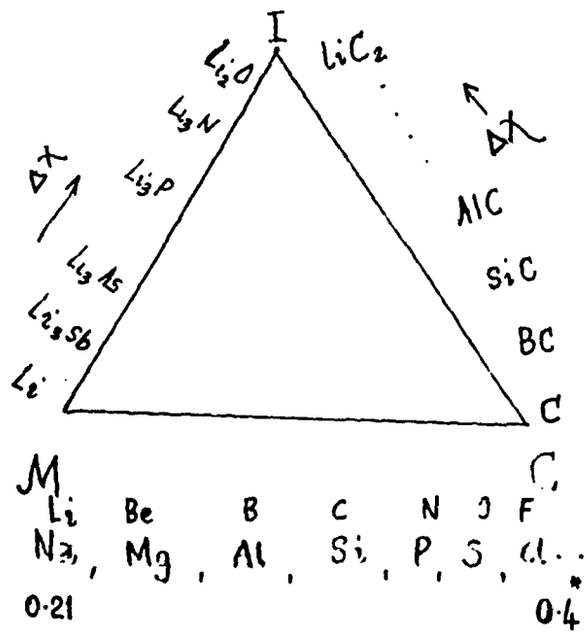

- 'Position' of H_2 requires reshuffling?

RELEVANCE OF χ w.r.t. PERIODIC TABLE

- χ decreases down the group, (save for Si–Ge) for s, p elements

  Down the Group, the size (at. radii) increases, and s, p, d levels in the solid state converge.

  ~ difference in $\varepsilon_p - \varepsilon_d$ comes down.

  ~ increased delocalization

  ~ increased metallicity

  χ value decreases.

  If $\chi \approx$ av. one e^{-n} energy of valence shell then this trend is accepted.

- Slight upward shift in Si → Ge

  Si : p block element – no d-band

  Ge – imperfect screening by d-band of the valence s and p. As a net result there is a slight d-band contribution → shifting it to semiconductivity.

- Compared to Si, Ge has a lower band gap. (and high χ)

* SCALE FOR 72 ELEMENTS

X — ELEMENT SYMBOL

72 H 0.9106														
69 Li 0.2328	68 Be 0.2218											67 B 0.21107	70 C 0.34485	71 N 0.37283
66 Na 0.2059	51 Mg 0.1538											54 Al 0.15647	57 Si 0.16179	48 P 0.14614
63 K 0.17953	38 Ca 0.12919	27 Sc 0.1057	25 Ti 0.102256	32 V 0.11522	35 Cr 0.124167	47 Mn 0.14509	36 Fe 0.12543	46 Co 0.14227	49 Ni 0.1480	65 Cu 0.1913	64 Zn 0.19447	52 Ga 0.15425	62 Ge 0.17935	44 As 0.13556
61 Rb 0.17338	34 Sr 0.11935	16 Y 0.09834	7 Zr 0.08788	2 Nb 0.08411	11 Mo 0.08933	26 Tc 0.1035	29 Ru 0.10771	33 Rh 0.11931	41 Pd 0.1317	59 Ag 0.16164	58 Cd 0.1633	53 In 0.15477	43 Sn 0.1335	39 Sb 0.12073
60 Cs 0.1693	31 Ba 0.11462	4 La 0.087928	8 Hf 0.08793	5 Ta 0.0868	3 W 0.0848	18 Re 0.09276	24 Os 0.1009	28 Ir 0.10635	30 Pt 0.11004	40 Au 0.13181	55 Hg 0.15649	56 Tl 0.161147	50 Pb 0.14745	45 Bi 0.13762

RARE EARTHS

1 +4 Ce 0.0842	9 Pr 0.0889	12 Nd 0.08969	10 Pm 0.0891	13 Sm 0.0903	14 +3 Eu 0.09046	15 Gd 0.0983	17 Tb 0.09151	19 Dr 0.09305	21 Ho 0.09453	20 Er 0.09583	22 Tm 0.09547	23 +3 Yb 0.0963	Lu 0.095032
+3 Ce 0					0. +2 Eu 0.12668							0. +2 Yb 0.13323	

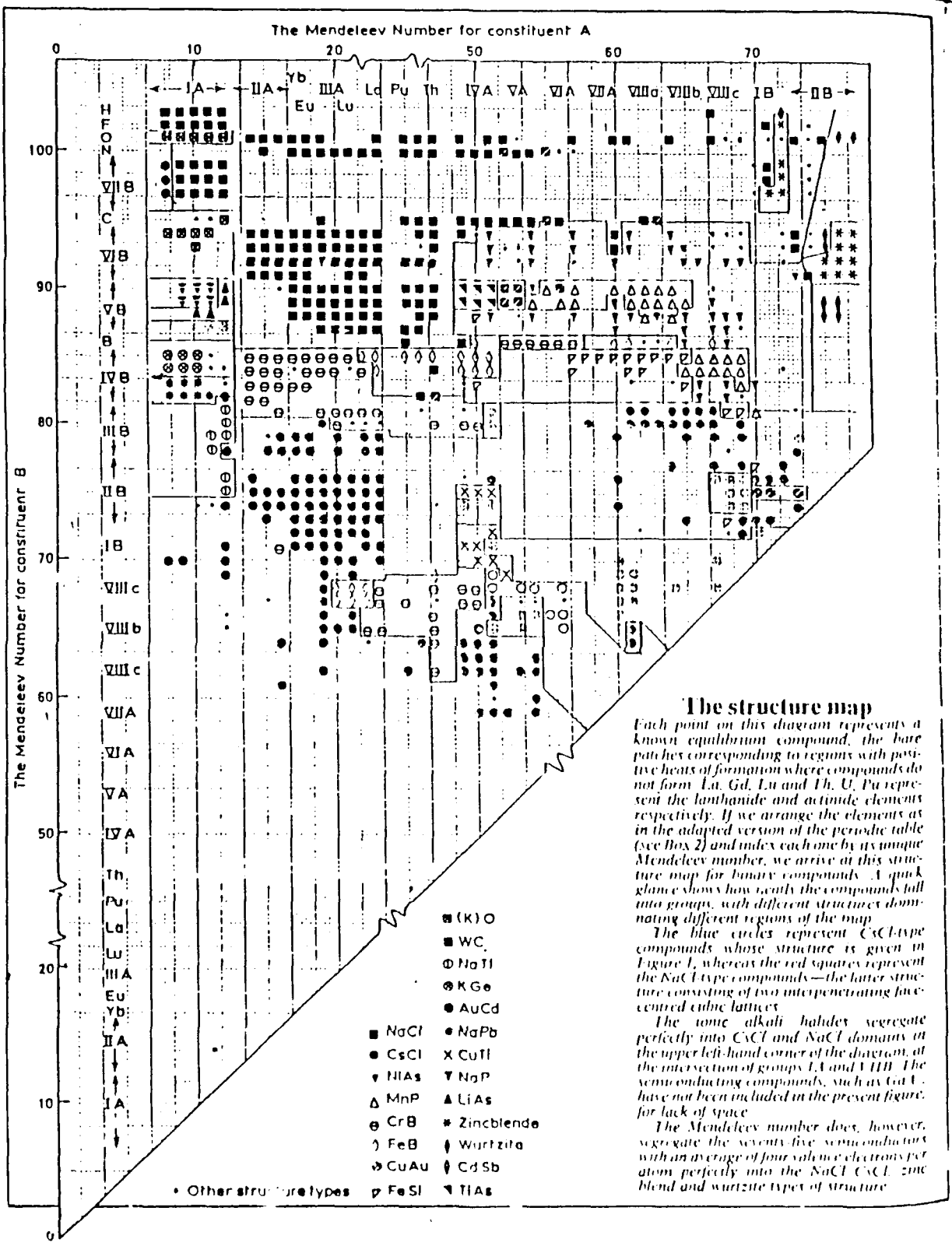

The structure map

Each point on this diagram represents a known equilibrium compound, the bare patches corresponding to regions with positive heats of formation where compounds do not form. La, Gd, Lu and Th, U, Pu represent the lanthanide and actinide elements respectively. If we arrange the elements as in the adapted version of the periodic table (see Box 2) and index each one by its unique Mendeleev number, we arrive at this structure map for binary compounds. A quick glance shows how neatly the compounds fall into groups, with different structures dominating different regions of the map.

The blue circles represent CsCl-type compounds whose structure is given in Figure 1, whereas the red squares represent the NaCl-type compounds—the latter structure consisting of two interpenetrating face-centred cubic lattices.

The ionic alkali halides segregate perfectly into CsCl and NaCl domains in the upper left-hand corner of the diagram, at the intersection of groups IA and VIIB. The semiconducting compounds, such as GaAs, have not been included in the present figure, for lack of space.

The Mendeleev number does, however, segregate the seventy-five semiconductors with an average of four valence electrons per atom perfectly into the NaCl, CsCl, zinc blend and wurtzite types of structure.

PRELIMINARY CONCLUSIONS ABOUT χ

- For s, p elements, the metallic state valence orbitals
- retain a large portion of atomic character and therefore χ exhibits a trend, coinciding with an atomic electronegativity

- The more the 's' orbitals are involved in bonding the larger is the χ. This is evidenced by $\chi_{Li} > \chi_{Be}$ etc..
  $\chi_{Na} > \chi_{Mg}$

- Transition Metals exhibit a low range of $\Delta\chi$, besides having low χ themselves.

- Rare earths tend to group, mingle with the d-transition metals, thus unifying the general metallicity of these group. Note, the present form of periodic table tends to <u>muddle</u> this trend. ie, After La, Ce → Lu must be followed: But we write La-Hf-Ta-W ... etc..

BASIC STEPS

CELL PREPARATION

$A^{\circ} \rightarrow \underline{A}$

$\rho_{A^{\circ}}$ $\quad$ $\rho_{\underline{A}}$ $\quad$ $V_{A^{\circ}} < V_{\underline{A}}$

$V_{A^{\circ}}$ $\quad$ $V_{\underline{A}}$ $\quad$ $\rho_{A^{\circ}} > \rho_{\underline{A}}$

$B^{\circ} \Rightarrow \underline{B}$

$\rho_{B^{\circ}}$ $\quad$ $\rho_{\underline{B}}$ $\quad$ $V_{B^{\circ}} > V_{\underline{B}}$

$V_{B^{\circ}}$ $\quad$ $V_{\underline{B}}$ $\quad$ $\rho_{B^{\circ}} < \rho_{\underline{B}}$

CELL PREPARATION STEP: VOLUME EFFECT

Generates repulsive forces

CHARGE TRANSFER STEP

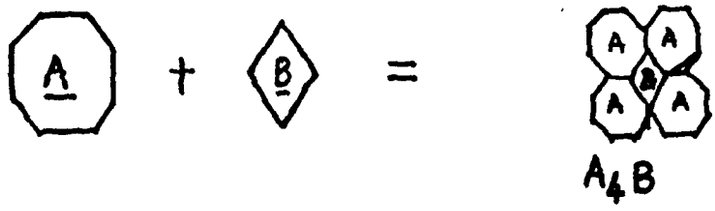

THIS IS ATTRACTIVE AS CHARGE TRANSFER, DRIVEN BY CHEMICAL POTENTIAL GRADIENT. ($\Delta\phi^*$)

ELECTRO CHEMICAL FACTOR.

THUS ρ, ϕ COULD BE BASIC ALLOY THEORY PARAMETERS.

BESIDES, THEY ARE CONNECTED TO ΔH_f.

ELECTRON DENSITY

$$\rho \text{ or } n = \left(V/Z\right)^{-1}$$

$$4/3\, \pi r_s^3 = V/Z$$

$$r_s = r_s/a_0$$

- Z cannot be solved exactly in 3-D
- H is a composite term, again exact calculations are impossible
- Approximations at this very basic level
  - Adiabatic approximation
  - one electron approximation
  - Self consistent treatments of e-e
    (Various band structure models, DFT, PPT)
    EMA, Molecular dynamics, cluster calculations)
- Incorporation of temperature effects
  - harmonic, quasi harmonic models
  - inadequate portrayal of lower T regime
- Calculational accuracy
  < lev (~~13.6 kJ~~ 23 kCal/g.atom)

REQUIRED INPUT

- Set of Z_i
- eqlm. spacing (Vegard's Law : Zen's Law)
- Core size, Madelung Constant

OUTPUT

FORMATION ENTHALPY.

ELECTRONEGATIVITY

BULK MODULUS (?)

SFE, APBE (?)

ORDERING ENERGY

VALIDITY

ONLY S, p ALLOYS

ATTRACTION

SIMPLE, ALLOWS EASY BREAK UP

INPUT

W_i, n_i $(i = A, B)$; W_{AB} ,

SIMPLE ;

NO STRUCTURE DEPENDENCE

ABSENCE OF REPULSION TERM

BUT EXPERIMENTAL AGREEMENT

GOOD ?

How ?

How to incorporate structure ?

STRATEGY

(i) $N(E)$ → density of states, structure sensitive.

(ii) FORCE THEOREM

Consider C Covalent sp^3 / tetrahedral

Si, Ge] tetrahedral sc

Sn - White tin, sc, tetragonal lower χ,

Pb - Fcc, metal, lower χ

Further Al Si P $\chi_{Si} = \frac{\chi_{Al} + \chi_P}{2}$

Ga Ge As $\chi_{Ge} = \frac{\chi_{As} + \chi_{Ga}}{2}$

In Sn Sb $\chi_{Sn} = \frac{\chi_{In} + \chi_{Sb}}{2}$

Al P
Ga As are also semiconducting.
In Sb

As we go from Left → right in the periodic table we move from

Metallic → Covalent binding

Li, Be, Ba etc ..

B, C, N_2, P, As. O_2 F_2 etc ...

$\chi \longrightarrow$

What is special about transition metals ?

d electrons - spatially localized
- Covalent interaction
- Strongly bound to the core

TIGHT BINDING SCHEME

$$E = \underbrace{U_{att} + U_{rep}}_{U_d + U_{s-d} + U_{others}}$$

RECTANGULAR BAND ASSUMPTION

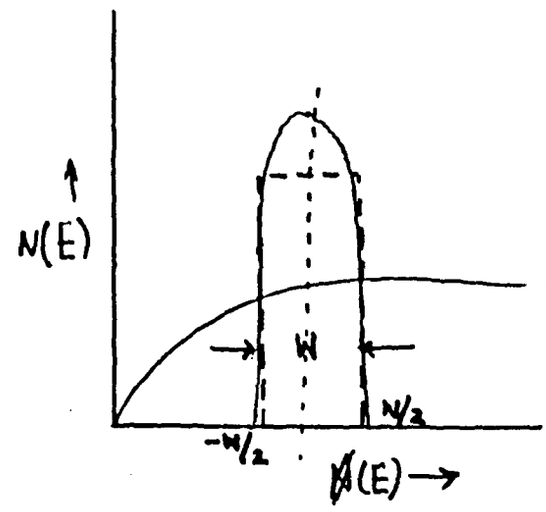

TRANSITION METAL COHESION

$$E = E_d + E_{s,p} + E_{s+d} + \text{others}$$

$E_d =$ band theory route

$E_{s,p} =$ Pseudo potential

$E_{s+d} =$ Tight binding

$E_{others} =$ Magnetic.

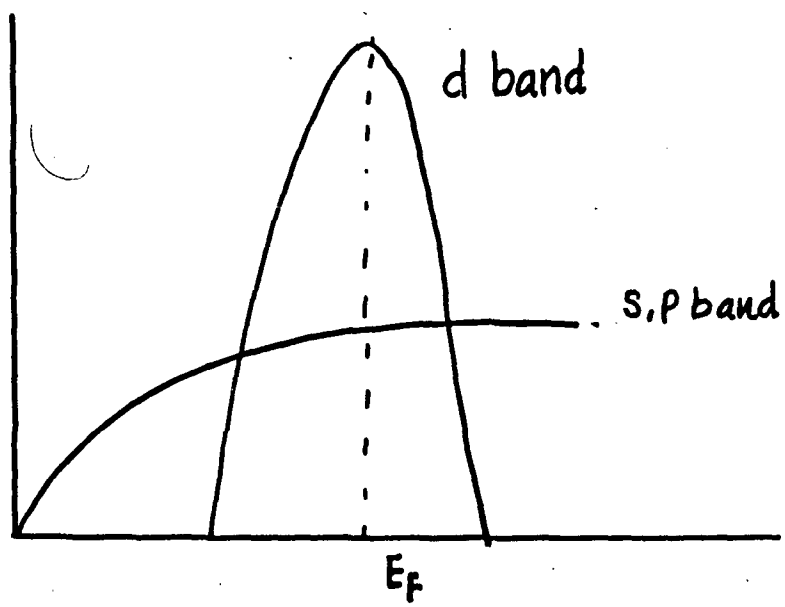

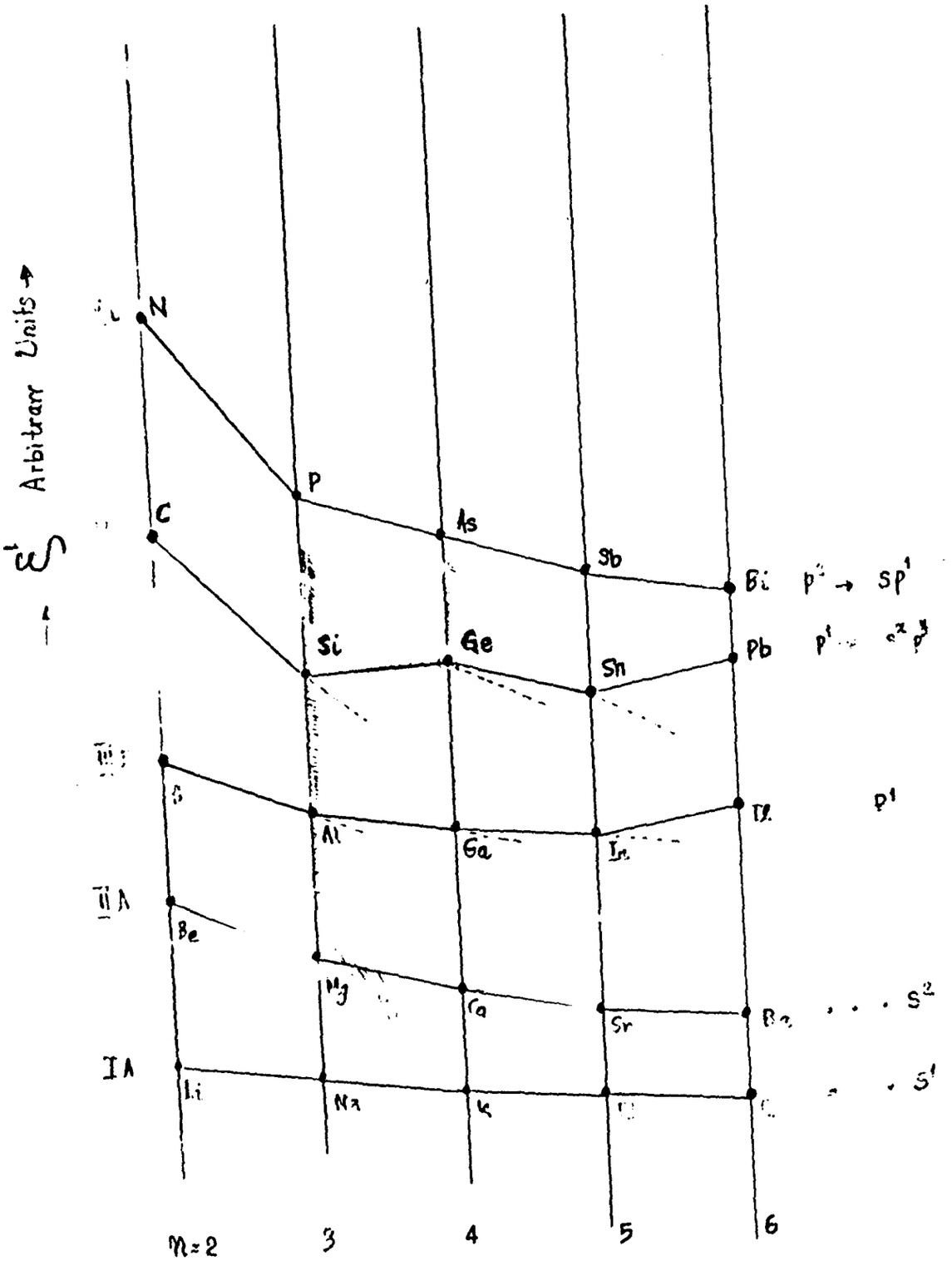
Arbitrary Units
N
P
As
Sb
Bi
C
Si
Ge
Sn
Pb
Al
Ga
In
Tl
Be
Mg
Ca
Sr
Ba
Li
Na
K
n=2
3
4
5
6

OCCURRENCE OF $MgCu_2$ STRUCTURE

'B' COMPONENT ELEMENTS

Li	Be															
Na	Mg											Al	Si		S	
K	Ca	Sc	Ti	V	Cr	Mn	Fe	Co	Ni	Cu	Zn	In				
Rb	Sr	Y	Zr	Nb	Mo	Tc	Ru	Rh	Pd	Ag						
Cs	Ba	La	Hf	Ta	W	Re	Os	Ir	Pt	Au		Pb	Bi			

--RAREEARTHS Ce Pr Nd Pm Sm Eu Gd Tb Dy Ho Er Tm Yb Lu

→ACTINIDES Th Pa U Np Pu Am Cm ← Lack of data →

(X) BOTH 'A' AND 'B' ELEMENTS

[X] PREDICTED NOT TO FORM $MgCu_2$ STRUCTURE

(X) PREDICTED TO FORM $MgCu_2$ WITH SUITABLE 'B' ELEMENT $ThIn_2$, $ErSi_2$, DrS_2, $AgBe_2$, $FeBe_2$, $CuBe_2$, $LiPt_2$ ARE SPECIAL CASES.

OCCURRENCE OF $MgZn_2$ STRUCTURE

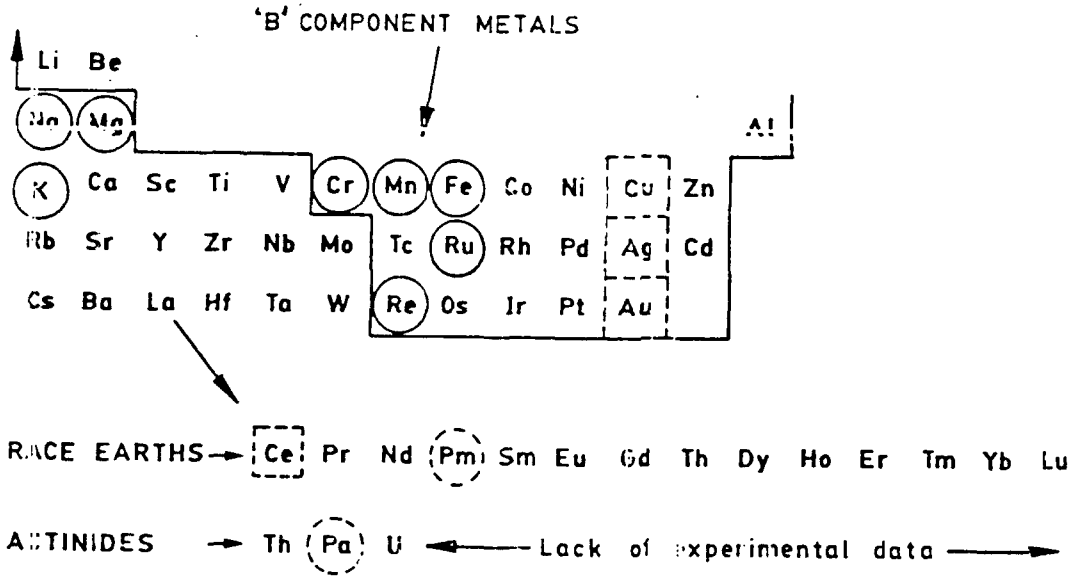

(X) BOTH 'A' AND 'B' ELEMENTS

[X] PREDICTED TO FROM $MgCu_2$

(X) PREDICTED TO FORM $MgZn_2$

Cr, Mn, Fe, Ru, Re FORM 'A' ELEMENTS ONLY WITH Be as 'B'

$CaLi_2$ SPECIAL CASE

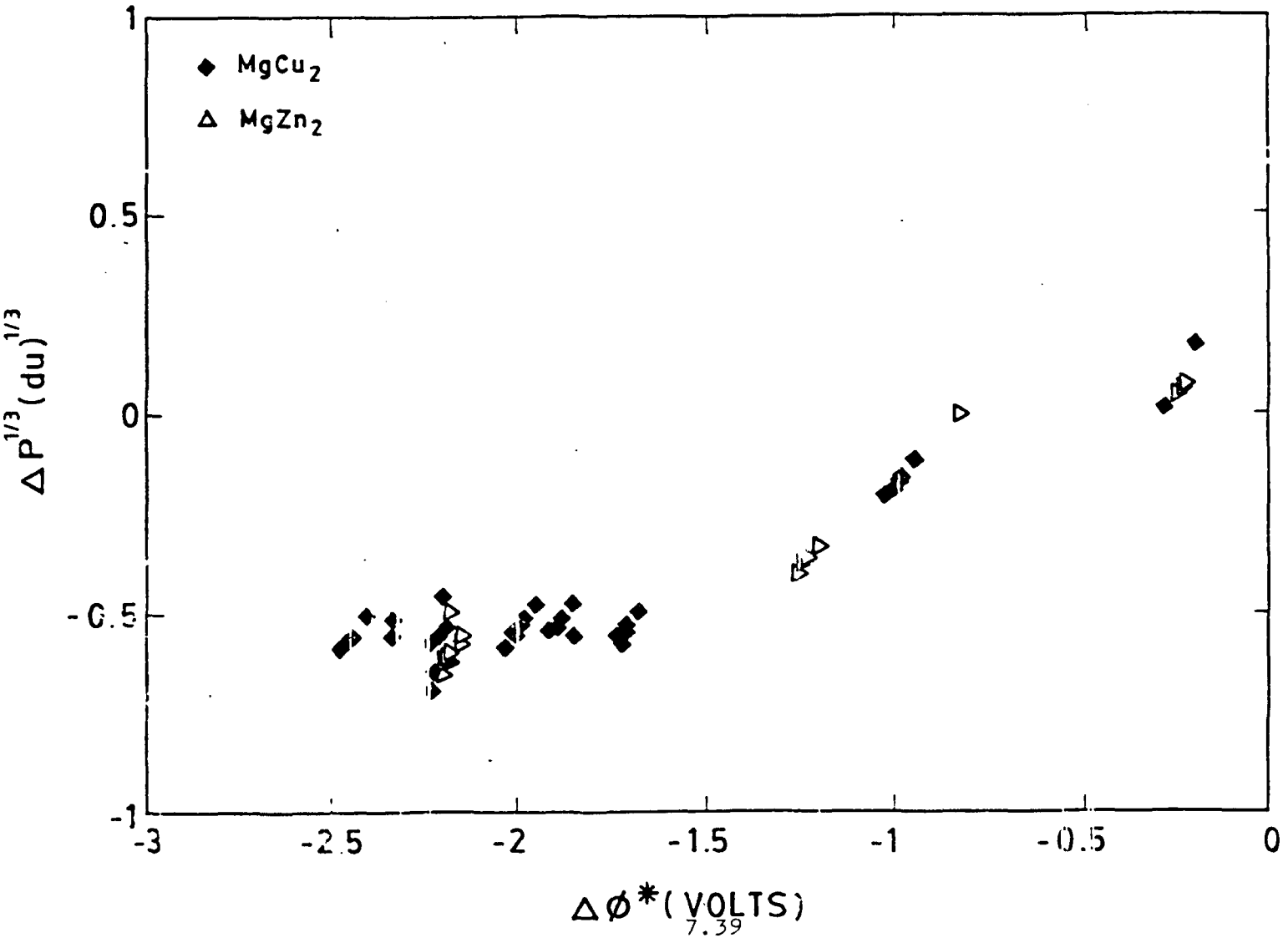
MgCu2
MgZn2
1
0.5
0
-0.5
-1
-3
-2.5
-2
-1.5
-1
-0.5
0
ΔP^1/3 (du)^1/3
ΔØ* (VOLTS)

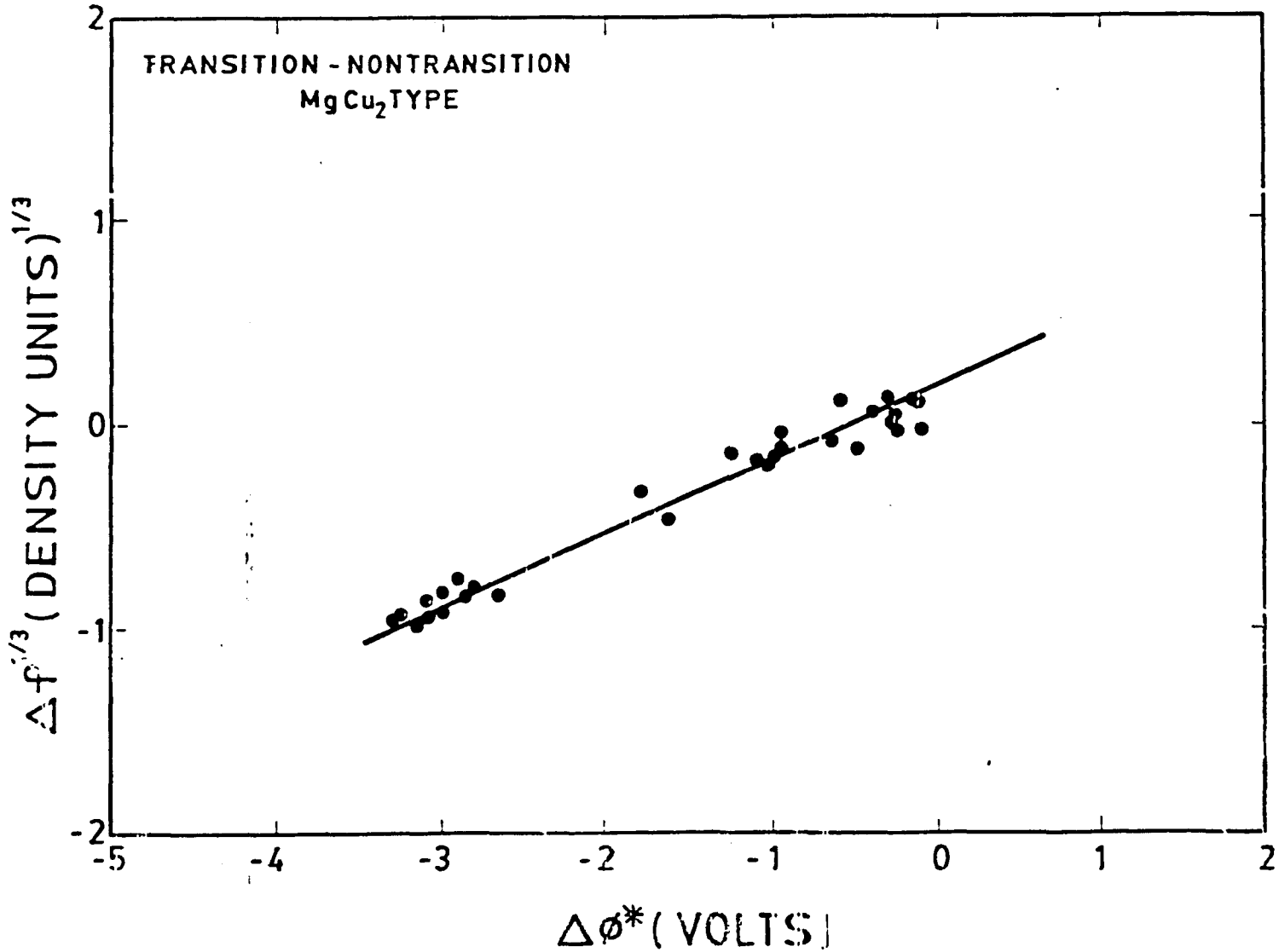
TRANSITION - NONTRANSITION
$MgCu_2$ TYPE
$\Delta\rho^{1/3}$ (DENSITY UNITS)$^{1/3}$
$\Delta\phi^*$ (VOLTS)
2
1
0
-1
-2
-5
-4
-3
-2
-1
0
1
2

7.40

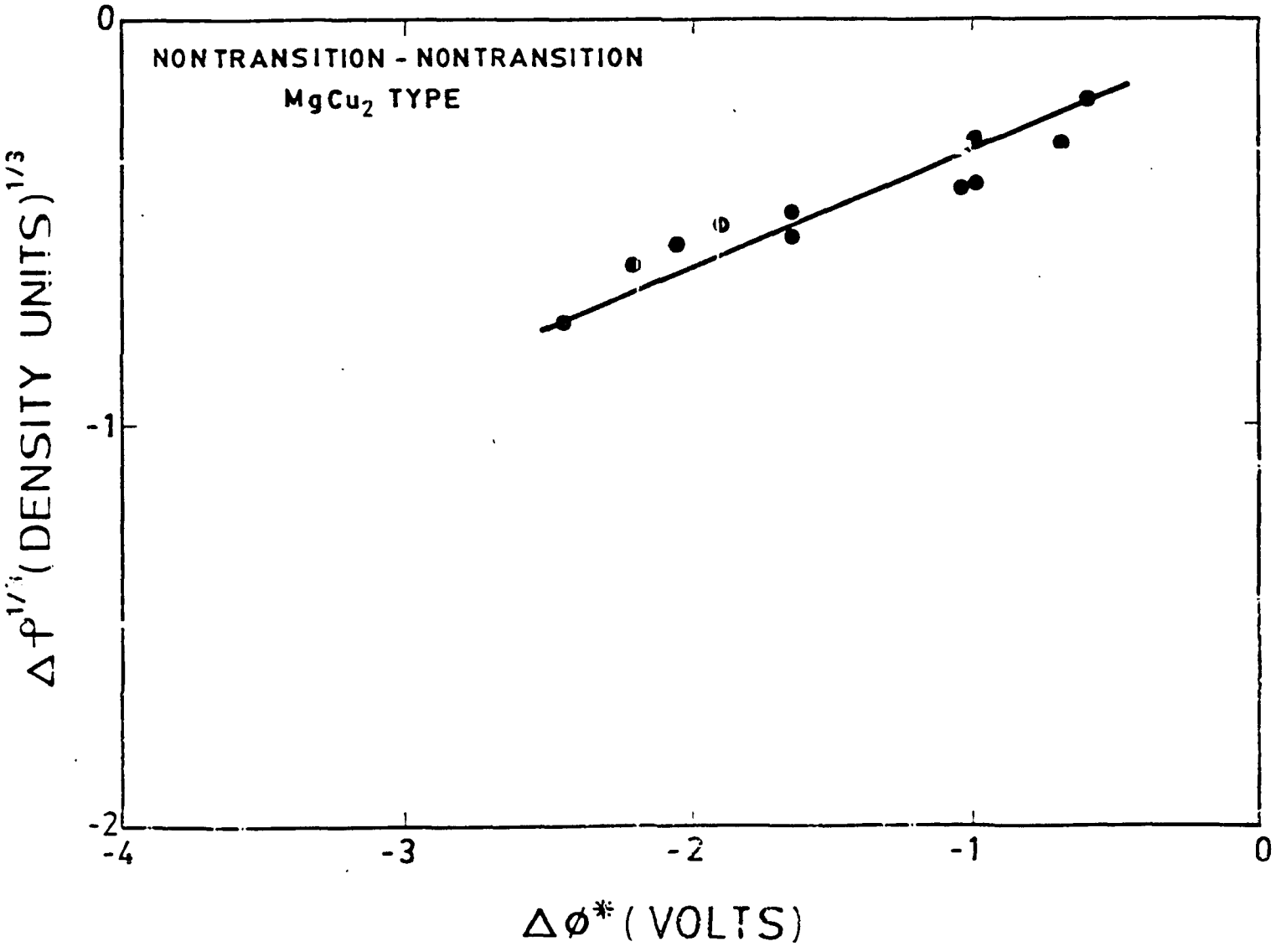
NONTRANSITION - NONTRANSITION
MgCu2 TYPE
0
-1
-2
-4
-3
-2
-1
0
Δρ^1/3 (DENSITY UNITS)^1/3
Δφ* (VOLTS)

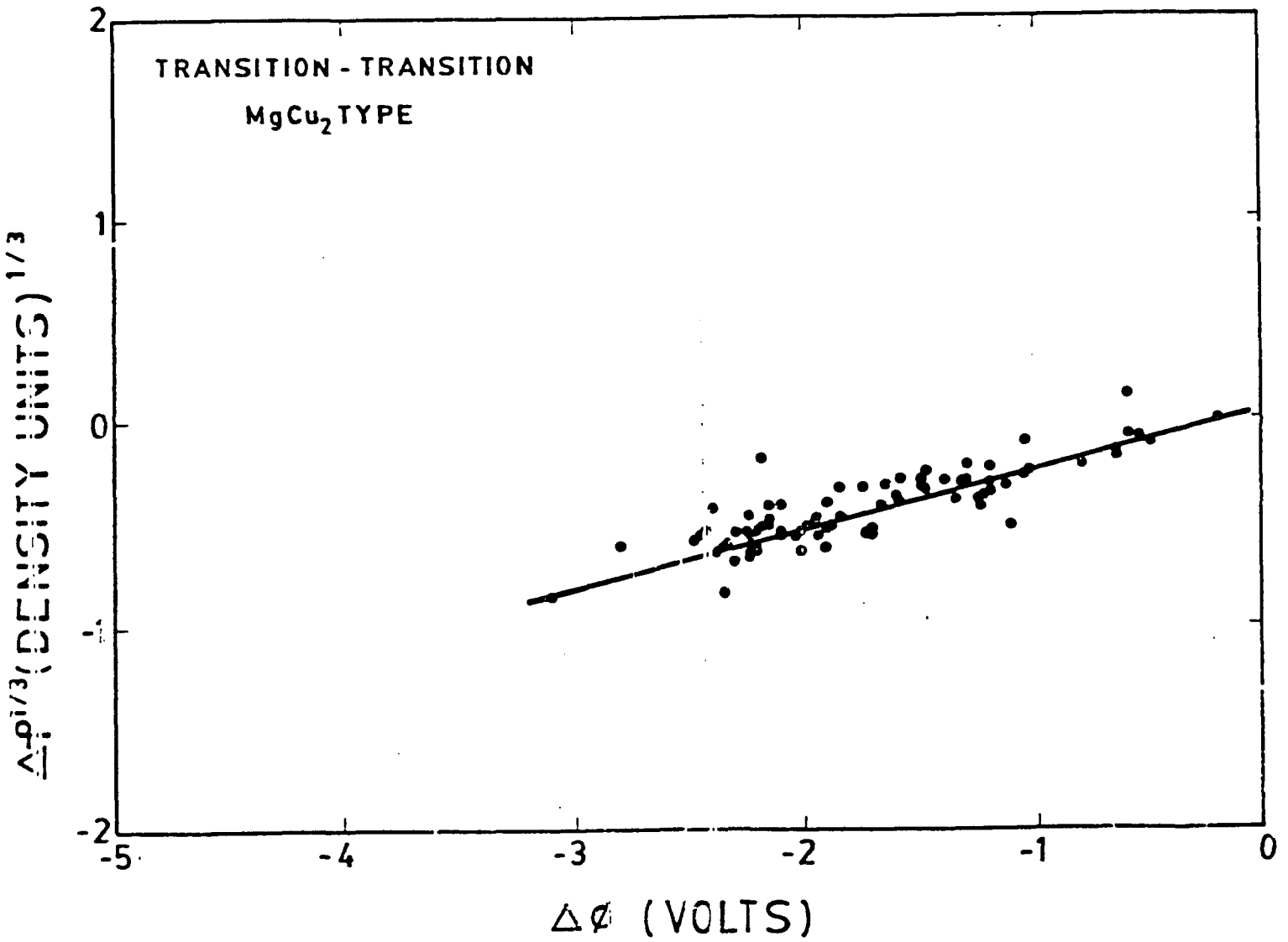
TRANSITION - TRANSITION
MgCu2 TYPE
2
1
0
-1
-2
-5
-4
-3
-2
-1
0
Δφ (VOLTS)

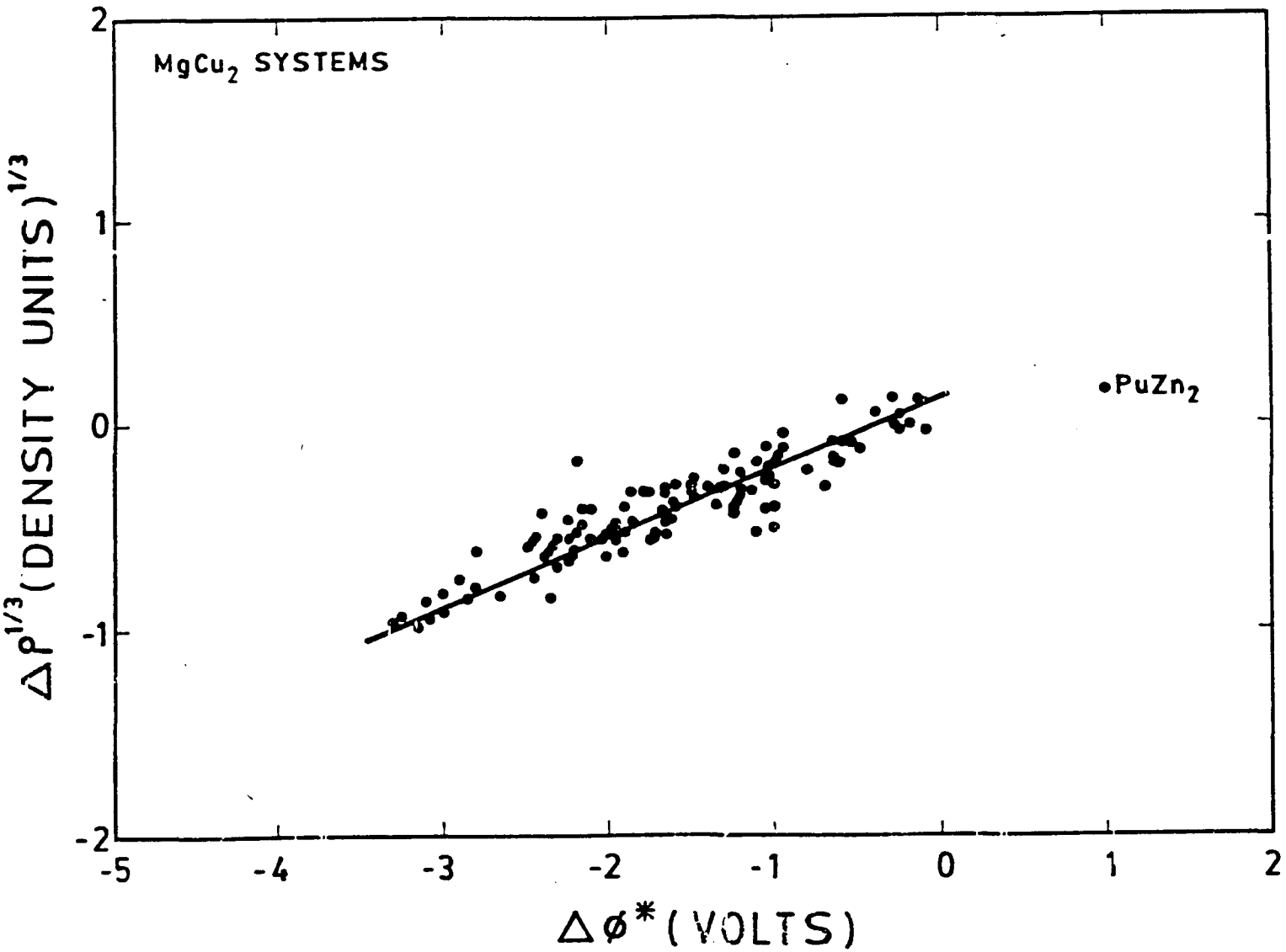
MgCu2 SYSTEMS
•PuZn2
ΔP^1/3 (DENSITY UNITS)^1/3
Δφ* (VOLTS)
2
1
0
-1
-2
-5
-4
-3
-2
-1
0
1
2

7.43

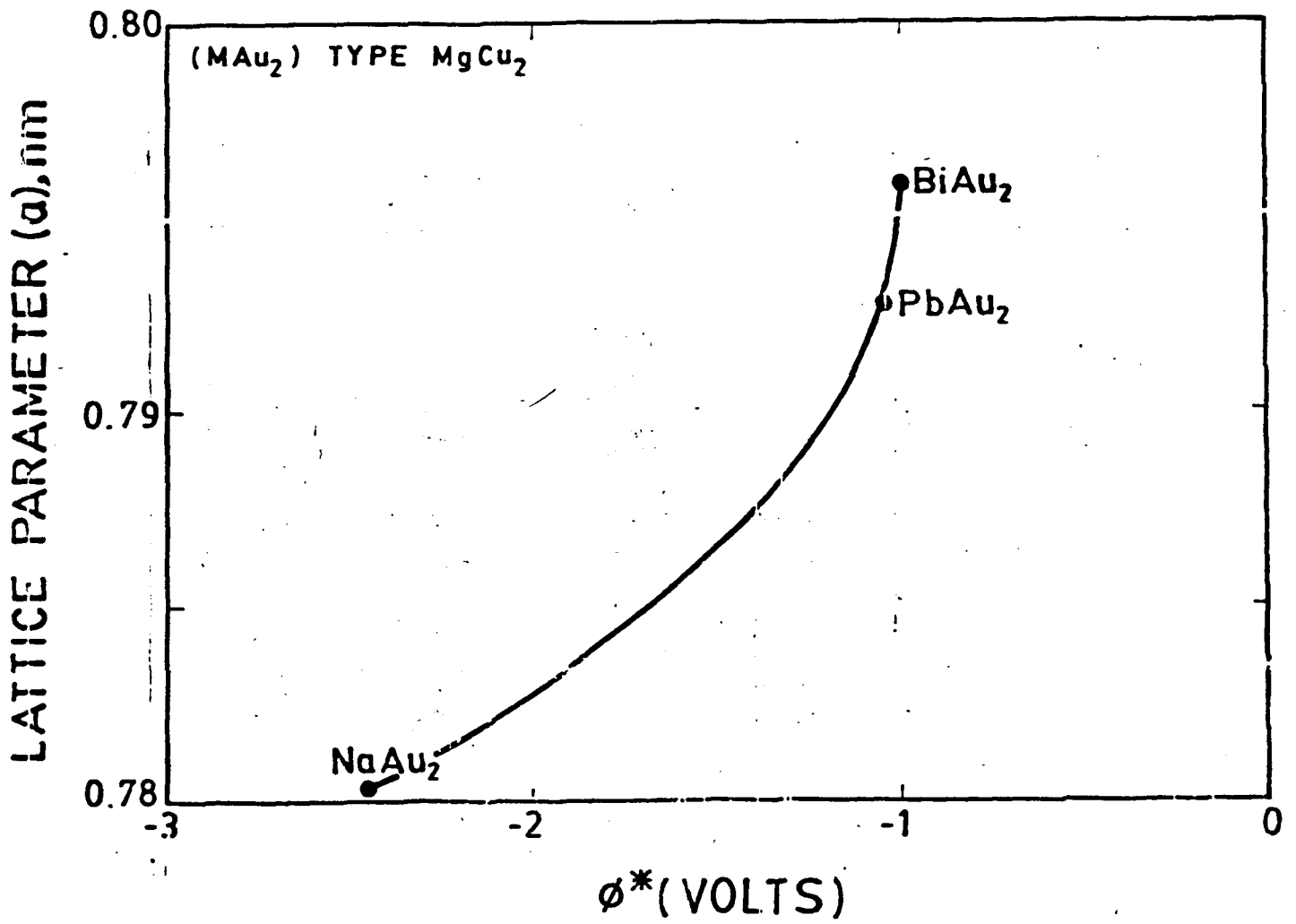
(MAu2) TYPE MgCu2
BiAu2
PbAu2
NaAu2
LATTICE PARAMETER (a), nm
0.80
0.79
0.78
-3
-2
-1
0
ø*(VOLTS)

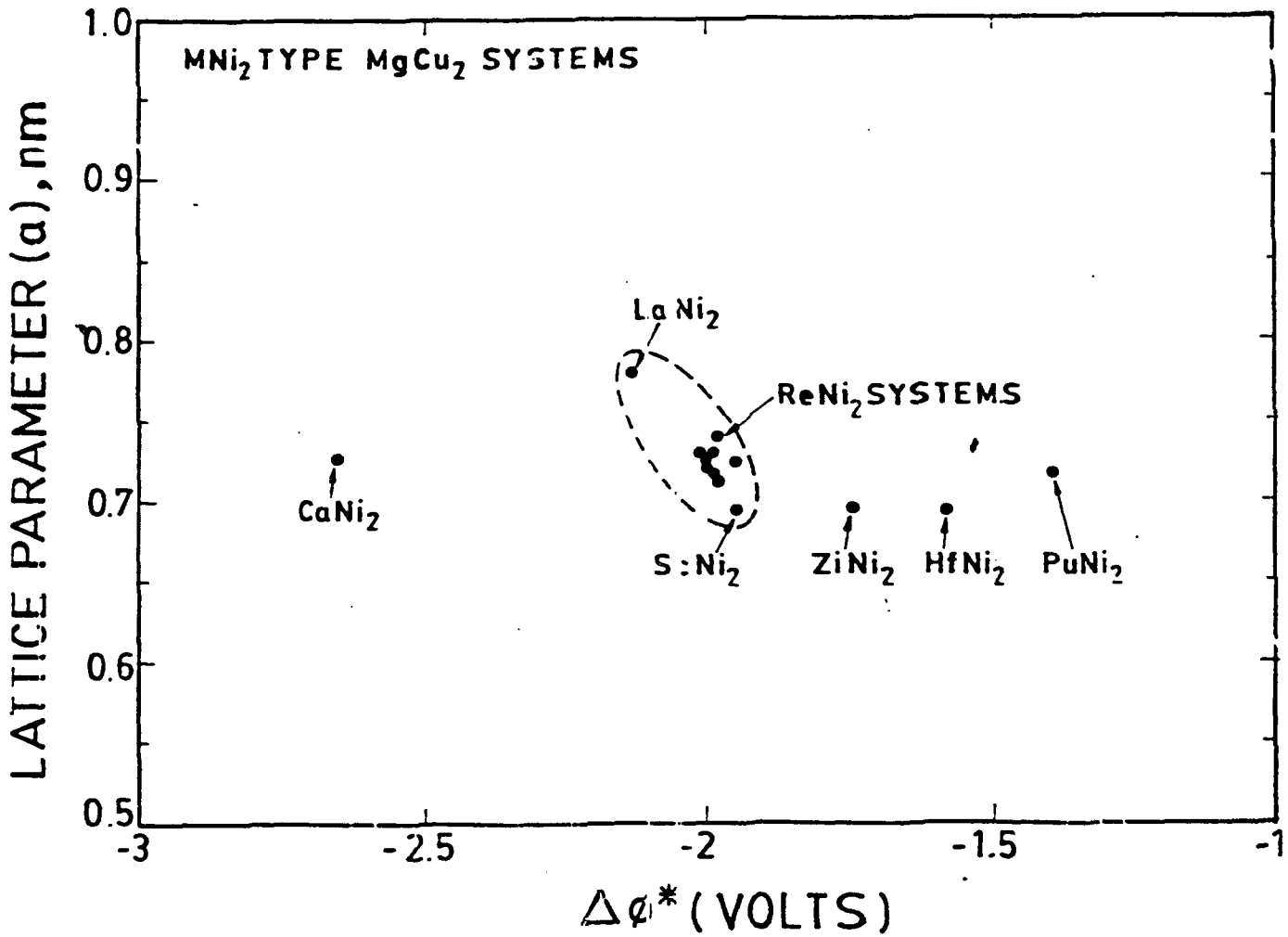
MNi2 TYPE MgCu2 SYSTEMS
LATTICE PARAMETER (a), nm
1.0
0.9
0.8
0.7
0.6
0.5
-3
-2.5
-2
-1.5
-1
Δφ* (VOLTS)
LaNi2
ReNi2 SYSTEMS
CaNi2
S:Ni2
ZiNi2
HfNi2
PuNi2

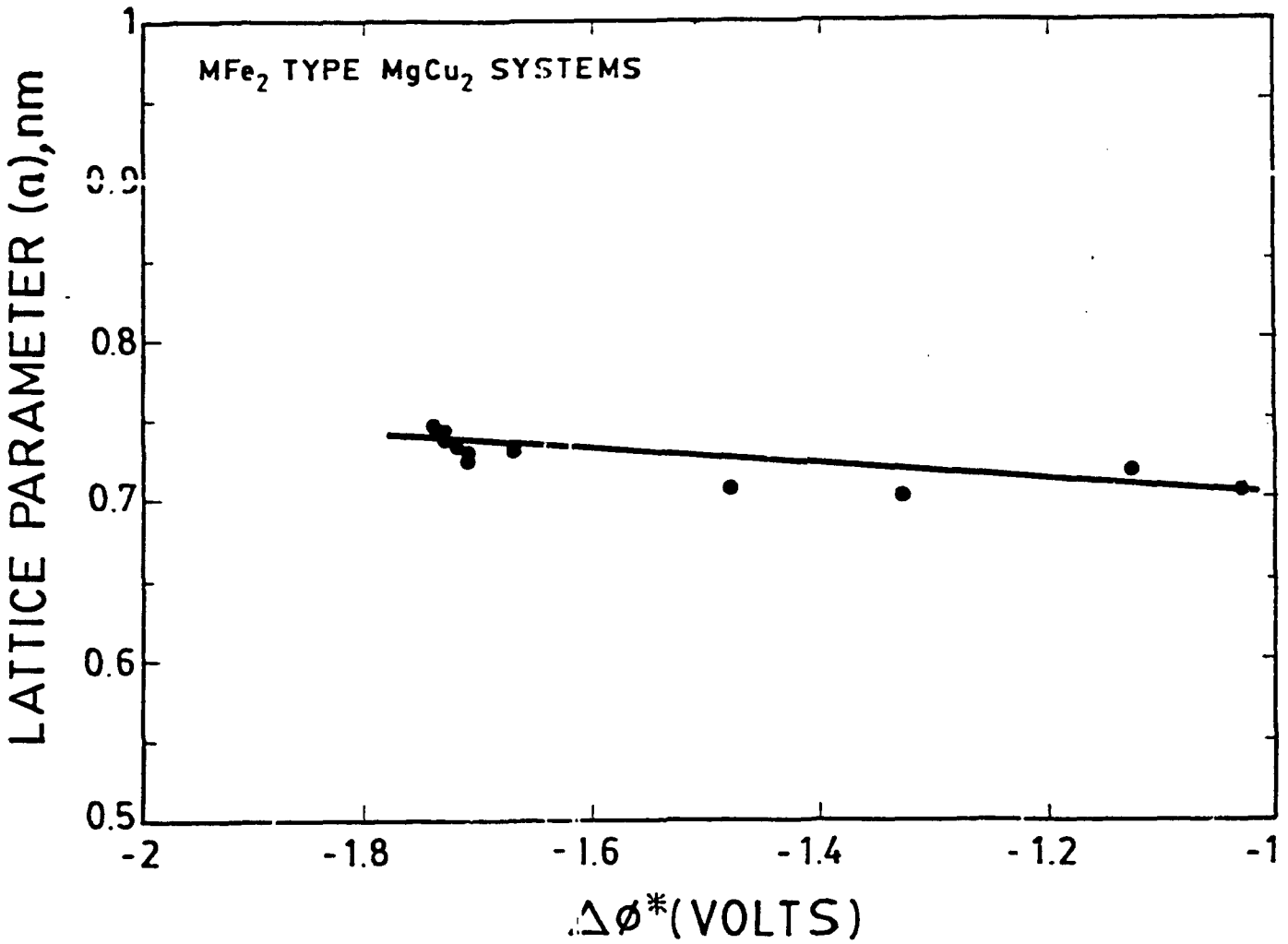
MFe$_2$ TYPE MgCu$_2$ SYSTEMS
LATTICE PARAMETER (a),nm
1
0.9
0.8
0.7
0.6
0.5
-2
-1.8
-1.6
-1.4
-1.2
-1
Δø*(VOLTS)

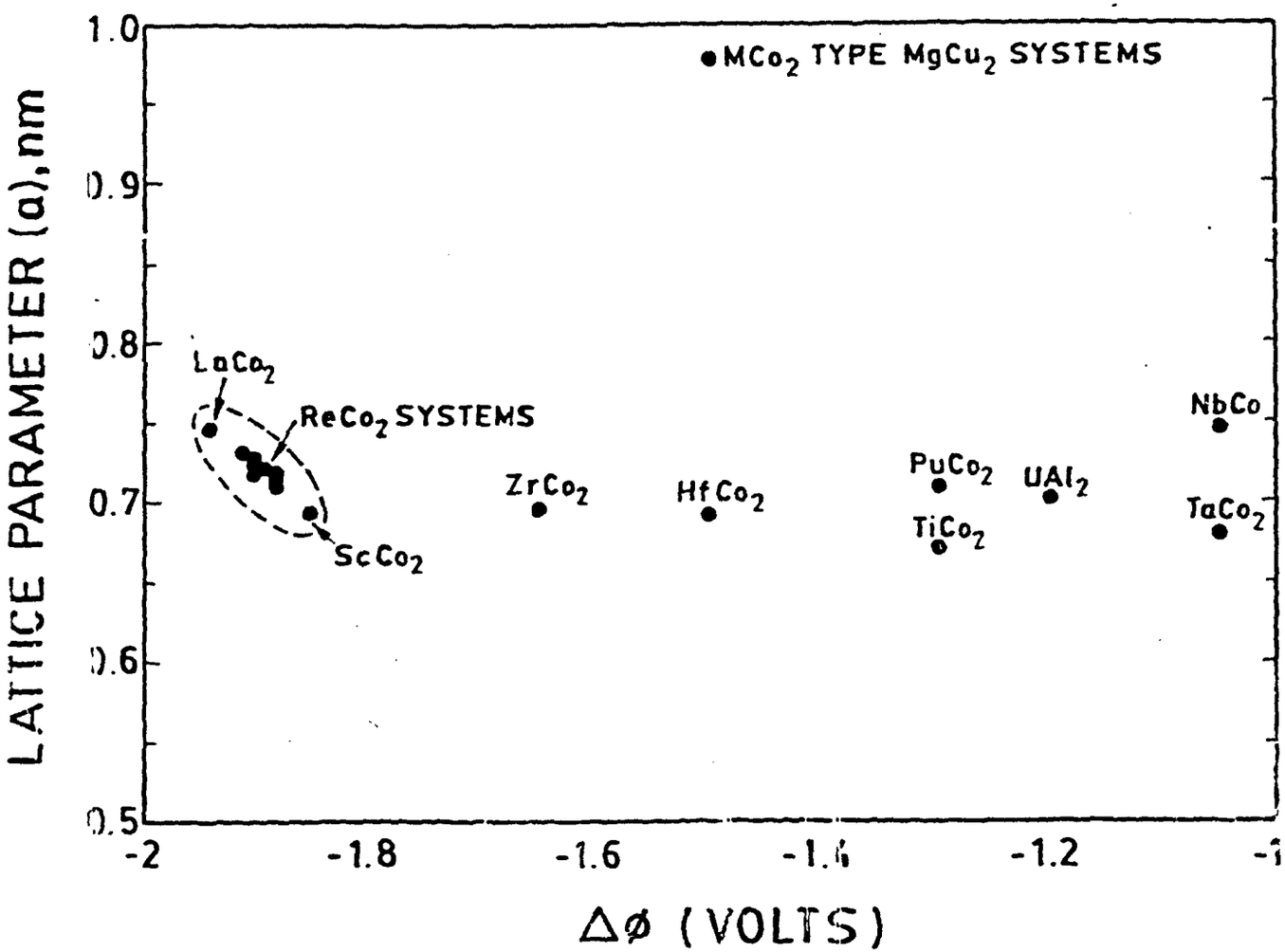
LATTICE PARAMETER (a), nm
1.0
0.9
0.8
0.7
0.6
0.5
-2
-1.8
-1.6
-1.4
-1.2
-1
Δø (VOLTS)
● MCo2 TYPE MgCu2 SYSTEMS
LaCo2
ReCo2 SYSTEMS
ScCo2
ZrCo2
HfCo2
PuCo2
TiCo2
UAl2
NbCo
TaCo2

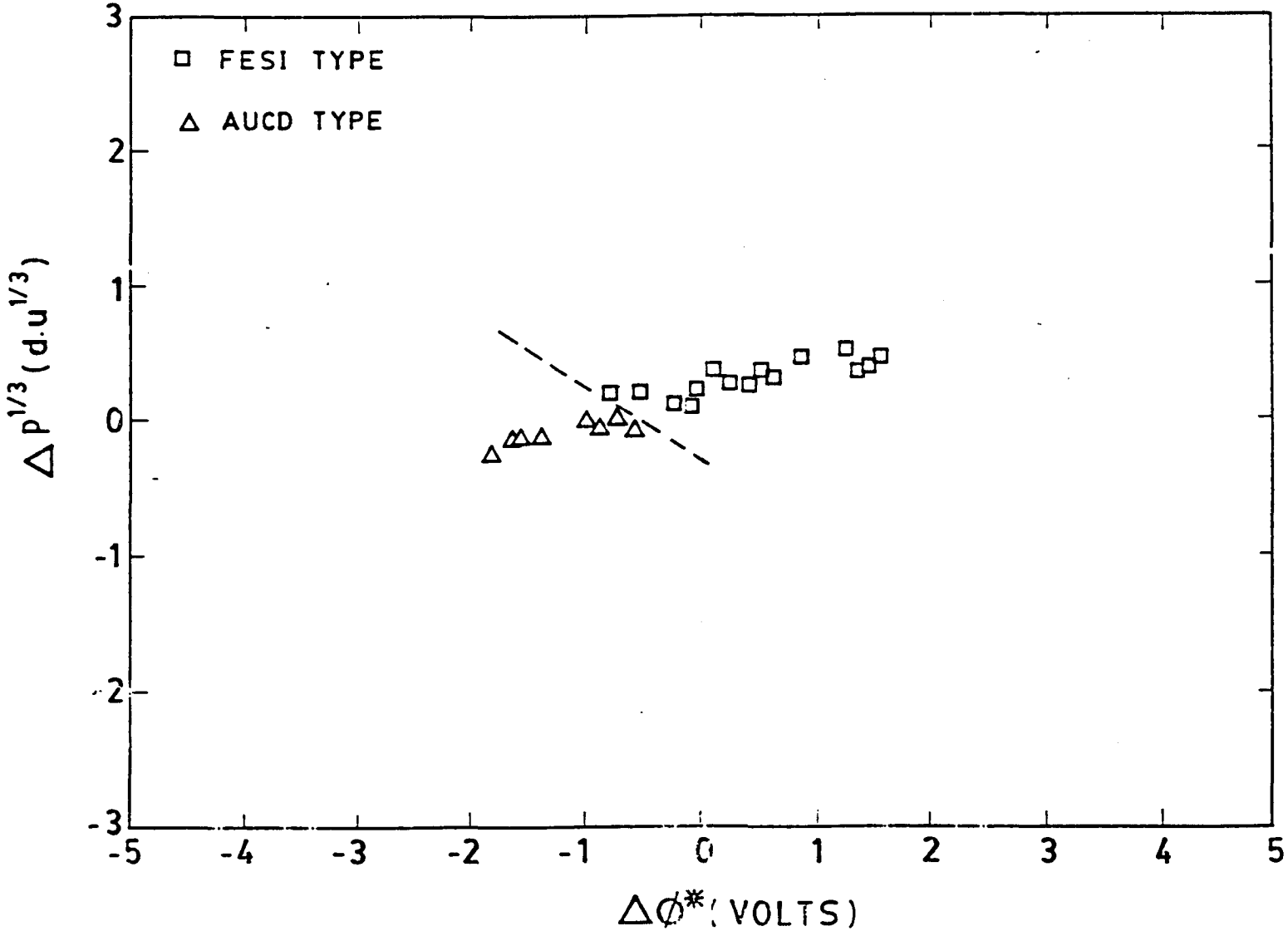
FESI TYPE
AUCD TYPE
$\Delta P^{1/3}$ (d.u$^{1/3}$)
$\Delta\phi^*$ (VOLTS)
3
2
1
0
-1
-2
-3
-5
-4
-3
-2
-1
0
1
2
3
4
5

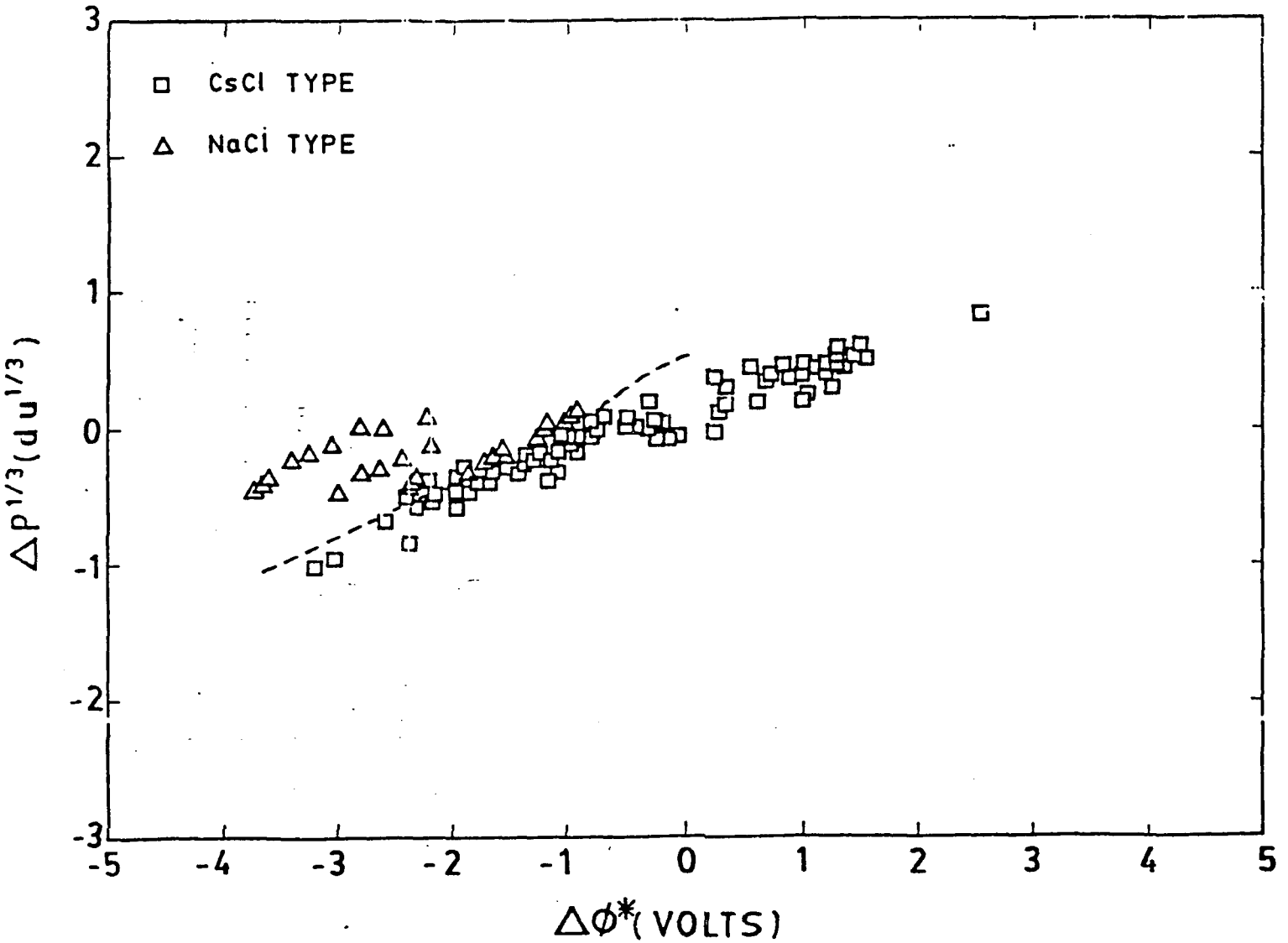
CsCl TYPE
NaCl TYPE
$\Delta P^{1/3}(du^{1/3})$
$\Delta\phi^*$(VOLTS)
3
2
1
0
-1
-2
-3
-5
-4
-3
-2
-1
0
1
2
3
4
5

7.49

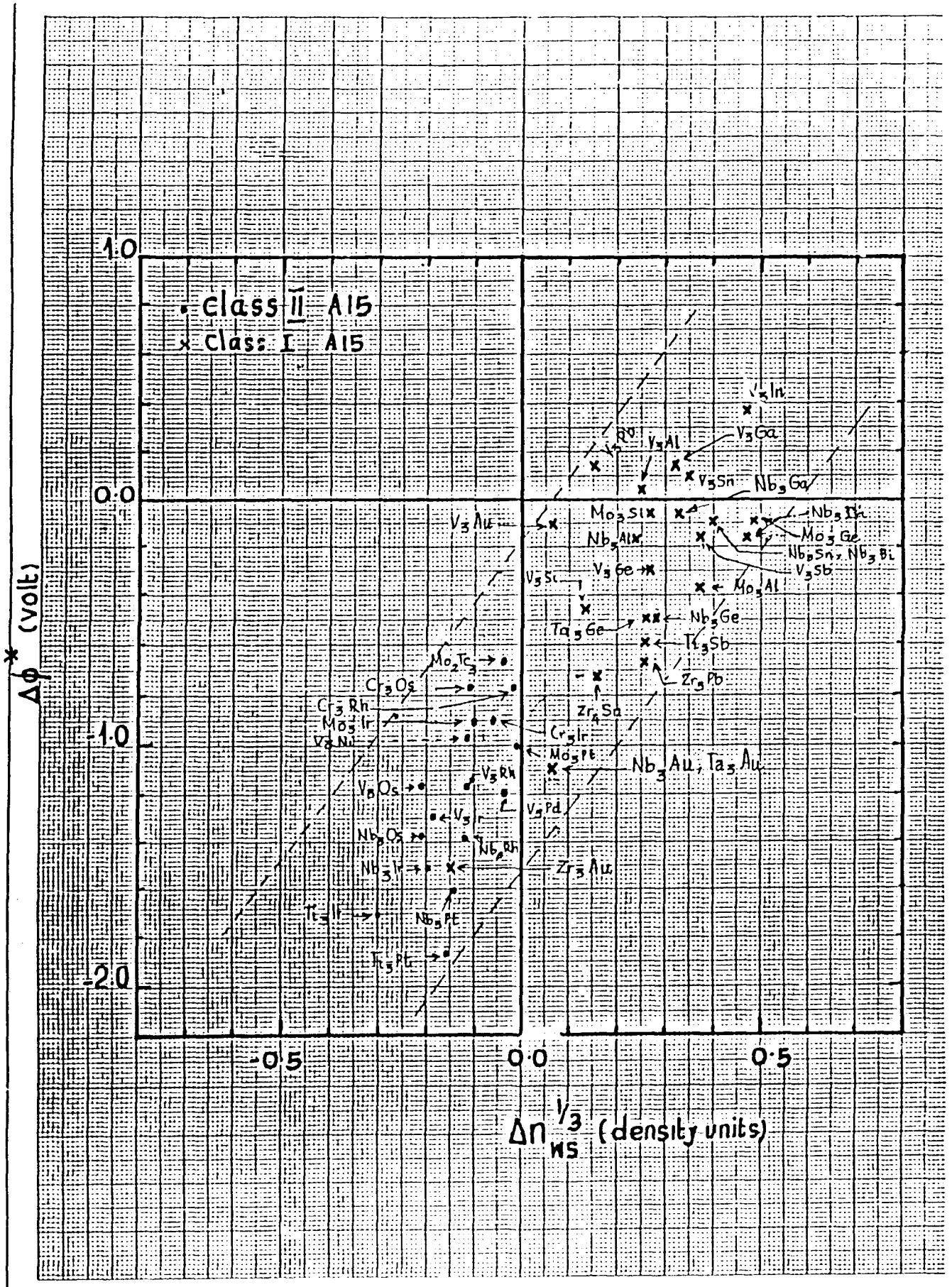
• Class II A15
× Class I A15
1.0
0.0
-1.0
-2.0
-0.5
0.0
0.5
Δφ* (volt)
Δn^1/3 ws (density units)
V3In
V3Ga
V3Al
V3Sn
Nb3Ga
Mo3Si
Nb3Al
Nb3Ge
Mo3Ge
Nb3Sn, Nb3Bi
V3Sb
V3Si
V3Ge
Mo3Al
Ta3Ge
Nb3Ge
Ti3Sb
Zr3Pb
Zr3Sn
Cr3Ir
Mo3Pt
Nb3Au, Ta3Au
Zr3Au
V3Pd
V3Au
Mo2Tc3
Cr3Os
Cr3Rh
Mo3Ir
V3Ni
V3Os
V3Rh
V3Ir
Nb3Os
Nb3Rh
Nb3Ir
Ti3Ir
Nb3Pt
Ti3Pt

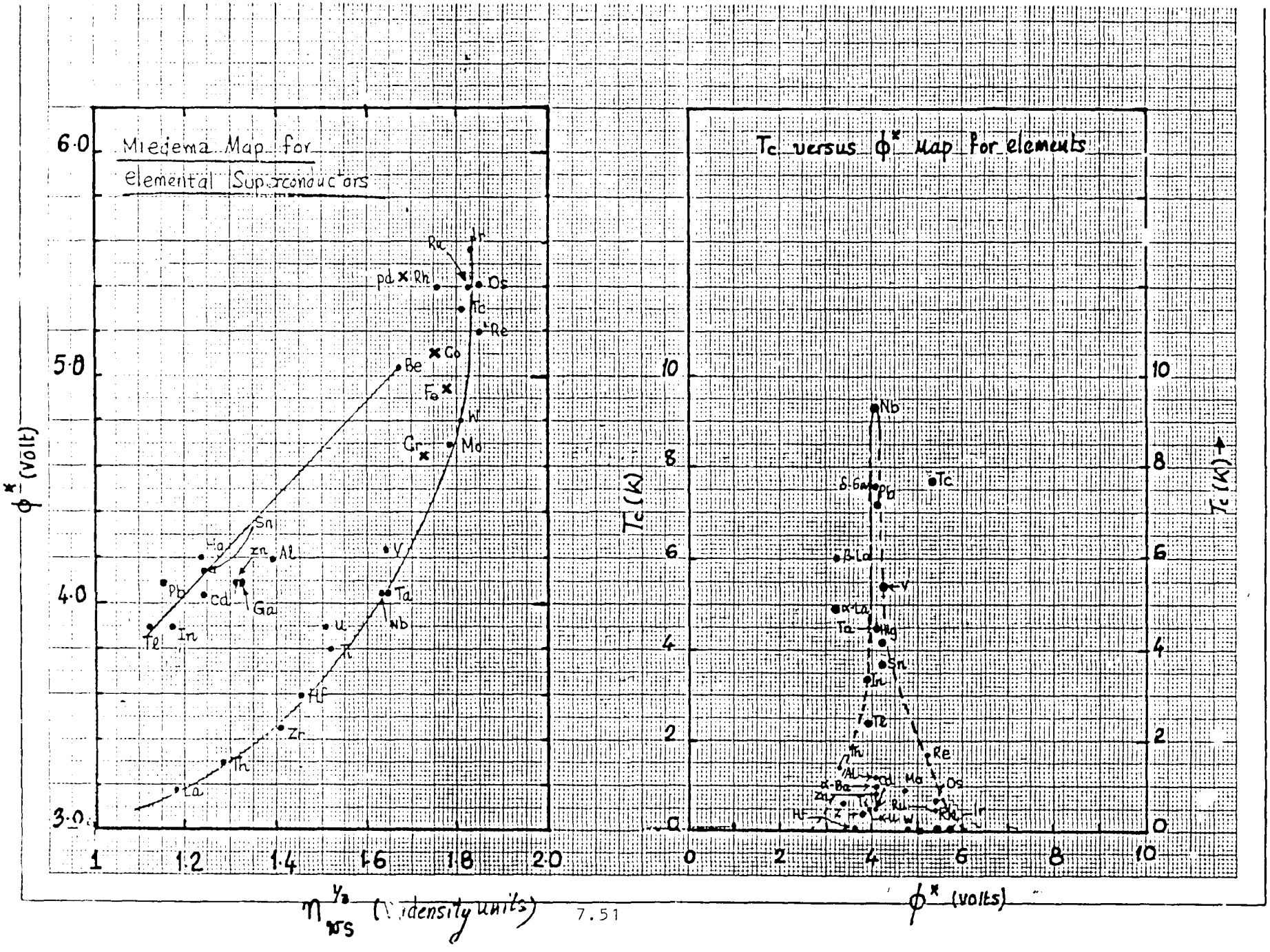
Miedema Map for
elemental Superconductors
ϕ^* (volt)
$n_{ws}^{1/3}$ (density units)
Re
Ir
Pd
Rh
Os
Tc
Re
Co
Be
Fe
W
Cr
Mo
Sn
Ga
Zn
Al
V
Pb
Cd
Ga
Ta
Nb
Tl
In
U
Ti
Hf
Zr
Th
La
Tc versus ϕ^* map for elements
T_c (K)
ϕ^* (volts)
Nb
δ-Ga
Pb
Tc
β-Cd
V
α-Ta
Ta
Hg
Sn
In
Tl
Re
Th
Al
α-Ba
Cd
Mo
Os
Zn
Ru
Rh
Ir
Hf
Zr
U
W

7.51

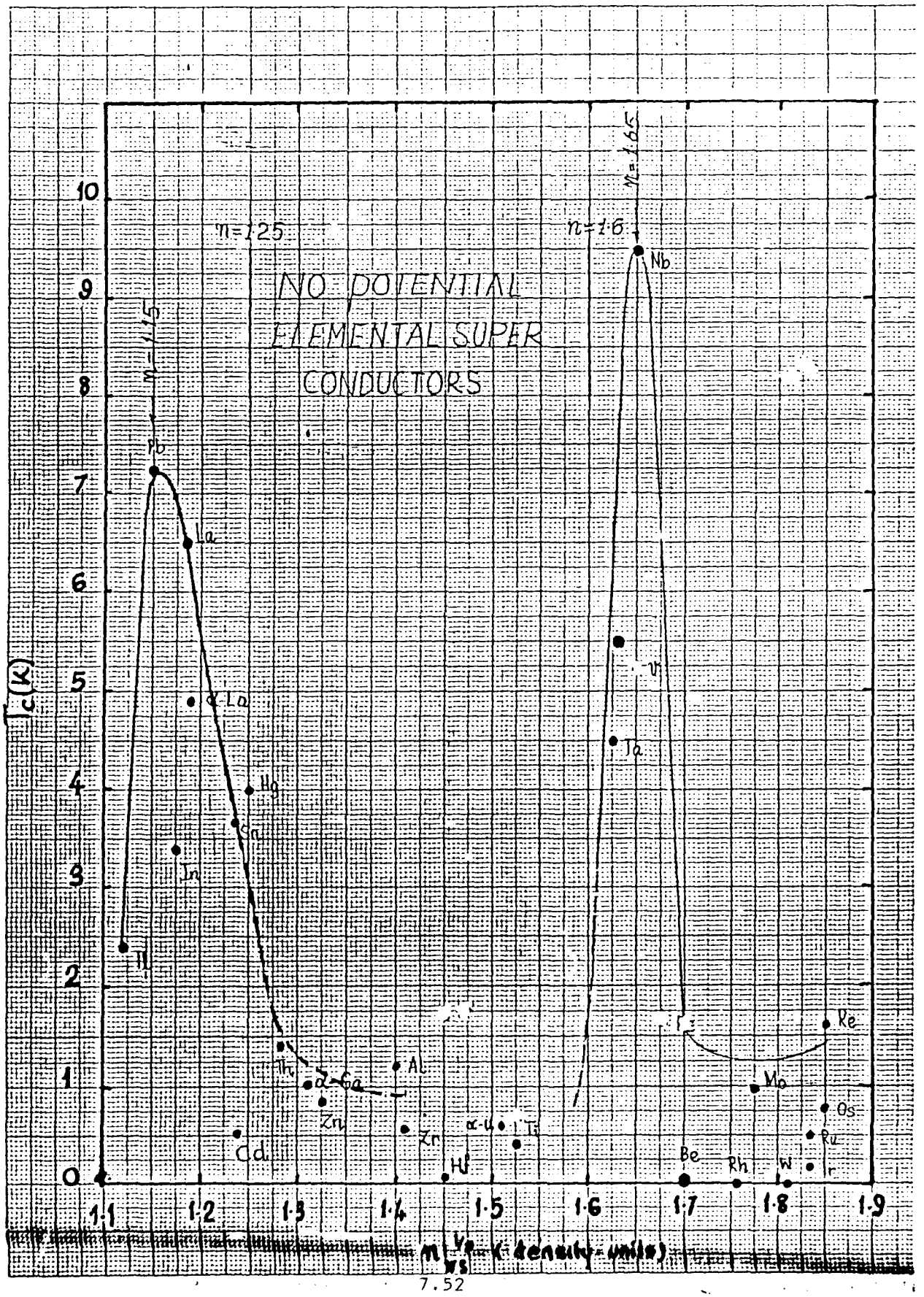
NO POTENTIAL
ELEMENTAL SUPER
CONDUCTORS
n=1.25
n=1.15
n=1.6
n=1.65
Pb
La
α-La
Hg
Sn
In
Tl
Th
α-Ga
Al
Zn
Cd
Zr
α-U
Ti
Hf
Nb
V
Ta
Re
Mo
Os
Ru
Be
Rh
W
Ir
T_c (K)
0
1
2
3
4
5
6
7
8
9
10
1.1
1.2
1.3
1.4
1.5
1.6
1.7
1.8
1.9
$n \frac{V_0}{V_{ws}}$ (density units)

CONCLUSION # 1

The direct method is seldom transparent and transferable

but

It offers to validate or otherwise a successful empirical correlation

CONCLUSION # 2

Miedema coordinates : Bond Indicators ?

STRUCTURE SORTING PARAMETERS

Pettifor's vs Miedemas